INFORMATION TO USERS

The most advanced technology has been used to photograph and reproduce this manuscript from the microfilm master. UMI films the original text directly from the copy submitted. Thus, some dissertation copies are in typewriter face, while others may be from a computer printer.

In the unlikely event that the author did not send UMI a complete manuscript and there are missing pages, these will be noted. Also, if unauthorized copyrighted material had to be removed, a note will indicate the deletion.

Oversize materials (e.g., maps, drawings, charts) are reproduced by sectioning the original, beginning at the upper left-hand corner and continuing from left to right in equal sections with small overlaps. Each oversize page is available as one exposure on a standard 35 mm slide or as a 17″ × 23″ black and white photographic print for an additional charge.

Photographs included in the original manuscript have been reproduced xerographically in this copy. 35 mm slides or 6″ × 9″ black and white photographic prints are available for any photographs or illustrations appearing in this copy for an additional charge. Contact UMI directly to order.

Accessing the World's Information since 1938

300 North Zeeb Road, Ann Arbor, MI 48106-1346 USA

Order Number 8822425

Synthesis and ^{1}H NMR conformational analysis of potent and mu opioid receptor selective cyclic peptides: Topographical design utilizing a conformationally stable template

Kazmierski, Wieslaw Mieczyslaw, Ph.D.

The University of Arizona, 1988

U·M·I
300 N. Zeeb Rd.
Ann Arbor, MI 48106

PLEASE NOTE:

In all cases this material has been filmed in the best possible way from the available copy. Problems encountered with this document have been identified here with a check mark __√__.

1. Glossy photographs or pages _____
2. Colored illustrations, paper or print _____
3. Photographs with dark background _____
4. Illustrations are poor copy _____
5. Pages with black marks, not original copy __√__
6. Print shows through as there is text on both sides of page _____
7. Indistinct, broken or small print on several pages __√__
8. Print exceeds margin requirements _____
9. Tightly bound copy with print lost in spine _____
10. Computer printout pages with indistinct print _____
11. Page(s) _____ lacking when material received, and not available from school or author.
12. Page(s) _____ seem to be missing in numbering only as text follows.
13. Two pages numbered _____. Text follows.
14. Curling and wrinkled pages _____
15. Dissertation contains pages with print at a slant, filmed as received _____
16. Other _____

_____

_____

SYNTHESIS AND ^{1}H NMR CONFORMATIONAL ANALYSIS OF POTENT AND MU OPIOID RECEPTOR SELECTIVE CYCLIC PEPTIDES: TOPOGRAPHICAL DESIGN UTILIZING A CONFORMATIONALLY STABLE TEMPLATE

by

Wieslaw Mieczyslaw Kazmierski

A Dissertation Submitted to the

DEPARTMENT OF CHEMISTRY

In Partial Fulfillment of the Requirements
For the Degree of

DOCTOR OF PHILOSOPHY

In the Graduate College

THE UNIVERSITY OF ARIZONA

1 9 8 8

THE UNIVERSITY OF ARIZONA
GRADUATE COLLEGE

As members of the Final Examination Committee, we certify that we have read the dissertation prepared by Wieslaw Mieczyslaw Kazmierski

entitled Synthesis and ^{1}H NMR Conformational Analysis of Potent and Mu Receptor Selective Cyclic Peptides: Topographical Design Utilizing Conformationally Stable Template.

and recommend that it be accepted as fulfilling the dissertation requirement for the Degree of Doctor of Philosophy.

Dr. Victor J. Hruby	May 6, 1988 Date
Dr. Eugene A. Mash	May 6, 1988 Date
Dr. Robert B.Bates	May 6, 1988 Date
Dr. Michael Barfield	May 6, 1988 Date
Dr. Krishna Vemulapalli	May 6, 1988 Date

Final approval and acceptance of this dissertation is contingent upon the candidate's submission of the final copy of the dissertation to the Graduate College.

I hereby certify that I have read this dissertation prepared under my direction and recommend that it be accepted as fulfilling the dissertation requirement.

Dissertation Director Dr. Victor J. Hruby	May 6, 1988 Date

STATEMENT BY AUTHOR

This dissertation has been submitted in partial fulfillment of requirements for an advanced degree at The University of Arizona and is deposited in the University Library to be made available to borrowers under the rules of the Library.

Brief quotations from this dissertation are allowable without special permission, provided that accurate acknowledgment of source is made. Requests for permission for extended quotation from or reproduction of the manuscript in whole or in part may be granted by the copyright holder.

SIGNED: 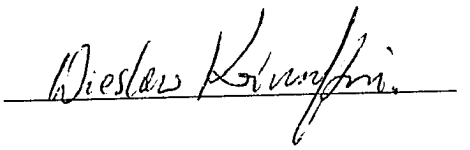

ACKNOWLEDGEMENTS

This work was supported by U.S. Public Health Service Grants: NS 19972, DA 04248 and DK 36289. The mass spectral determinations were performed by the Midwest Center for Mass Spectrometry, a National Science Foundation Regional Instrumentation Facility (Grant No. CHE 8211164).

The author would like to thank his research director, Dr. Victor J. Hruby, for the opportunity to work in his laboratory, his support and enthusiasm, as well as the scientific freedom the author has enjoyed during his graduate studies. Many thanks also go to all the professors who have served as members of my committee: Dr. Michael Barfield, Dr. Robert B. Bates, Dr. Eugene A. Mash, Jr., and Dr. Krishna Vemulapalli.

The author would also like to thank Dr. Henry I. Yamamura, Dr. Thomas F. Burks, Dr. Jennifer E. Shook, Dr. Richard J. Knapp, William S. Wire and George Lui for their bioassay work which has contributed to this study.

The author would like to express his thanks to his colleagues: Dr. Christian Zechel, Dr. Dirk Tourwe, Dr. Terry Matsunaga, Dr. Andy Kawasaki, Dr. Geza Toth, Dr. David Smith, Dr. Sunan Fang, Dr. Ramalinga Dharanipragada, Dr. Sam Sanderson, Dr. Om Prakash, Dr. Kate Toth, Cathy Gehrig, Casey Russell, Geoff Landis, Fahad Al-Obeidi, Min-Shine Chao and Dev Trivedi.

Long and insightful discussions with Dr. Elizabeth Sugg helped the author to form his views on many aspects of peptide research.

Dr. Andrzej Lipkowski (Warsaw University) is gratefully acknowledged for his help and guidance.

Finally, words of undescribed gratitude are directed to my parents Mieczyslaw and Jozefa, as well as to my wife Maria and my little son Konstantin for their sacrifice of not being able to see me during the three and one-half year period while I was engaged in my graduate studies.

TABLE OF CONTENTS

Page

LIST OF ILLUSTRATIONS..... 7

LIST OF TABLES..... 11

ABSTRACT..... 13

1. INTRODUCTION..... 15
   Somatostatin: Structure and Biological Action..... 15
   Concepts of Conformational Constraints..... 20
   Existing Models of μ and δ Opiate Receptor Ligands.. 27

2. EXPERIMENTAL AND THEORETICAL METHODS IN THE SYNTHESIS AND CONFORMATIONAL ANALYSIS OF SOMATOSTATIN ANALOGUES..... 35

   Theoretical Aspects of 2D NMR..... 35
   Introduction to chemical shift correlated spectroscopy... 35
   Phase sensitive spectroscopy..... 44
   Cross relaxation and chemical exchange..... 45
   Experimental Methods In the Synthesis of Somatostatin Analogues.. 48
   Methods of peptide bond formation..... 48
   Protecting groups in peptide synthesis..... 53
   Polymeric support in a solid phase peptide synthesis.... 53
   Coupling schemes..... 55
   Experimental Section..... 59
   General methods..... 59
   Reduced ring size peptides..... 65
   N- and C-terminally modified peptides..... 68
   Synthesis of alkylamino peptide bond isosteres.... 75
   Experimental Conditions for NMR Experiments..... 83

3. PHARMACOLOGICAL PROPERTIES OF THE SYNTHETIC SOMATOSTATIN ANALOGUES: RECEPTOR BINDING AND IN VITRO EXPERIMENTS..... 86

   General Remarks..... 86
   Reduced Ring Size Analogues..... 90
   Design Rationale..... 90
   Analogues With N-terminal Modifications..... 93
   Modifications on the C-terminal Position.....105

4. CONFORMATIONAL ANALYSIS AND DYNAMICS OF CONSTRAINED SOMATOSTATIN ANALOGUES: NUCLEAR MAGNETIC RESONANCE STUDIES...111
N-terminally Modified Cyclic Octapeptides.....111
Pseudopeptides and Bicyclic Peptides.....133
Design rationale of pseudopeptides.....133
Comparison of Results Obtained in this Work With the Literature Data.....164
Summary and Future Perspectives.....166

REFERENCES.....169

LIST OF ILLUSTRATIONS

Page

Figure 1. Opioid peptides and receptors - possible physiological roles..... 18

Figure 2. Hierarchy of information transfer in the biological system..... 19

Figure 3. Some common secondary structures found in peptides and proteins (top). Dihedral angles and theoretically observable NOE cross - relaxations in βII' turns (bottom)..... 22

Figure 4. Concept of template-assembled synthetic proteins..... 23

Figure 5. Structures of some β-turn peptido-mimetics..... 25

Figure 6. A γ-turn template proposed by Kemp and Carter (1987).. 26

Figure 7. Turn stabilization by a proline residue by Gierasch et al., (1981)..... 28

Figure 8. Possible side chain conformations of D-tetrahydroisoquinoline..... 29

Figure 9. Structure of 1,2,3,4-tetrahydro-β-carboline..... 30

Figure 10. The normal lineshape resulting from the 2D FT of a phase modulated signal (right) is a combination of a double absorption (left) and double dispersion (middle)..... 46

Figure 11. Definition of transition probabilities in double quantum NMR Spectroscopy..... 46

Figure 12. Mechanisms of peptide bond formation..... 49

Figure 13. Peptide bond formation via 8-hydroxyquinoline active esters..... 51

Figure 14. Principles of a racemization free method of peptide bond formation..... 51

Figure 15. Attachment of the first amino acid to the resin..... 52

Figure 16. Two strategies of Pam resin synthesis by Merrifield (1978)..... 56

Figure 17. Two methodologies of p-MBHA resin synthesis; Path A (used in this work) by Orlowski et al., (1976), and Path B (Bryan, 1986)..... 57

Figure 18. Coupling scheme used for stepwise elongation of peptide chain, synthesis of peptides 1-22 and 25..... 58

Figure 19. Chemical scheme for the ninhydrin based detection of the free amino group..... 60

Figure 20. Scheme of synthesis and purification techniques applied for analogues 1-27, example of peptide 2..... 61

Figure 21. Typical RP HPLC chromatogram of crude (after cyclization) peptides 10 (A; 10-30%/60 min.) and 23 (B; 10-40%/30 min.)..... 63

Figure 22. Reduction scheme for conversion of amides into aldehydes, according to Fehrentz and Castro (1983)... 52

Figure 23. Long range COSY spectrum of Gly-D-Tic-Cys-Tyr-D-Trp-Orn-Thr-Pen-Thr-NH_2 (303K, d_6-DMSO)..... 85

Figure 24. NOESY spectrum of D-Pgl-Cys-Tyr-D-Trp-Lys-Thr-Pen-Thr-NH_2, 303K, d_6-DMSO..... 94

Figure 25. NOESY spectrum of PCTP, fragment illustrating NH^5/NH^6 cross - relaxation (d_6-DMSO, 303K)..... 95

Figure 26. NOESY cross-relaxation off-diagonal signals between $Cys_\alpha{}^2$ and $Pen_\alpha{}^7$, d_6-DMSO, 303K, PCTP..... 96

Figure 27. Structures of amino acids replacing D-Phe on the N-terminal position, applied in this work..... 97

Figure 28. Conformations of D-Tic-Cys-Tyr-D-Trp-Orn-Thr-Pen-Thr-NH_2 (top), and D-Pgl-Cys-Tyr-D-Trp-Orn-Thr-Pen-Thr-NH_2 (bottom), energy minimized with use of the NMR constraints (CHARMM).
Both structures have the same backbone conformations, but different topographies.....101

Figure 29. Newman representation of the first four residues of D-Tic-Cys-Tyr-D-Trp-Lys-Thr-Pen-Thr-NH_2.....102

Figure 30. Newman representation of relative aromatic ring relationship in Gly-D-Tic-Cys-Tyr-D-Trp-Orn-Thr-Pen-Thr-NH_2, consistent with the NMR data.....103

Figure 31. Conformations of Gly-D-Tic-Cys-Tyr-D-Trp-Orn-Thr-Pen-Thr-NH_2 (top) and D-Tic-Cys-Tyr-D-Trp-Orn-Thr-Pen-Thr-NH_2 (bottom), energy minimized with NMR constraints (CHARMM).
Both structures have the same backbone conformations, but different topographies.....104

Figure 32. Newman representations of aromatic ring determined topography in D-Phe-Cys-Tyr-D-Trp-Orn-Thr-Pen-Thr-NH_2 (top) and (determined by the ^1H NMR) D-Phe-Cys-Tic-D-Trp-Orn-Thr-Pen-Thr-NH_2 (bottom).....109

Figure 33. Newman representations of the aromatic ring topography determined for D-Phe-Cys-Tyr-D-Trp-Orn-Thr-Pen-Thr-NH_2 (top) and (putatively) in D-Phe-Cys-Tyr-D-Tca-Orn-Thr-Pen-Thr-NH_2 (bottom).....110

Figure 34. Phase sensitive COSY spectrum of D-Pgl-Cys-Tyr-D-Trp-Lys-Thr-Pen-Thr-NH_2, (303K, d_6-DMSO).....112

Figure 35. Definition of ψ, ϕ, and χ dihedral angles, determining protein/peptide conformation.....113

Figure 36. Rotamer Populations About the C_α-C_β Bond.....114

Figure 37. Distance vs dihedral angle ψ for cis and trans peptide bond of the Pro-Pro dipeptide, by Wüthrich et al., (1984).....118

Figure 38. 2D NOESY spectrum for TCTP in d_6-DMSO, with emphasis on αH region of Cys and Pen.....122

Figure 39. NOESY spectrum of Gly-D-Tic-Cys-Tyr-D-Trp-Orn-Thr-Pen-Thr-NH_2, 303K, d_6-DMSO.....127

Figure 40. NOESY spectrum of Gly-D-Tic-Cys-Tyr-D-Trp-Orn-Thr-Pen-Thr-NH_2, 303K, d_6-DMSO.....128

Figure 41. Conformational transformations of tetrahydroisoquinoline carboxylic acid (Tic).....132

Figure 42. NOESY spectrum of D-Phe-Cys-Tyr-D-Tca-Orn-Thr-Pen-Thr-NH_2, 303K, d_6-DMSO.....142

Figure 43. NOESY spectrum of D-Phe-Cys-Tyr-D-Tca-Orn-Thr-Pen-Thr-NH_2, 303K, d_6-DMSO.....143

Figure 44. Temperature dependence of aromatic resonances in D-Phe-Cys-Tyr-ψ[CH_2NH]-D-Trp-Orn-Thr-Pen-Thr-NH_2, d_6-DMSO.....146

Figure 45. Spectral types of the aromatic residues in peptides and proteins, due to their restricted rotation around the C_2 axis (BPTI example).....148

Figure 46. NOESY spectrum of D-Phe-Cys-Tyr-ψ[CH_2NH]-D-Trp-Orn-Thr-Pen-Thr-NH_2 (303K, d_6-DMSO).....152

Figure 47. Possible manifestation of the mobility of the pipecolic ring fragment in D-Phe-Cys-Tyr-ψ[CH_2N]-D-Tca-Orn-Thr-Pen-Thr-NH_2, by temperature spectral dependence.....154

Figure 48. NOESY spectrum of D-Phe-Cys-Tic-D-Trp-Orn-Thr-Pen-Thr-NH_2 (303K, d_6-DMSO).....159

LIST OF TABLES

Page

Table 1. Structure - receptor selectivity relationships in the somatostatin cyclic octapeptide series (Pelton et al., 1985a; Pelton et al., 1986; Pelton et al., 1985b). Starting structure D-Phe-Cys-Phe-D-Trp-Lys-Thr-Pen-Thr-OH is converted to D-Phe-Cys-Tyr-D-Trp-Arg-Thr-Pen-Thr-NH_2, 3 CTAP..... 17

Table 2. Protecting groups utilized in this work, their chemical stability and condition of removal..... 54

Table 3. Analytical Characterization of the Somatostatin Analogues Synthesized in This Work by HPLC, TLC and FAB MS..... 64

Table 4. Binding Affinities and Selectivities of CTP Analogues in Competition with [^{3}H]CTOP, [^{3}H]DPDPE and [^{125}I]CGP23,996 in Receptor Binding to Rat Brain Membranes..... 87

Table 5. Pharmacological characterization of selected somatostatin analogues in GPI assays..... 89

Table 6. Spectral assignments, coupling constants and temperature factors for PCTP, 8, 11, 12.....115

Table 7. Relative intensities of interresidual NOE cross-relaxations for the PCTP, 8, 11, 12.....116

Table 8. Possible dihedral angles (NH-CH_α) for PCTP, 8, 11, 12, determined from ^{1}H NMR coupling constants.....125

Table 9. Rotamer side chain populations for peptides 8 and 12, as calculated from vicinal coupling constants.....130

Table 10. Chemical shift and coupling constant assignments for model compound Boc-Tyr-(O-2,6-Cl_2-Bzl)-ψ[CH2N]-D-TcaOMe, 28, d_6-DMSO, 303K.....136

Table 11. Chemical shifts, coupling constant assignments and amide temperature coefficients for peptides D-Phe-Cys-Tyr-D-Tca-Orn-Thr-Pen-Thr-NH_2, 22, and D-Phe-Cys-Tic-D-Trp-Orn-Thr-Pen-Thr-NH_2, 25, d_6-DMSO, 303K.....137

Table 12. Side chain conformer population and accessible ψ angles derived from ^{1}H NMR analysis of D-Phe-Cys-Tyr-D-Tca-Orn-Thr-Pen-Thr-NH_2, 22, d_6-DMSO, 303K.....140

Table 13. Chemical shifts, coupling constants and amide temperature coefficients for D-Phe-Cys-Tyr-ψ[CH_2NH]-D-Trp-Orn-Thr-Pen-Thr-NH_2 (23), D-Phe-Cys-Tyr-ψ[CH_2N]-D-Tca-Orn-Thr-Pen-Thr-NH_2 (24), D-Phe-Cys-ψ[CH_2N]-Tic-D-Trp-Orn-Thr-Pen-Thr-NH_2 (26), d_6-DMSO.....150

ABSTRACT

There is a dogma in molecular biology that biological functions of peptides are determined by their structure ("function" code), coded in their primary structure ("structure" code).

This work describes a new approach that attempts to elucidate these relationships by peptide topology design based on intriguing conformational properties of pipecolic acid based amino acids - like 1,2,3,4 tetrahydroisoquinoline (Tic).

Opioid peptides, owing to the heterogeneity of opioid receptors, display a wide variety of physiological actions. The mu opioid receptor selective octapeptide I (D-Tic-Cys-Tyr-D-Trp-Orn-Thr-Pen-Thr-NH_2) is a model compound for topographical modifications induced by sequential substitutions by Tic residue. Thus, the closely related peptides I and II (Gly-D-Tic-Cys-Tyr-D-Trp-Orn-Thr-Pen-Thr-NH_2, obtained by coupling Gly residue to I) have contrasting affinities for the mu opioid receptor (IC_{50}= 1.2 and 278 nM, respectively). Conformational analysis of I and II by means of 1D and 2D ^1H NMR spectroscopy allowed to determine dramatic differences in the side chain orientation of D-Tic in both peptides and to propose features of the bioactive conformation. The extended conformation of I (due to g(-) side chain conformation of D-Tic) is well recognized by the mu receptor in contrast to the folded conformation of II (due to a g(+) side chain conformation of D-Tic[1], that places the aromatic ring on the opposite side

of the molecule), which is not.

Peptide III (D-Phe-Cys-Tic-D-Trp-Orn-Thr-Pen-Thr-NH_2), featuring replacement of Tyr^3 by Tic^3, binds very weakly to the mu opioid receptor, due to rotation of the Tic aromatic side chain to the opposite side of the molecule (Tic side chain is in a g(+) conformation again).

As these substitutions conserve the conformation of the backbone, constrained cyclic amino acids (picolic acid derivatives) can modify the topography of the peptide in a predictable manner, and (in conjunction with biological data) disclose structural elements of bioactive conformations.

The mechanism of pipecolic acid side chain rotamer selection, will be discussed in the context of design principles.

Chapter 1

INTRODUCTION

Somatostatin: Structure and Biological Functions.

The cyclic tetradecapeptide somatostatin, H-Ala-Gly-Cys-Lys-Asn-Phe-Phe-Trp-Lys-Thr-Phe-Thr-Ser-Cys-OH (SS-14), is a regulatory hormone that is distributed throughout the central nervous system, gastrointestinal tract and pancreas. Studies of its ability to inhibit growth hormone, glucagon, insulin and gastrin release have shown that a fragment of the native hormone, including the essential pharmacophore Phe-Trp-Lys-Thr, carries the full binding and transduction message of somatostatin (Veber et al., 1981; Veber and Holly, 1984). Further work has indicated that substitution of D-Trp for L-Trp increases the potency of the hormone. Veber and co-workers have developed a class of cyclic somatostatin-related hexapeptides, among which c(N-Me-Ala-Tyr-D-Trp-Lys-Val-Phe) is a potent inhibitor of growth hormone, insuline and glucagon release. The cyclic octapeptide D-Phe-Cys-Phe-D-Trp-Lys-Thr-Cys-Thr(ol), SMS-201995, synthesized by Bauer at al. (1982) is also an exceptionally potent inhibitor of growth hormone release.

In addition to its well-established role as a regulatory hormone (Vale et al., 1977), somatostatin has also been observed to have some neurotransmitter-like properties. These would include localization in presynaptic terminals (Eppelbaum ,1977), effects of spontaneous neuronal discharge following microionophoretic application

(Renaud et al., 1975) and behavioral effects after CNS administration (Kastin et al., 1978). Somatostatin also appears to bind weakly to CNS opioid receptors. High concentrations of somatostatin inhibit binding of naloxone and DADLE ([D-Ala, D-Leu]enkephalin) to rat brain homogenates and, in addition, it can give rise to an in vivo analgesic response in mice (Terrenius, 1976; Rezek et al., 1981). Moreover, SMS-201995 also binds moderately well to opioid receptors (Maurer et al., 1982). There exist at least three different opioid receptor systems generally referred to as mu, delta, and kappa (Chang et al., 1979; Lord et al., 1977; Martin et al., 1976), and subtypes of these major receptor systems have also been postulated (Figure 1). Utilizing various structural considerations in conjunction with conformational constraints (Hruby, 1982; Hruby, 1981; Meraldi et al., 1977), structure of truncated somatostatin analogues of the cyclic octapeptide type has been modified to enhance its affinity for the mu opioid receptor, while at the same time decreasing its affinity for delta opioid and somatostatin receptors, with which native hormone interacts with high affinity, in the process of converting a hormone agonist into a neurotransmitter antagonist. Structure-activity studies (Pelton et al., 1985a; Pelton et al., 1986; Pelton et al., 1985b) allowed this laboratory to modify structures related to SMS 201-995 to yield a potent mu opioid receptor antagonist D-Phe-Cys-Tyr-D-Trp-Arg-Thr-Pen-Thr-NH_2 (designated CTAP, 3). A summary of structural changes and their effects on peptide affinity to mu, delta opioid, and somatostatin receptor is shown in Table 1.

Table 1. Structure-receptor selectivity relationships in the somatostatin cyclic octapeptide series (Pelton et al., 1985a; Pelton et al., 1986; Pelton et al., 1985b). Starting structure D-Phe^{1}-Cys-Phe-D-Trp-Lys-Thr-Cys-Thr^{8}-OH is converted to D-Phe^{1}-Cys-Tyr-D-Trp-Arg-Thr-Pen-Thr^{8}-NH_2, 3 CTAP.

Modification	Position	Affinity to receptor type		
		μ opioid	δ opioid	somatostatin
$COOH/CONH_2$	C-terminal	↑83	↑4	↑2.3
Cys/Pen	7	↑5	≈	↓2
Tyr/Phe	3	↑3	≈	↑2
Arg,Orn/Lys	5	≈	≈	↓20

MU RECEPTORS - DAGO, MORPHICEPTIN

1. Analgesia -- Brain
2. Addiction -- Brain - severe
3. Gut Motility -- Inhibits transit via brain receptor
4. Respiration -- Depresses
5. Schizophrenia -- Either excess or deficiency
6. Hormone Release -- Prolactin (↑), ACTH (↓), GnRH (↓)
7. Cardiac Function -- Decreases

DELTA RECEPTORS - DPDPE, DPLPE

1. Analgesia -- Spinal cord, Brain?
2. Addiction -- Mild or None
3. Gut Motility -- No effect
4. Cardiac Function -- Little effect

KAPPA RECEPTORS - DYNORPHIN1-9

1. Analgesia -- Spinal cord, Brain
2. Addiction - Severe
3. Hormone Release -- AVP (↑↑), OT (↓)

Figure 1.

OPIOID PEPTIDES & RECEPTORS - POSSIBLE PHYSIOLOGICAL ROLES

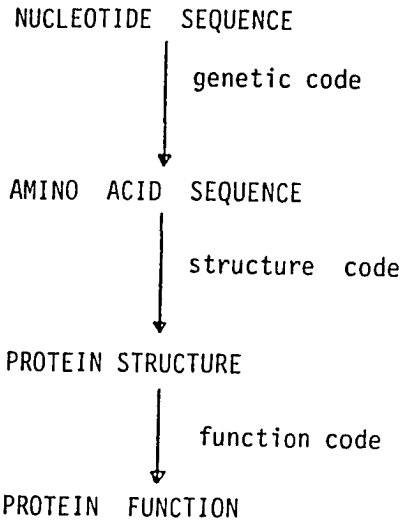

Figure 2. Hierarchy of information transfer in the biological system

Concepts of Conformational Constraints

One of the central questions of a molecular biology of peptides and proteins is the relation of their primary (amino acid sequence) to their secondary and consequently tertiary structure (Figure 2).

A description of a globular protein's 3D structure has been proposed to include the classification of globular proteins based on predominant type of secondary structure. Protein secondary structure refers to regular arrangement of the polypeptide chain backbone, which are stabilized by hydrogen bonds or other intramolecular attractive forces. Traditionally, secondary structure classification has been restricted to four major categories, i.e. α-helix, β-sheet, β-turns and random coil. However with improvements in protein structure resolution other secondary structures (e.g. γ turns, loops) have been found (Figure 3). For a peptide or protein chemist, the major question is what are the mechanisms of protein folding, and correspondingly, how can one utilize peptide/protein folding mechanisms to design a molecule with a predetermined three dimensional conformation giving access to macromolecules with tailor-made chemical, biological or catalytic properties.

Mutter (1985) pioneered the "Template Assembled Synthetic Protein Design" approach in which amphiphilic peptides with a potential for secondary structure formation are attached to a multifunctional template molecule which enhances the spatial accommodation of the peptide blocks to a well defined tertiary structure (Figure 4).

CD spectroscopy is used to prove that these peptides adopt well-developed secondary structures when assembled on a multifunctional template. On the other hand, the single peptide (not attached to the peptide matrix) in the blank experiment of identical sequence and chain length shows a disordered conformation. Consequently, the onset of stable secondary structures of these amphiphilic peptides after linkage to the template can only be rationalized by the formation of a tertiary structure.

Due to the inherent flexibility of most small peptide hormones and neurotransmitters, structure activity studies rarely provide insights into the "bioactive conformation" (or reciprocally the receptor topology) of peptide hormones and neurotransmitters (the host-guest problem). In addition most peptide neurotransmitters interact with several different receptors. For example, the opioid receptors, the subject of this work, exist as at least three different classes, μ, δ, and κ. Specific ligands for each class are needed to determine the biological functions of the different receptors. As a consequence of these and other problems, attempts to rationally design potent and receptor selective peptide ligands have been difficult, and the lack of highly selective ligands have obstructed efforts to understand the physiological roles of the multiple receptor systems found for most peptide hormones and neurotransmitters.

Another concept of conformational restrictions, via pseudo-isosteric cyclization, has been introduced (Hruby, 1982), which can be used in conjunction with local constraints imposed by sterically constrained amino acids and peptido-mimetics (Feigel, 1986; Kemp and

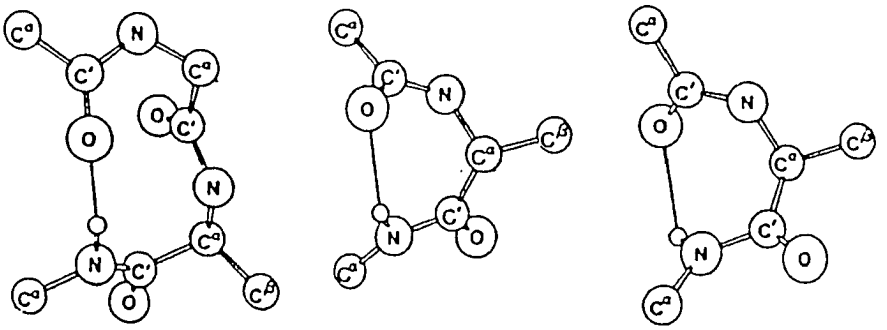

Type II' β-turn. γ-turn. inverse-γ-turn.

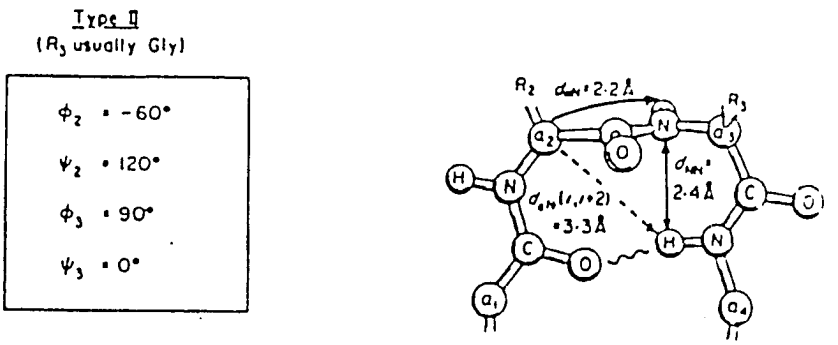

Figure 3. Some common secondary structures found in peptides and proteins (top).
Dihedral angles and theoretically observable NOE cross - relaxations in βII' turns (bottom).

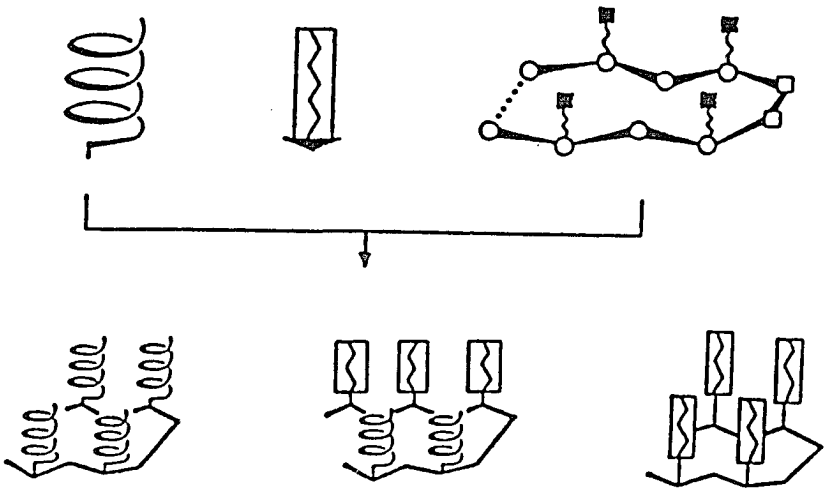

Figure 4. Concept of template-assembled synthetic proteins.

Carter, 1987; Sato and Nagai, 1986; Figure 5, Figure 6, respectively) to aid in the rational design of peptide analogues for specific receptors. For the latter purpose amino acids such as α,β-dehydro- (Nitz et al., 1986), N-methyl- (Vitoux et al., 1986), cyclopropyl- (Mapelli et al., 1985), α,α-dialkyl (Prasad and Balaram, 1984), and β,β-dialkyl- (Meraldi et al., 1977) amino acids have been used with considerable success.

Stabilization of an α-helix or 3_{10}-helix can be obtained with α-aminoisobutyric acid (Aib)- characterized by its restricted conformational space due to two α-methyl groups (Bonora et al., 1984). Quite interestingly, α,α-di-n-propylglycine (Dpg) residues occur in the region of fully extended conformation, thus tending to disrupt the α-helical structure.

Stability of β-turns in peptides and proteins may be greatly enhanced by a proline residue. Gierasch et al. (1981) has found (Figure 7) that in a β-turn consisting of four residues (i to i+3) the sequence Pro-Gly or Pro-D-Y leads to type IIβ turns (trans Pro residue in the i+1 position), the sequence Pro-D-Y leads to type Iβ turn (cis Pro residue in the i+1 position), and the sequence Gly-Pro-Val or D-X-Pro-Y leads to type II'β turns (cis Pro in i+2 position).

Yet another approach to peptide/protein design, is being attempted in this work. Unlike the already mentioned methods (vide supra) of secondary and tertiary structure stabilization that directly affect peptide/protein backbone conformation the approach presented here, called "Topographic Design on a Stable Conformational Template", alters the 3D architecture of a model octapeptide (derivative of

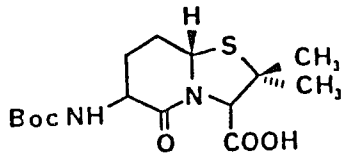

Structure of 8,8-dimethyl-BTD

Sato, K., and Nagai, U.(1986).J.Chem. Soc.Perkin Trans.1,1231

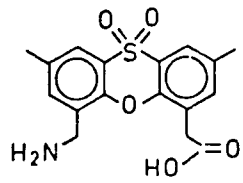

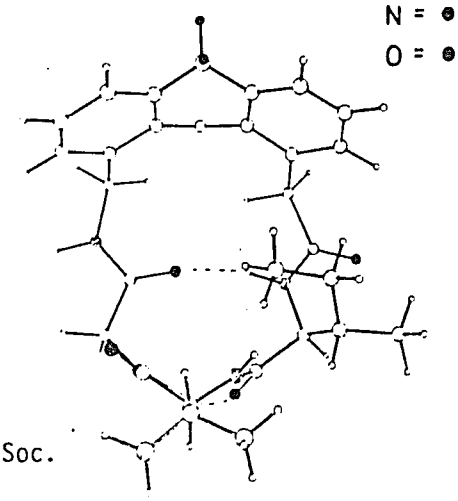

Feigel, M.(1986).J.Am.Chem.Soc. 108,181-182.

2,8-Dimethyl-4-(carboxymethyl)-6-(aminomethyl)phenoxathiin S-Dioxide

Figure 5. Structures of some β-turn peptido-mimetics.

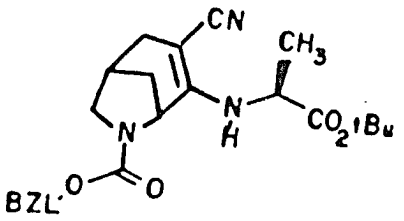

4-alkylamino-3-cyano-6-azabicyclo[3.2.1]oct-3-ene

Figure 6. A γ-turn template proposed by Kemp and Carter (1987).

somatostatin) without apparent modification of backbone conformation. Phenylalanine and tryptophan derivatives of pipecolic acid (1,2,3,4--tetrahydroisoquinoline and 1,2,3,4-tetrahydro- β-carboline carboxylic acid, Figure 8 and Figure 9, respectively) were found to possess a very distinct and well defined side chain conformation, strictly dependent on their position in the peptidic chain. These unusual amino acids (guests) while replacing phenylalanine or tryptophan in "native" peptides were not found to alter backbone conformation of the host.

Detailed description of the ^{1}H NMR experiments that allowed me to determine the topography of these peptide analogues and their correspondence to observed affinity to μ and δ opioid receptors is the subject of this work.

Existing Models of μ and δ Opiate Receptor Ligands.

Numerous investigations to elucidate the bioactive conformation of opioid agents, mostly enkephalins, have been undertaken. A commonly used theoretical approach was to match topologies of rigid opiates (morphine-like) with conformationally flexible opioid peptides, in an effort to establish possible bioactive conformations of the latter. This often resulted in conformations characterized by unacceptably (to be pharmacologically relevant) high energies (Loew and Burt, 1978; Isogai et al., 1977). Solution conformation investigation on flexible linear opioid peptides (Schiller et al., 1977; Fournie-Zaluski et al., 1977) usually provide "average" conformations, with often little apparent relevance to the bioactive one.

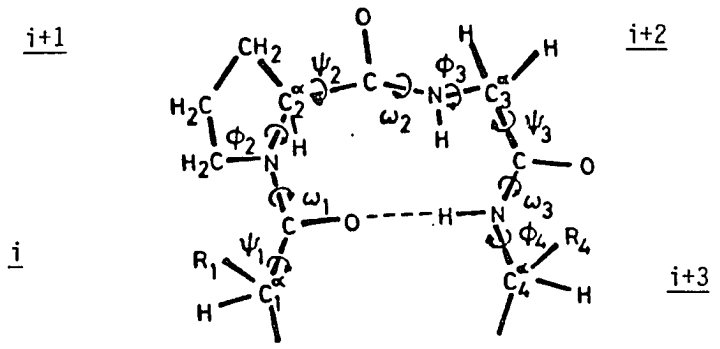

Pro $^{i+1}$	Pro $^{i+2}$
Pro-Gly Pro-D-Y ⇒ β II turn	Gly-Pro-Val D-X-Pro-Y ⇒ β II' turn
Gly-Pro-Y ⇒ I turn	

Figure 7. Turn stabilization by a proline residue by Gierasch et al., (1981).

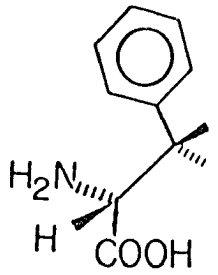

D-Phe

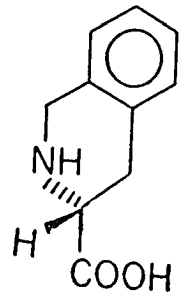

D-Tic

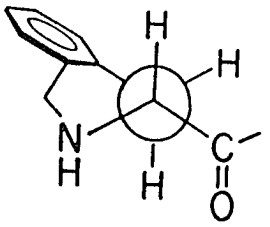

g-

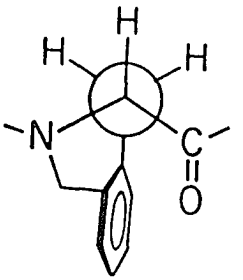

g+

Figure 8. Possible side chain conformations of D-tetrahydroisoquinoline.

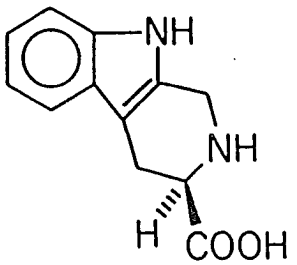

D

Figure 9. Structure of 1,2,3,4-tetrahydro-β-carboline.

The inherent flexibility of most endogenous peptides makes it very difficult, if not impossible, to obtain any reliable information about their bioactive conformation by theoretical calculations (a large number of energetically similar conformational families is usually found; Loew et al., 1986) or by physicochemical methods with relatively slow time scales (e.g. NMR, CD). This factor has caused a significant number of contradictory claims regarding the bioactive conformation of opioid ligands in general as well as mu or delta opioid receptor selective ligands. Some of these will be briefly discussed below, and then compared with results obtained in these studies.

Early structure-activity relationship studies revealed certain distinct structural differences between mu and delta ligands. The hypothesis that a mu receptor prefers a compact (folded) conformation of an endogenous enkephalin, and a delta opioid receptor requires an extended form of the neurotransmitter, has been suggested based on X-ray studies (Camerman et al., 1983).

DiMaio et al. (1986) described the use of a "Bimolecular Energy Refinement" of the semi-rigid alkaloid 7α-[(1R)-1-methyl-1-hydroxy-3-phenylpropyl]-6,10-endo-ethanetetrahydrooripavine (PEO) and a mu opiate selective cyclic peptide H-Tyr-cyclo[D-N^{δ}-Orn-Gly-Phe-Leu], on which ^{1}H NMR studies had previously been reported by Kessler et al. (1983). A systematic search of low energy conformers with significant spatial overlap for both compounds afforded several sets of conformers in which the distance between the aromatic groups of the peptide has been estimated to be between 8.3 and 10.6 Å.

Empirical energy calculations by Doi et al. (1987) suggested that the two primary forms of Met^5- and Leu^5-enkephalins, found by X-ray diffraction methods (the type I'β turn and the dimeric antiparallel extended structure), could be superimposed without significant energy expense. Thus, the apparent flexibility of these linear peptides allow them to attain both conformational states, claimed to be bioactive for the mu and delta opioid receptors, respectively. While the correctness of this claim can be disputed, these computations may confirm that a low interconversion energy is a factor causing the experimentally observed, low receptor selectivity of these endogenous peptidic ligands.

Wilkes and Schiller (1987) have reported the results of a molecular mechanics aided search of low energy conformers of a mu selective agonist H-Tyr-c(D-Orn-Phe-Asp)-NH_2. Four major conformatio nal classes have been found, generally characterized by aromatic ring stacking. Different results were obtained by Loew et al. (1986) and Gorin et al. (1977). In both cases empirical energy calculations for a family of active and inactive analogues of mu opioid receptor selective morphiceptin (Tyr-Pro-Phe-Pro-NH_2) yielded low energy classes of conformation, with separations of the aromatic groups ranging from 6 to 12 Å (Gorin et al., 1977).

^1H NOE difference experiments carried on by Gupta et al. (1986) suggested a spatial proximity between aromatic rings (less than 3.5 Å), though these results were not confirmed (Motta et al., 1987). Fluorescence energy transfer experiments for potent [Trp^1, Met^5]-enkephalin indicated average distances between the aromatic rings of about

10.0±1.1 Å (Schiller et al., 1977). This brief review underlines a number of controversies existing with regard to proposed bioactive conformations of opioid ligands.

There seem to exist two strategies to overcome the flexibility problem inherent for endogenous peptides. One of them involves TNOE (Transferred NOE) conformational investigations on receptor bound peptides (thus rigidized by a receptor matrix). Due to fast exchange between a free and a bound form, the free conformation "remembers" structural parameters of the bound form, which can then be investigated by standard NOE techniques (Clore and Gronenborn, 1982). Glasel and Borer (1986) have studied conformations of nalorphine and levorphanol bound to their binding sites in two anti-opiate antibodies. A significant conformational heterogeneity of free and bound forms suggested that even for relatively rigid molecules, the bioactive conformation may be different from the statistical one observed in the free state.

Another method which provides insight into the guest structure involves imposing conformational restrictions on the peptide (Hruby, 1982) via either isosteric side chain to side chain cyclization, or restriction of rotational mobility of amino acid side chains. Both these methodologies were successfully utilized at different stages of mu opioid selective peptide development, to be presented in this work. Conformational restriction is not a necessary structural feature of the molecule to exhibit high potency and selectivity. The main advantage seems to be in a limitation of the number of attainable

conformations, a factor that renders results of physicochemical investigations much more reliable.

Chapter 2

EXPERIMENTAL AND THEORETICAL METHODS IN THE SYNTHESIS AND CONFORMATIONAL ANALYSIS OF SOMATOSTATIN ANALOGUES.

Theoretical Aspects of 2D NMR.

Introduction to chemical shift correlated spectroscopy.

A standard 2D experiment consists of four basic elements: Preparation, evolution, mixing, and detection periods. During the preparation period a nonequilibrium state of the system is created by applying a suitable train of pulses (either selective or nonselective). During the evolution time t_1 (any modulation that takes place in this period is carried over to further periods of evolution) the system evolves to a suitably tailored (via pulse sequence) Hamiltonian. In the third period of mixing (not applicable for shift correlated spectroscopy), suitable pulses are employed that affect coherence transfer, or monitor cross-relaxation or chemical exchange (NOE). In the fourth period (usually no pulses applied) acquisition of the final response of the spin system is carried out, so that a time domain signal matrix $S(t_1,t_2)$ is obtained, then converted to a frequency domain matrix $S(\omega_1,\omega_2)$. Assuming single phase detection:

[1] $$S(t_1,t_2) = \exp(-t_1/T^a_2)\cos(\omega_a t_1+\theta_a)\times\exp(-t_2/T^b_2)\cos(\omega_b t_2+\theta_b)$$

which after 2D FT with phase correction yields

[2] $$S(\omega_1,\omega_2) = [T^a{}_2/(1+(T^a{}_2(\omega_1-\omega_a))^2)][T^b{}_2/(1+(T^b{}_2(\omega_2-\omega_b))^2)]$$

Equation [2] describes a peak located at coordinates (ω_a,ω_b). A peak of this kind at position $(\omega_1,\omega_2)=(\omega_a,\omega_b)$ indicates connectivity between the two spins resonating at frequencies ω_a and ω_b. In more complicated case $(\omega_1,\omega_2)=(\omega_a+\omega_x,\omega_m)$ if spin "m" is connected to both spins "a" and "b" .

For a system of weakly coupled two spin systems (spin 1/2), the spin-Hamiltonian during free precession is (throughout this work I=S=1/2 , "_" denotes an operator):

[3] $$\underline{H}_S(\pm x) = -(\pm\hbar\gamma_I B_1 \underline{I}_x) \qquad \underline{H}_I(\pm y) = -(\pm\hbar\gamma_I B_1 \underline{I}_y)$$

$$\underline{H}_S(\pm x) = -(\pm\hbar\gamma_S B_1 \underline{S}_x) \qquad \underline{H}_I(\pm y) = -(\pm\hbar\gamma_S B_1 \underline{S}y)$$

$$\underline{H}^{p+q}{}_{I+S} = \underline{H}^p{}_I + \underline{H}^q{}_S \qquad (p,q = +x, -x, +y, -y)$$

These equations are valid for heteronuclear systems, for homonuclear system (to be used in this work) there are two cases:

i) non-selective pulses

$$\underline{H}^{\pm p}{}_{I+S} = -(\pm\gamma h B_1(\underline{I}_p+\underline{S}_p)) \qquad p=x,y$$

ii) pulses selective for I or S spin only.

To define a multiple pulse NMR experiment it is necessary to specify which Hamiltonian is valid for each moment during the experiment.

Thus, a heterocorrelated spectroscopy experiment is described by the following pulse train (associated Hamiltonians are indicated):

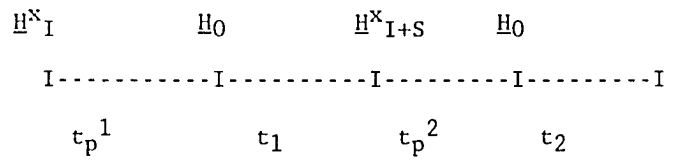

Homocorrelated spectroscopy would be described by a train of Hamiltonians, generated by a pulse sequence $90°\text{-}t_1\text{-}90°\text{-}t_2$:

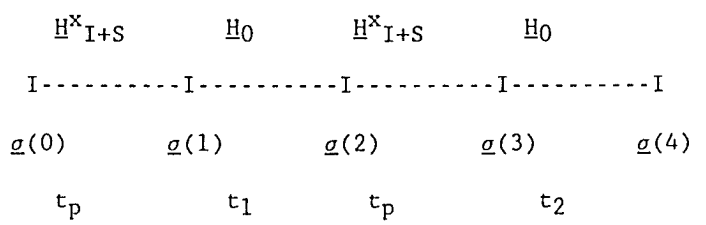

To describe the state of the spin system at any moment during an experiment one needs to know the spin-density operator $\underline{\sigma}$. This operator will be used to calculate the ensemble averaged expectation value <P> of a spin property:

[4] $$<P> = \text{trace}(P.\sigma) = \sum_i \sum_j <\theta_i|\underline{P}|\theta_j><\theta_j|\underline{\sigma}|\theta_i>$$

For a two-spin system the set of basis functions can be chosen as $\theta_1 = \alpha\alpha$, $\theta_2 = \alpha\beta$, $\theta_3 = \beta\alpha$, $\theta_4 = \beta\beta$. Similarly, operators for a two spin system are formed from the one spin operator by taking products of $\underline{E}$,

$\underline{I}_x$, $\underline{I}_y$, $\underline{I}_y$, $\underline{E}$, $\underline{S}_x$, $\underline{S}_y$, $\underline{S}_z$ operators. This gives sixteen operators $\underline{O}_k$, with matrix elements defined as:

[5] $$(O_k)_{rc} = \langle\theta_r|\underline{O}_k|\theta_c\rangle$$

The density operator for our two-spin system is a linear combination of $\underline{O}_k$. Since operators $\underline{O}_k$ are orthonormal it can easily be shown that

[6] $$\underline{\sigma} = \sum^{16}_{k=1}\langle O_k\rangle\underline{O}_k$$

Thus $\underline{\sigma}$ is an element of a 16-dimensional space and the projections of $\underline{\sigma}$ on the axes $\underline{O}_k$ are directly proportional to $\langle O_k\rangle$, which are detected during time t_2.

The basic equation describing the time development of the density operator σ during any NMR experiment is:

[7] $d\underline{\sigma}/dt = (-i/\hbar)[\underline{H}\underline{\sigma}-\underline{\sigma}\underline{H}]=(-i/h)\underline{H}'\sigma$, where $\underline{H}'$ is a superoperator.

For the time independent Hamiltonian:

[8]

$$\underline{\sigma}(t) = \exp(-i\underline{H}'t/h)\underline{\sigma}(0)=\underline{\sigma}(0)+(-it/h)[\underline{H},\underline{\sigma}(0)]+(it/h)^2/2[\underline{H},[\underline{H},\underline{\sigma}(0)]]+\ldots$$

Assuming that $\underline{H} = \sum_p\underline{h}_p$, where all the $\underline{h}_p$ are mutually commuting

[9] $$\underline{\sigma}(t)=\Pi_p\exp(-i\underline{h}_pt/h)\sigma(0)$$

Since terms $\underline{h}_p$ are directly proportional to $\underline{O}_k$ operators one can rewrite equation 9 as

[10] $\underline{\sigma}(t)=\sum_k<O_k(t)>\underline{O}_k=\sum_j<O_j(0)>\Pi_p\exp(i\omega_p t\underline{O}'_p)\underline{O}_j$

Multiplication of both sides of this equation with $\underline{O}_l$ and calculation of a trace gives:

[11] $<O_l(t)> = \mathrm{Tr}\ \underline{O}_l[\sum_j<O_j(0)>\Pi_p\exp(i\omega_p t\underline{O}'_p)\underline{O}_j]$

Equation [11] allows one to evaluate $<O_l(t)>$ which is detected during the NMR experiment. To accomplish that task 256 possible terms [12] need to be evaluated (Banwell and Primas, 1963) :

[12] $\exp(i\theta\underline{O}'_p)\underline{O}_j$

Equation [12] may be simplified as follows:

[13] $\exp(i\theta\underline{O}'_p)\underline{O}_q = \underline{O}_q+i\theta[\underline{O}_p,\underline{O}_q]-(\theta^2/2)\underline{O}_q-i\theta^3/3![\underline{O}_p,\underline{O}_q]..+..=$

$= \underline{O}_q\cos(\theta)+i[\underline{O}_p,\underline{O}_q]\sin(\theta)$

Equation [13] allows for convenient evaluation of equation [11]; thus it is possible to describe the development of $<O_l(t)>$ at every moment during the NMR experiment.

Illustration of the above derived formalism of a multi-pulse experiment for Correlated Spectroscopy requires thermodynamic equilibrium conditions for a homonuclear system :

[14] $\underline{\sigma}(0) = (\underline{E}/4)+\beta(\underline{I}_z+\underline{S}_z)$, where $\beta = \gamma B_0/4kT$

At the end of the time interval (t_p) following a 90° rotation

[15] $\underline{\sigma}(t_1) = \exp(i\theta\underline{I}'_x)\exp(i\theta\underline{S}'_x)\underline{\sigma}(0)$

Combination of [13,14,15] gives (substituting $\pi/2$ as θ)

$$\underline{\sigma}(t_1) = I_0(\underline{I}_y+\underline{S}_y)$$

During the evolution period one needs to consider three rotations: a free precession caused by J-modulation (two spin system), as well as free precessions of spins I and S around the static longitudinal field (setting $J=2\pi J$):

[16] $\underline{\sigma}_I(t_1,t_2) = \exp(i\omega_I\underline{I}'_z t_1)\exp(i\omega_s\underline{S}'_z t_1)\exp(-iJ\underline{I}'_z\underline{S}'_z t_1)\underline{I}_y$

for spin I (an analogous equation can be written for a spin S). Application of equation [13] allows one to write eq. [16] in an analytical form:

[17] $\underline{\sigma}_I(t_1,t_2) = \cos(Jt_1/2)(\underline{I}_y\cos\omega_I t_1+\underline{I}_x\sin\omega_I t_1)-$
$\sin(Jt_1/2)(2\underline{I}_x\underline{S}_z\cos\omega_I t_1-2\underline{I}_y\underline{S}_z\sin\omega_I t_1)$

Combination of result [17] and an analogous one obtained for spin S gives a total density matrix at the evolution time period. It is important to note, without necessity to simplify further eq. [17] by means of eq. [13], that multiplication of both cos terms in eq. [17] gives a term related to the average value of the I spin operator:

[18] $\langle I_y \rangle \propto \cos(\omega_I t_1)\cos J t_1/2$

which rearranged gives [19]

[19] $\langle I_y \rangle \propto 1/2[\cos(\omega_I+J/2)t_1+\cos(\omega_I-J/2)t_1]$

Thus, a doublet at ω_I is expected (the same holds for ω_S, since application of a nonselective pulse allows permutation of the results). To consider development of the density matrix during the second nonselective 90° pulse, one may use the formalism developed by van de Ven and Hilbers (1983). Considering only those terms coming from the $\underline{I}_Y$ operator (for simplicity)-eq [17] -and utilizing eq [13] (equivalent to the approach of van de Ven and Hilbers) one can trace what happens with the $\underline{I}_X$, $\underline{I}_Y$, $\underline{I}_X\underline{S}_Z$, $\underline{I}_Y\underline{S}_Z$ operators:

[20a] $\underline{I}_Y$------ $-\underline{I}_Z$

the $\cos(\omega_I t_1)\cos(Jt_1/2)$ term is carried over from eq. [17]

[20b] $\underline{I}_X\underline{S}_Z$------ $\underline{I}_X\underline{S}_Y$

[20c] $\underline{I}_X$------ $\underline{I}_X$

the $\sin(\omega_I t_1)\cos(Jt_1/2)$ term is carried over from the first evolution period eq. [17]

[20d] $\underline{I}_Y\underline{S}_Z$------ $-\underline{I}_Z\underline{S}_Y$

the $\sin(\omega_I t_1)\sin(Jt_1/2)$ term is carried over from the first evolution period, eq.[17]

Thus, by the second pulse a single quantum coherence ($\Delta m_I = \pm 1$, $\Delta m_S = 0$) I_YS_Z is transferred into a single quantum coherence with $\Delta m_I = 0$, $\Delta m_S = \pm 1$ (I_ZS_Y). This step of coherence transfer via weakly coupled systems contains the essence of a COSY experiment.

The time dependence of the coherence in the last period t_2 (where they still evolve under the influence of static magnetic field as well as spins of the coupled partner) will be described with van de Ven and Hilbers formalism for only those coherences that will be detected as M_y magnetization.

[21a] $\underline{I}_X$------- $-\underline{I}_Y\cos(Jt_2/2)\sin(\omega_I t_2)$

the $\sin(\omega_I t_1)\cos(Jt_1/2)$ term is carried over from eq. [20c]

[21b] $-2\underline{I}_Z\underline{S}_Y$--- $-\underline{S}_Y\sin(Jt_2/2)\sin(\omega_I t_2)$

the $\sin(\omega_I t_1)\sin(Jt_1/2)$ term is carried over from eq. [20d]

The above considerations are valid not only for spin I, but also for spin S. Application of nonselective pulses in the pulse scheme allows one simple permutation of the spins to obtain an analogous solution for spin S. Thus, M_Y magnetization can be detected:

$$[22] \quad -M_Y = (\langle I_Y\rangle+\langle S_Y\rangle)=\cos(Jt_1/2)\cos(Jt_2/2)[\sin(\omega_I t_1)\sin(\omega_I t_2)+\sin(\omega_S t_1)\sin(\omega_S t_2)]+\sin(Jt_1/2)\sin(Jt_2/2)[\sin(\omega_I t_1)\sin(\omega_S t_2)+\sin(\omega_S t_1)\sin(\omega_I t_2)]$$

Equation [22] may be worked up to describe J-splitting; considering spin I and expanding two first terms of eq. [22] one obtains respectively:

$$[23] \quad (1/4)[\sin(\omega_I+J/2)t_1+\sin(\omega_I-J/2)t_1][\sin(\omega_I+J/2)t_2+\sin(\omega_I-J/2)t_2]$$

$$[24] \quad (1/4)[\cos(\omega_I-J/2)t_1-\cos(\omega_I+J/2)t1][\cos(\omega_S-J/2)t_2-\cos(\omega_S+J/2)t_2]$$

Equations [23] and [24] describe the FID detected during time t_2 that undergoes FT yielding a square with sides of length J, of four peaks situated around coordinates $(\omega_1,\omega_2)=(\omega_I,\omega_I)$-diagonal peaks (from eq. [23]), and four peaks centered around (ω_I,ω_S)-off diagonal peaks. These equations also show that there is a 90° phase-twist between the time-domain cross- and diagonal-peaks. This means that if the spectrum is phased to produce absorption lineshapes for the cross-peaks, the diagonal peaks will have dispersion lineshapes. The cross-peaks

originate, as it has already been mentioned, from the term $2I_YS_Z$ which is result of a J modulation during time t_1.

Phase sensitive spectroscopy.

A short account of the principles of phase sensitive spectroscopy will be presented here, as most COSY as well as NOESY (to be discussed in the next paragraph) experiments can be carried on in that mode. The advantage of using phase sensitive spectroscopy for COSY is related to the possibility of extracting coupling constants directly from the 2D spectrum. It has in practical form been realized by Kessler et al. (1985) in his DISCO technique. For a two spin system the total FID is described by equation [25]:

$$[25] \qquad FID = \exp(-i\omega_1 t_1 - t_1/T_2)\exp(-i\omega_2 t_2 - t_2/T_2)$$

Two dimensional Fourier transformation of the free induction decay results in a product of respective 1D decay functions. Thus:

$$[26] \qquad S(\omega_1,\omega_2)=[A(\omega_1)+iD(\omega_1)][A(\omega_2)+iD(\omega_2)]=$$
$$=(A_1A_2-D_1D_2) +i(A_1D_2+A_2D_1)$$

A and D represent well known Lorentzian lineshapes in the absorption and dispersion mode, respectively. It is clear therefore that the real part of the spectrum is not simply a purely positive product of absorption lineshapes in both dimensions, but the sum of a doubly ab-

sorptive and doubly dispersive term. The cross sections through the center of the peak are therefore simple Lorentzian absorption lineshapes, but as slices are taken further and further from the center the dispersive contributions grow (Figure 10). The "phase-twist" in a real phase modulated signal is a source of relatively low resolution of 2D spectra.

The presence of long dispersion tails makes it difficult to identify cross-peaks which lie in the vicinity of the diagonal. Furthermore, since they have alternating signs, the cross-peak multiplet components tend to cancel when incompletely resolved.

A solution of this problem has been proposed by Marion and Wuthrich (1983). By appropriate phase cycling of the pulses and the receiver it is possible in the phase sensitive experiment to construct two complementary pulses that will give the same modulation frequencies but with the opposite signs. Thus, addition of $F_-(t) \propto \exp(-i\omega t)$ and $F_+(t) \propto \exp(i\omega t)$ results in a $\cos(\omega t)$ function, which gives rise to pure absorption lineshapes.

Cross relaxation and chemical exchange.

For the previously discussed case of Correlation Spectroscopy J-connectivities could be made manifest for different spin-systems. It also is possible to detect cross-relaxation or chemical exchange by means of a 2D NMR experiment. Solomon (1955) showed that longitudinal relaxation of two interacting spins I and S can be described by the rate-equations:

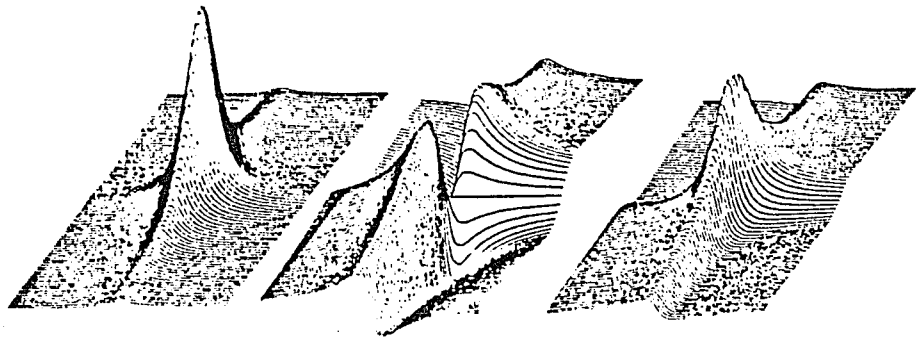

Figure 10. The normal lineshape resulting from the 2D FT of a phase modulated signal (right) is a combination of a double absorption (left) and double dispersion (middle). combination of a double absorption (left) and

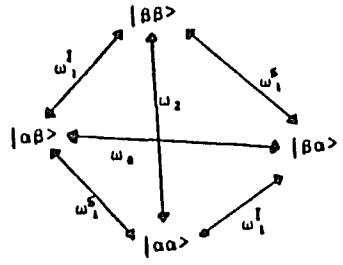

Figure 11. Definition of transition probabilities in double quantum NMR Spectroscopy.

[25] $d\langle I_Z\rangle/dt = -\lambda_I(\langle I_Z\rangle - I_0) - \eta_{SI}(\langle S_Z\rangle - S_0)$

[26] $d\langle S_Z\rangle/dt = -\lambda_S(\langle S_Z\rangle - S_0) - \eta_{IS}(\langle I_Z\rangle - I_0)$

where

[27] $\lambda_I = w_0 + 2w^I{}_1 + w_2 \qquad \lambda_S = w_0 + 2w^S{}_1 + w_2 \qquad \eta_{IS} = \eta_{SI} = w_2 - w_0$

Quantities w_0, $w^I{}_1$, $w^S{}_1$ and w_2 are transition probabilities per unit time between the eigenstates $|m_I, m_S\rangle$ (Figure 11).

The dipolar interaction between I and S is modulated by isotropic motion of the molecule:

[28] $w^I{}_1 = 1.5qJ(w_I) \quad w^S{}_1 = 1.5qJ(w_S) \quad w_0 = qJ(w_I - w_S)$

$w2 = 6qJ(w_I + w_S)$

where $J(w) = \tau_c/(1 + w^2\tau_c{}^2)$

q is a quantity proportional to $(r_{IS})^{-6}$

Thus detection of cross-relaxation rates may provide information about inter-nuclear distances. Employing double resonance methods, the longitudinal magnetization of one spin is perturbed and the effect of its relaxation is detected. A technique called NOESY (Nuclear Overhauser Effect) is the practical solution to a problem of cross-relaxation in a multispin systems. This technique utilizes the following pulse sequence: $90°\text{-}t_1\text{-}90°\text{-}\tau_{mix}\text{-}90°\text{-}t_2$. The first pulse creates transverse magnetization. During the evolution time t_1 each spin precesses with its characteristic Larmor frequency in the transverse plane. This process is described by similar density matrix evolution as for the initial phase of a COSY experiment. The second pulse converts transverse magnetization back to longitudinal magnetization. The amplitude of this longitudinal magnetization will be perturbed

differently by each spin system, depending on its Larmor precession frequency as well as on systematically varied t_1. During the mixing time cross-relaxation will be effective, depending on molecular motions (molecular tumbling as well as internal motions), and distances between relaxing spins. During this phenomenon a part of the intensity of one spin system is transferred to intensity of the other system. This magnetization (as well as all others) is then converted back to transverse magnetization by the third pulse and detected as an FID.

Experimental Methods In the Synthesis of Somatostatin Analogues.

Methods of peptide bond formation.

To date there exist over fifty methods of peptide bond formation. Some of relevance to this work will be discussed below.

The carbodiimide method was introduced by Sheehan and Hess (1955), with dicyclohexylcarbodiimide (DCC) and diisopropylcarbodiimide (DIC) currently being the most popular versions. A reaction scheme representing the basic chemistry of peptide synthesis is presented in Figure 12. The first stage of this reaction is an addition of the carboxyl group to the diimide and formation of an O-acyl lactim (derivative of an isourea); that is followed by transformation to a peptide derivative and N,N'-dicyclohexylurea (path A) or to the symmetric anhydride and N,N'-dicyclohexylurea (path B). The anhydride then undergoes aminolysis, with formation of peptide derivative and

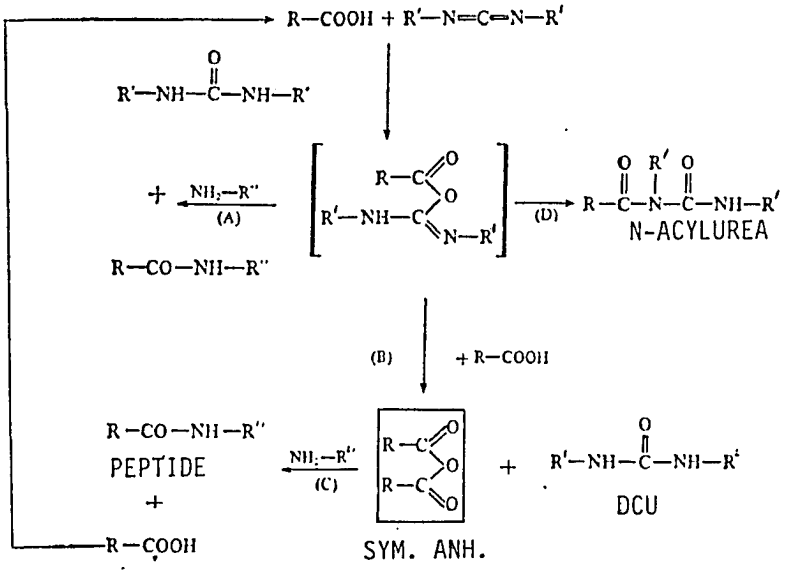

Figure 12. Mechanisms of peptide bond formation.

regeneration of 1M of acyl derivative (path C). An undesired side reaction is formation of the acylurea derivatives (path D) as a result of O-acylation transformation. The carbodiimide method is generally the fastest coupling method, though substantial racemization has been detected in several investigations. Thus, Weygand et al. (1968) found 12.5% D-Phe after a fragment coupling of Z-Leu-Phe-OH and Val-O-Bu^t in THF (20°C). Generally, use of the DCC method requires removal of the urea byproduct (DCU) by using an ethanol cycle in SPPS (solid phase peptide synthesis). This can be avoided by use of some of new generation diimides: DIC (DIU is soluble in DCM) and N-ethyl-N'-(-dimethyl-aminopropyl)carbodiimide are used mostly in solution methods of peptide synthesis, due to formation of a water soluble urea.

The active ester method allows us to suppress racemization, though a drawback may be its prolonged reaction time. Active esters are usually obtained by methods utilizing DCC or mixed anhydrides. At present, the most popular method involves use of HOBt (N-hydroxybenzotriazole) and HOSu (N-hydroxysuccinimide).

In 1965 two very interesting methods of peptide coupling were introduced. They utilize esters of N-hydroxypiperidine (Beaumont et al., 1965) and 8-hydroxyquinoline (Jakubke, 1965). Aminolysis of these esters is very fast and goes with activation of the carboxyl group and simultaneous extraction of the proton from the amino group of the nucleophile component of the reaction (Figure 13).

The azide method of peptide bond formation was introduced by Curtius (1902), and still remains a very attractive technique (racemization free) in solution PS. It is depicted in Figure 14.

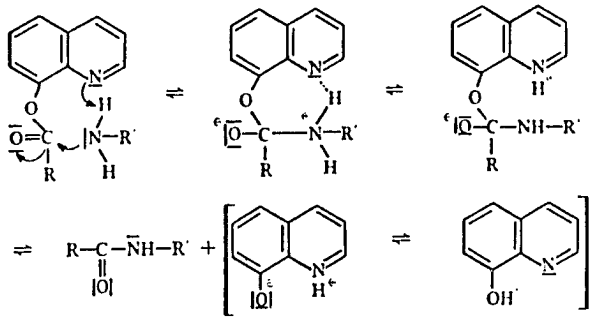

Figure 13. Peptide bond formation via 8-hydroxyquinoline active esters.

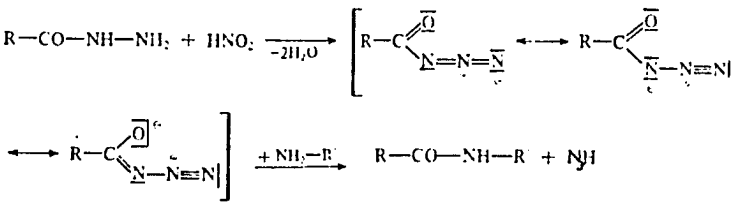

Figure 14. Principles of a racemization free method of peptide bond formation.

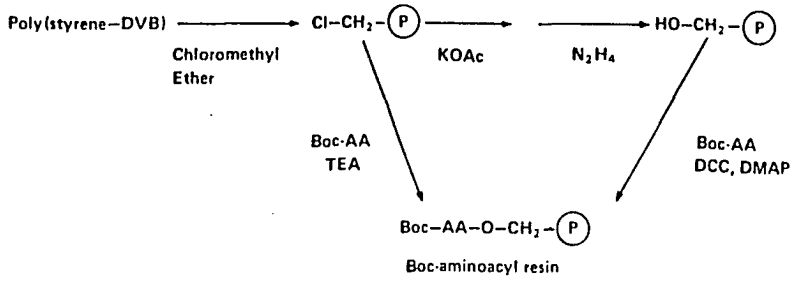

Figure 15. Attachment of the first amino acid to the resin.

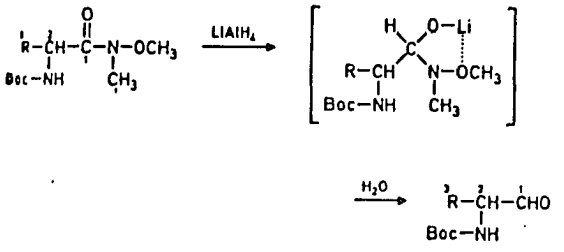

Figure 22. Reduction scheme for conversion of amides into aldehydes, according to Fehrentz and Castro (1983).

Protecting groups in peptide synthesis (orthogonal protection).

Table 2 lists all the protecting groups utilized in this work, with emphasis on their stability under different reaction conditions, as well as methods of their removal.

Polymeric support in a solid phase peptide synthesis.

Cross-linked polystyrene containing 1% of DVB (divinylbenzene) remains the most convenient solid phase in peptide synthesis. Functional groups are introduced into this polymer by chloromethylation, usually with methyl chloromethyl ether or formaldehyde and hydrochloric acid. The schemes for coupling of the first amino acid to such functionalized resin are presented in Figure 15. Amino acids which contain easily alkylated functional groups cause difficulty in the esterification reaction, due to the presence of active chloromethyl groups on the resin (path A). Such amino acids are histidine, cysteine and methionine. All these problems can be avoided by using a hydroxymethyl resin for attachment of the first amino acid (path B). The first Boc-amino acid may thus be added by means of DCC-mediated esterification. DMAP is a catalyst added to accelerate the reaction, though its excess may cause partial racemization of the amino acid. Unfortunately, the ester linking the peptide to the resin is slightly labile to the TFA used for deprotection (about 1% loss on each cycle). This loss may be of serious consequences in the synthesis of long sequences. Increased stability of this bond may be obtained by substitution of the resin with electron withdrawing groups.

Table 2. Protecting groups utilized in this work, their chemical stability and condition of removal.

Functional group	Protecting group	Reference
1. α-amino	t-butoxycarbonyl stable:H_2/Pd, Na/NH_3 cleaved: TFA, HCl	Merrifield, 1964 Voelter, 1980
2. δ-amino (Orn)	benzyloxycarbonyl stable: TFA (slow) cleaved: HF, Na/NH_3	Bergman and Zervas, 1932
3. ε-amino (Lys)	2-chlorobenzyloxycarbonyl stable: TFA cleaved: HF, Na/NH_3	
4. N^G-amino (Arg)	4-toluenesulfonyl (Tos) stable:TFA, HCl, HF (low HF procedure) cleaved:Na/NH_3, HF (high HF procedure)	Erickson and Merrifield, 1976 Rudinger, 1973 Steward and Young, 1984
5. β-hydroxyl (Thr, Ser)	benzyl (O-Bzl) stable:TFA, HCl cleaved: HF, Na/NH_3, H_2/Pd, HBr/TFA	
6. phenolic (Tyr)	2,6-dichlorobenzyl stable: TFA cleaved:HF	Erickson and Merrifield, 1973
7. Sulfhydryl (Cys, Pen)	4-methylbenzyl (S-4-MeBzl) stable:TFA cleaved: HF, Na/NH_3	

The Pam (p-acetamide) resin introduced by Mitchell et al. (1978) increases the stability of the peptide-resin link by a factor of 100 over that of the classical system. The two alternative schemes for Boc-Aminoacyl-Pam resin synthesis are shown in Figure 16.
Polyamide resins have solvating properties similar to those of a peptide chain. Thus, it was suggested by Atherton et al. (1978) that a single solvent might effectively solvate both the peptide and the carrier matrix, avoiding peptide chain collapse upon itself, which sometimes occurs for the Merrifield-type resin as a result of incompatibility between the natures of the growing peptide chain and the polystyrene resin. Three alternative methods of p-MBHA resin synthesis are presented in Figure 17. Path A has been employed in this work.

Coupling schemes.

A coupling scheme for a standard synthesis of peptides (analogues 1-22 and 25) is presented on Figure 18. A coupling problem quite commonly found in some of the syntheses appeared after the deprotection of Boc-Pen-(S-4-MeBzl)-AA-resin. In several cases the result of the ninhydrin test (even after repeated deprotection and neutralization) was negative. While the reasons for this synthetic problem are not known (they may be related to already discussed chain collapse for some sequences), it was found that initial swelling of the resin with TFA and consequent neutralization (steps 1 and 2, Figure 18) afforded trouble-free synthesis with yields of the final product about 30-50% higher than if step 1 was omitted in the coupling scheme.

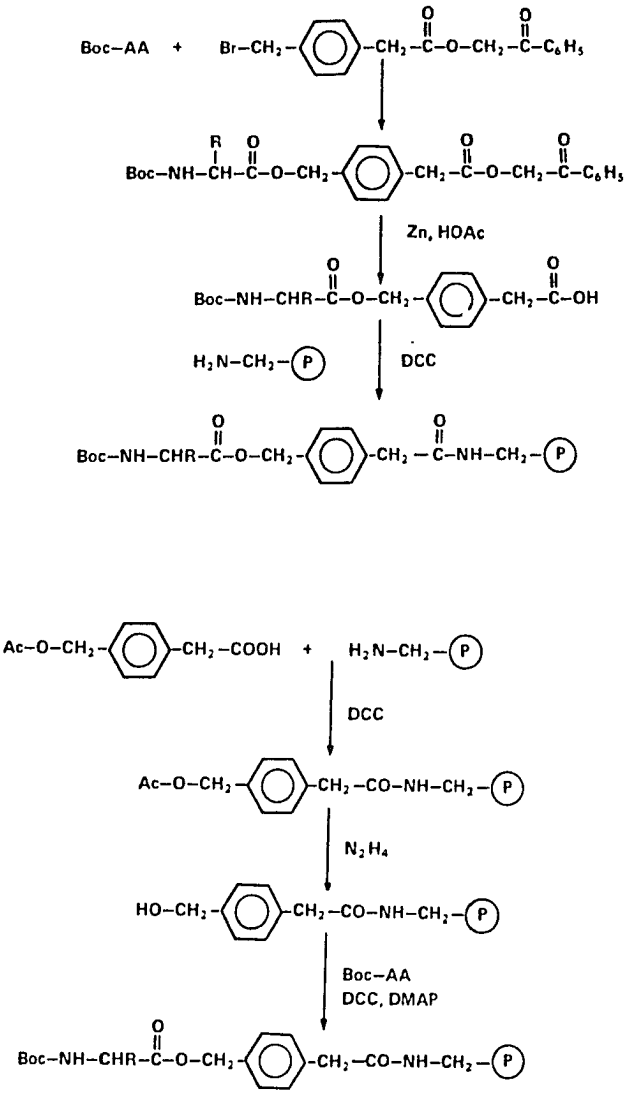

Figure 16. Two strategies of Pam resin synthesis by Merrifield (1978).

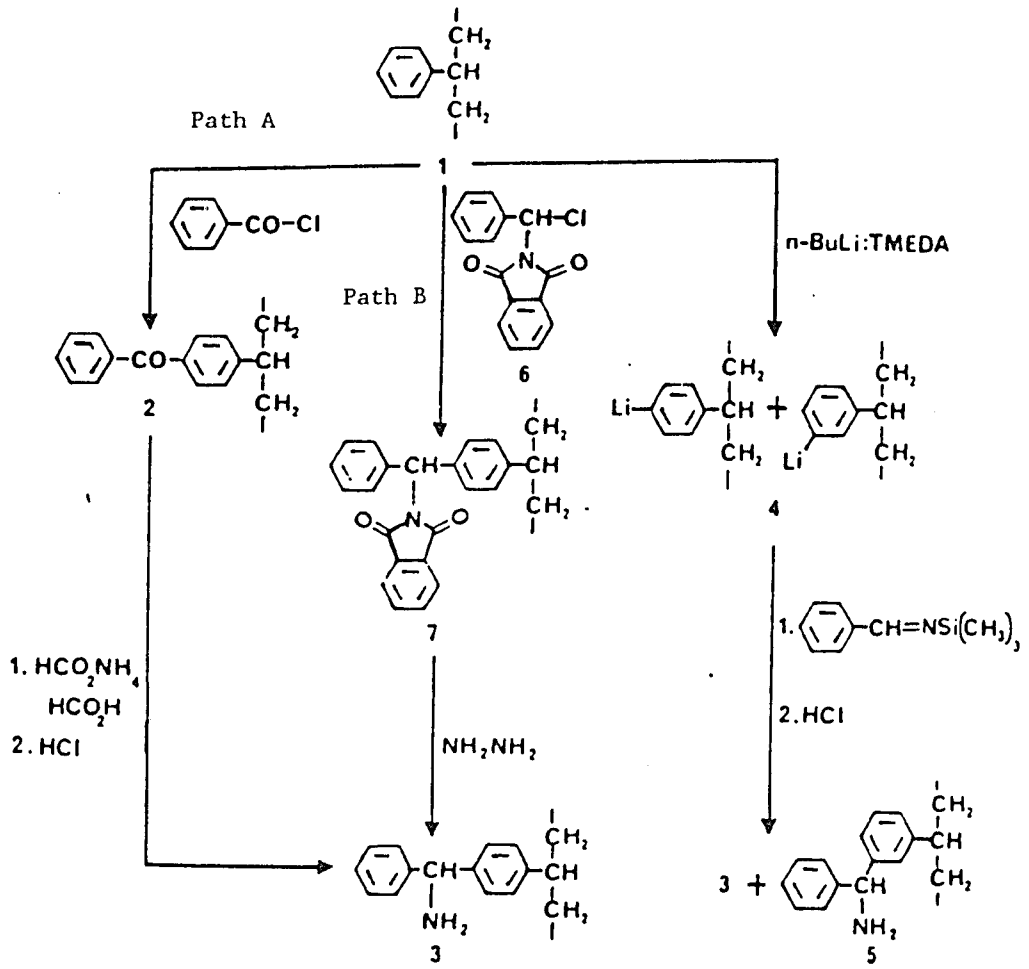

Figure 17. Two methodologies of p-MBHA resin synthesis; Path A (used in this work) by Orlowski et al., (1976), and Path B (Bryan, 1986).

Figure 18. Coupling scheme used for stepwise elongation of peptide chain, synthesis of peptides 1-22 and 25.

Description	solvent/reagent	repet.	time (min)
1. Swell the pMBHA resin in TFA	50% TFA, 2% anisole in DCM	1	20
2. Neutralize	10% DIEA in DCM	3	2
3. Wash	DCM	4	1
4. Free amino group monitoring	ninhydrin test		
5. Coupling	active ester or summ. anhydride of amino acid	1	30
6. Coupling anal.	ninh. test		
7. Wash	DCM	3	1
8. Acetylation of the free amino group (if free amino group)	AcIm, 10 fold excess	1	20
9. Wash	DCM	3	1
10. Deprotection	50% TFA, 2% anisole in DCM. If D-Trp, Tyr 20% Me_2S, 10% dithio-ethane added.	1 1	2 20
11. Wash	DCM	4	1
12. Neutralize	10% DIEA in DCM	3	2
13. Wash	DCM	3	1
14. Free amino group analysis	Ninhydrin or chloranil tests		
15. Go to step 5 and cycle.			

In the case of reductive alkylation (analogues 23, 24, 26, and 27) the only change in the coupling scheme (Figure 18) would involve step 5.

Ninhydrin-aided detection of the free amino group is based on oxidative deamination of amino acids (Figure 19).

General scheme of peptide synthesis and purification.

This scheme (Figure 20) is intended to be a guide, with numerous references to methodologies already mentioned in the text (e.g. Figure 18, Table 2), and others (related to peptide work-up, cyclization, purification, analysis, etc.) which will be discussed in the text to follow.

Experimental Section

General methods.

Syntheses of CTP (1), CTAP (2), and CTOP (3) were accomplished as previously reported (Pelton et al., 1985a; Pelton et al., 1986). Peptides 4-29 were also prepared (with the exception of dipeptide 28) by solid phase synthetic techniques (Upson and Hruby, 1976; Stewart and Young, 1984), using Vega (Tucson, Az) Model 250 and 1000 peptide synthesizers. Amino acids were either purchased from

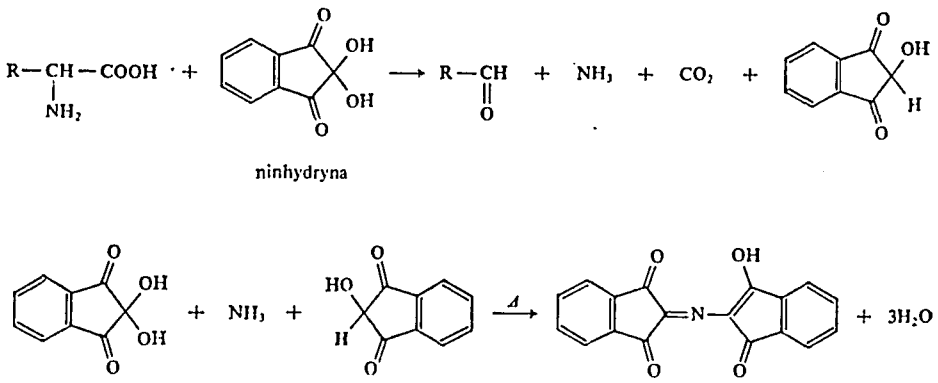

Figure 19. Chemical scheme for the ninhydrin based detection amino of the free amino group.

Figure 20. Scheme of synthesis and purification techniques applied for analogues 1-27, example of peptide 2.

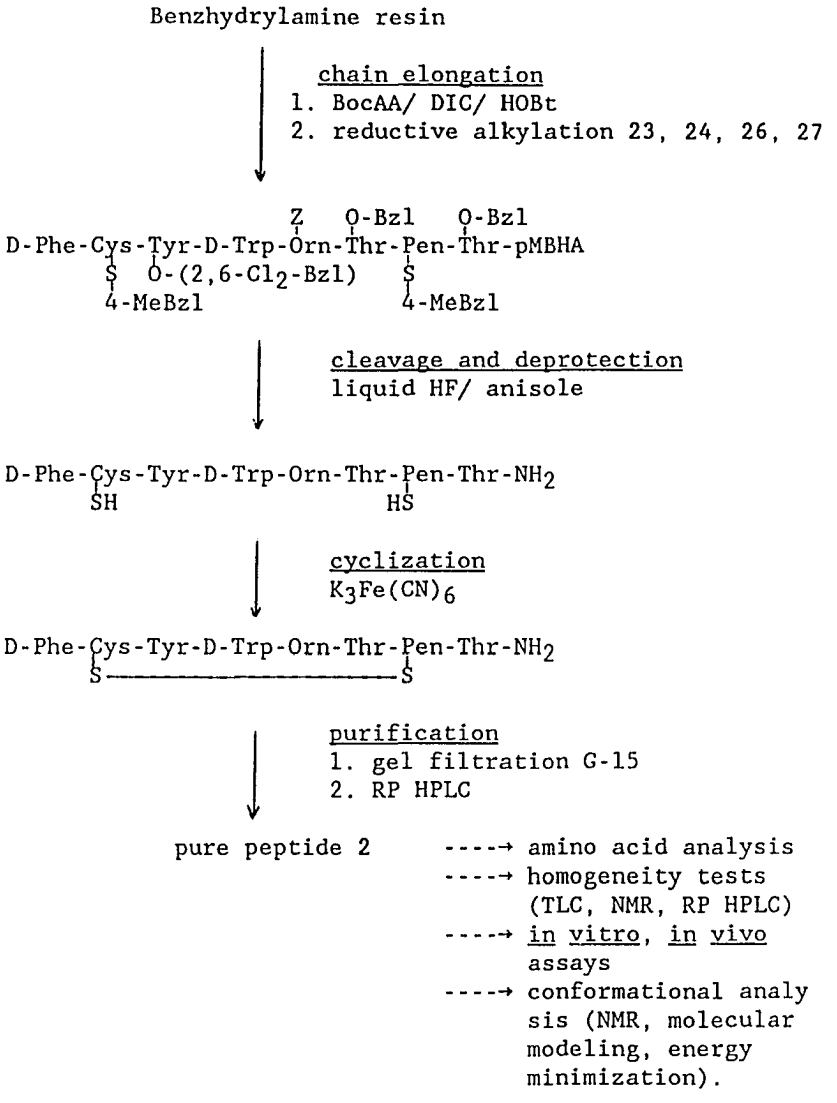

Bachem (Torrance, Ca) or were prepared by literature methods (Stewart and Young, 1984). Carboxamide peptides were synthesized using a p-methylbenzhydrylamine (pMBHA) resin which was prepared by literature methods (Orlowski et al., 1976); resin substitution was 1.0 mM/g. A 1.5 M excess of preformed symmetrical anhydrides or a 3M excess of hydroxybenzotriazole active esters was used for coupling reactions, which were monitored by ninhydrin (Kaiser et al., 1970) or chloranil tests (Christensen, 1979). Purity of the final peptide was assessed by TLC in four different solvents, HPLC, FAB-MS, amino acid analysis and ^{1}H NMR (Table 3). Capillary melting points were determined on a Thomas-Hoover apparatus and are uncorrected. Purity for each amino acid was established by the ninhydrin test, ^{1}H NMR, optical rotation (sodium D line, Rudolph Research Auto-Pol III polarimeter), and TLC. Purification of peptides was accomplished by a combination of gel filtration, partition chromatography and reversed phase high performance liquid chromatography. For most cases gel filtration (G-15) followed by RP HPLC were sufficient to obtain a peptide of high purity (>95%). Respective chromatograms for peptides 1 and 23 are shown on Figure 21. Gel filtrations were performed on a Sephadex G-15 (Pharmacia Fine Chemicals, Piscataway,NJ) column (2.65 x 75cm) applying a 5% solution of acetic acid isocratically, connected with a Buchler Monostatic Pump (20-30 ml/hr, over 20 hrs), Buchler Fracto-Scan (254 nm) and Buchler Automatic Fraction Collector. Preparative RP-HPLC was performed on a Perkin-Elmer Series 3B Liquid chromatograph equipped with an LC-75 Spectrophotometric Detector and

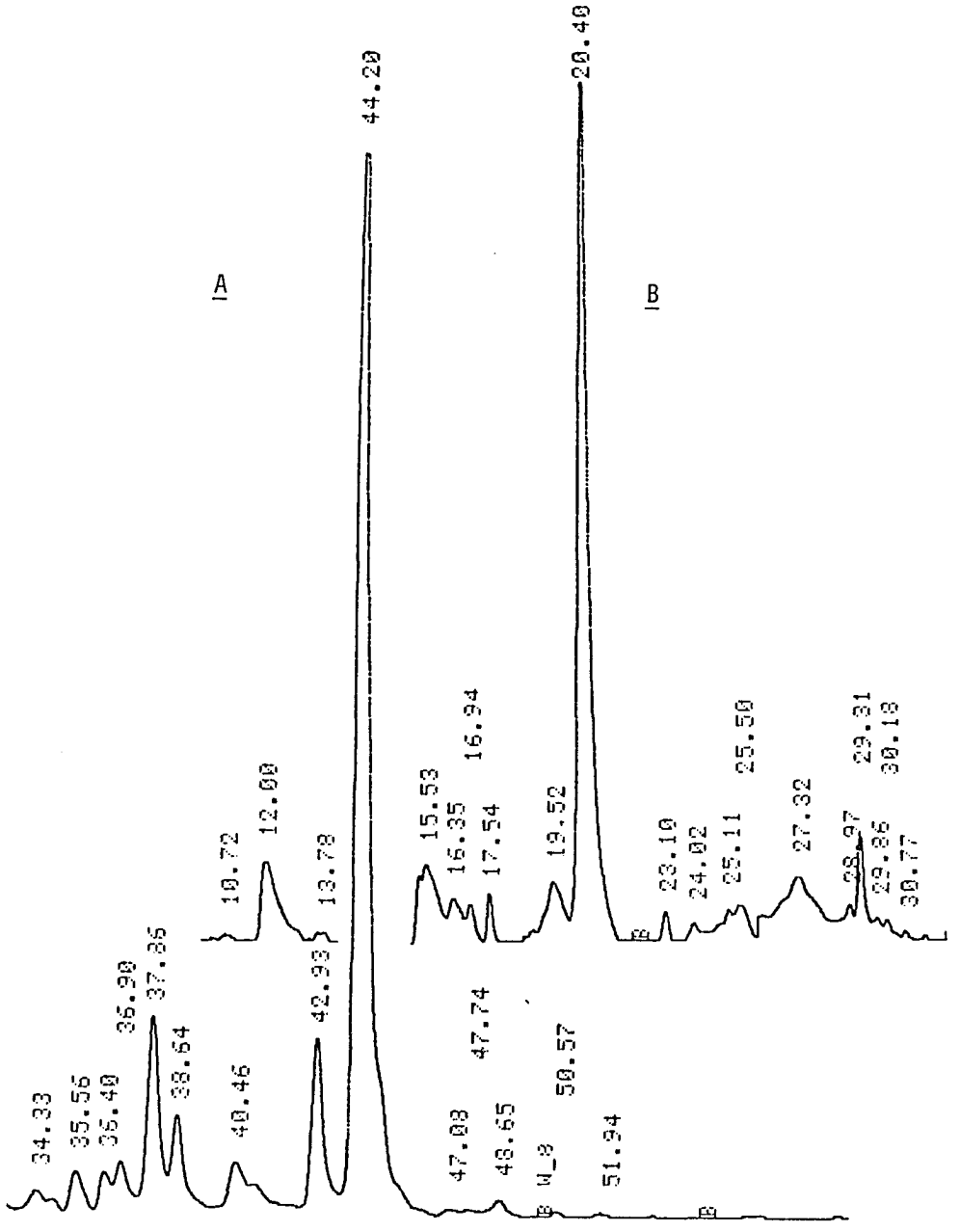

Figure 21. Typical RP HPLC chromatogram of crude (after cyclization) peptides 10 (A; 10-30%/60 min) and 23 (B; 10-40%/30 min.)

Table 3. Analytical Characterization of the Somatostatin Analogues Synthesized in This Work by HPLC, TLC and FAB MS.

Peptide	Thin-Layer Chromatography[a] R_f Values I	II	III	IV	HPLC[b] K' values	FAB-MS $[M+H]_{obs}$	$[M+H]_{cal}$
4.	0.47	0.72	0.79	0.75	0.0	775	775
5.	0.45	0.67	0.80	0.75	0.4	775	775
6.	0.63	0.79	0.84	0.81	1.7	949	949
7.	0.36	0.60	0.77	0.72	0.7	976	976
8.	0.45	0.68	0.77	0.74	4.8	1088	1088
9.	0.44	0.69	0.77	0.74	3.5	1075	1075
10.	0.47	0.58	0.78	0.75	4.8	1116	1116
11.	0.43	0.69	0.77	0.73	3.5	1077	1077
12.	0.38	0.68	0.74	0.71	3.2	1131	1131
13.	0.45	0.65	0.77	0.73	7.9	1115	1115
14.	0.37	0.64	0.76	0.73	1.5	988	988
15.	0.50	0.74	0.78	0.75	3.0	961	961
16.	0.36	0.68	0.72	0.73	2.9	976	976
17.	0.39	0.65	0.76	0.72	2.7	1090	1090
18.	0.37	0.66	0.71	0.67	1.8	1089	1089
19.	0.63	0.70	0.79	0.75	6.4	1086	1086
20.	0.44	0.66	0.77	0.74	3.2	1062	1062
21.	0.43	0.67	0.77	0.74	4.1	1075	1075
22.						1074	1074
23.						1048	1048
24.						1060	1060
25.						1058	1058
26.						1037*	1037
27.						1050*	1050
28.						638	638

* $[M+Li]$ recorded

[a]Silica gel GF 250 microns (Analtech) glass plates were used. The following solvent system has been applied: (I) n-BuOH/AcOH/H_2O, 4/1/5 (v/v); (II) iPrOH/NH_3/H_2O, 3/1/1 (v/v); (III) n-BuOH/AcOH/H_2O/Py, 6/1/5/6 (v/v); (IV) n-BuOH/AcOH/H_2O/Py 15:3/10/12 (v/v).

[b]Vydac 218 TP 104 C_{18} column (25 cm x 4.5 mm), 0.1%TFA/CH_3CN 80/20, flowrate 2.5 mL/min, monitored at λ = 214 nM

an LCI-100 Laboratory Computing Integrator, or on a Spectra-Physics Liquid Chromatograph equipped with a Spectra-Physics SP 8800 ternary pump, SP 8500 dynamic mixer, Spectroflow 757 Absorbance Detector and SP4270 Integrator. Fractions were monitored at 280 nm or 254 nm (if no Tyr residue was present). A Vydac C_{18} semi-preparative (10 mm, 10 mmx25 cm) column was used with either isocratic or linear gradient elution in a mobile phase of varying concentrations of acetonitrile in aqueous TFA (0.10%). Amino acid analyses were obtained as described by Spackman et al. (1958) on a Beckman Instruments Model 120C or Beckman 7300 amino acid analyzer, after acid hydrolysis in sealed tubes with 4 M methanesulfonic acid for 24 hrs. D-Trp, Cys, and Pen undergo oxidation under these conditions and are not detected. FAB-MS and NMR served for composition confirmation for these as well as other amino acids. In all cases when reporting the amino acid composition of a peptide, a value in a bracket refers to the theoretical number of residues of a given type in a molecule.

Reduced ring size peptides.

D-Tyr-Cys-Phe-Asn-Pen-Thr-NH_2, 4.

N-$^{\alpha}$-Boc-Thr(O-Bzl) was coupled to 0.5 mM of pMBHA resin using the active ester method, followed by deprotection using 50% TFA in dichloromethane (DCM) (2% anisole added) for 2 and 20 min. Stepwise coupling and deprotection of N^{α}-Boc-Cys(S-4-MeBzl), N^{α}-Boc-Asn, N^{α}-Boc-Phe, N^{α}-Boc-Cys(S-4-MeBzl) and N^{α}-Boc-D-Tyr(O-2,6-Cl_2-Bzl) was then accomplished by standard methods of solid phase synthesis. For N^{α}-Boc-Asn coupling an active ester derivative was chosen to avoid nitrile formation. After coupling of the last amino acid, the N^{α}-Boc

protecting group was removed, the amino group neutralized with diisopropylethylamine and the resulting D-Tyr(O-2,6-Cl_2-Bzl)-Cys(S-4-MeBzl)-Phe-Asn-Pen(S-4-MeBzl)-Thr(O-Bzl)-resin was dried in vacuo. Cleavage of all side protecting groups as well as peptide from the resin was achieved with liquid HF (approx. 15 ml) with addition of 1 ml anisole, at 0°C. The product was washed with ethyl ether (3x20 ml), extracted with 10% aqueous HOAc (3x20 ml) followed by glacial HOAc (2x20 min); both fractions were lyophilized separately. Next the linear peptide was cyclized by dissolving in 1.5 l of water (pH adjusted with aqueous ammonia to 8.5), oxidized with 0.01 N $K_3Fe(CN)_6$ until the yellow color persisted for 1 hr. After the reaction was terminated, the pH was adjusted to 4.5 with AcOH, excess ferro- and ferricyanides were removed by 15 ml of Amberlite IRA-45 (mesh 15-60, Cl^-form), the mixture was stirred for 1 hr., filtered, and the solution concentrated in vacuo and lyophilized. Gel filtration on 100 x 2.5 cm Sephadex G-15 with 5% (v/v) aqueous HOAc was generally applied. Final purification was achieved by RP-HPLC using a gradient of acetonitrile and 0.1% TFA. the total yield of 4 was 12%. Amino acid analysis : Asn 0.95 (1.0), Thr 0.98 (1.0), D-Tyr 0.98 (1.0), Phe 1.03 (1.0). The structure was also confirmed by ^1H NMR assignments. Integration: D-Tyr(Ar, 4 H, 1.0), Cys(α) 0.97 H (1.00), Pen (α) 0.98 H, (1.0). The TLC, analytical HPLC and FAB-MS data are given in Table 3.

D-Phe-Cys-Tyr-Asn-Pen-Thr-NH_2, 5.

The protected peptide resin of 5 was prepared by sequential coupling of N^{α}-Boc-Pen(S-4-MeBzl), N^{α}-Boc-Asn, N^{α}-Boc-Tyr(O-2,6-Cl_2-Bzl), N^{α}-Boc-Cys(S-4-MeBzl), and N^{α}-D-Phe to Thr(O-Bzl)-pMBHA, resulting in D-Phe-Cys(S-4-MeBzl)-Tyr(O-2,6-Cl_2-Bzl)-Asn-Pen(S-4-MeBzl)-Thr(O-Bzl)-resin. The workup was identical to that described for 4. The yield was 13%. Amino acids analysis: D-Phe 0.98 (1.0), Tyr 0.97 (1.0), Asn 1.01 (1.0), Thr 0.98 (1.0). Additionally, a ^{1}H NMR spectrum confirmed the amino acid constitution and relative abundance: Tyr(Ar), 4 H (1.0), Cys(α) 0.98 H (1.0), Pen(γ) 6.3 H (1.0). The TLC, HPLC, FAB-MS data are presented in Table 3.

D-Phe-Cys-Tyr-D-Trp-Thr-D-Pen-Thr-NH_2, 6.

The protected peptide resin D-Phe-Cys(S-4-MeBzl)-Tyr(O-2,6-Cl_2-Bzl)-D-Trp-Thr(O-Bzl)-D-Pen(S-4-MeBzl)-Thr(O-Bzl)-resin was obtained by sequential coupling of the constituent amino acids to pMBHA resin. The workup was identical to that described for 4. The yield was 16%. Amino acids analysis: D-Phe 0.98 (1.0), Tyr 1.01 (1.0), Thr 1.91 (2.0). Additionally, a ^{1}H NMR spectrum confirmed the amino acid constitution and relative abundance: Tyr(Ar), 4 H (1.0), Cys(α) 1.10 H (1.0), Pen(α) 1.1 H (1.0), D-Trp(C5H) 0.98 H (1.0). The TLC, HPLC, FAB-MS data are presented in Table 3.

D-Phe-Cys-Tyr-D-Trp-Lys-D-Pen-Thr-NH_2, 7.

The same scheme was applied, except that N^{α}-Boc-Lys(N^{ϵ}-2-ClZ) was coupled instead of N^{α}-Boc-Thr(O-Bzl) in the 5 position, resulting in D-Phe-Cys(S-4-MeBzl)-Tyr(O-2,6-Cl_2-Bzl)-D-Trp-Lys(N^{ϵ}-2-ClZ)-Pen(S-4-

MeBzl)-Thr(O-Bzl)-resin. The workup was identical to that described for 4. The yield was 16%. Amino acids analysis: D-Phe 0.98 (1.0), Tyr 0.98 (1.0), Thr 1.05. (1.0), Lys 1.05 (1.0). Additionally, a ^1H NMR spectrum confirmed the amino acid constitution and relative abundance: Tyr(Ar), 4 H (1.0), Cys(α) 0.97 H (1.0), Pen(α) 0.99 H (1.0), D-Trp(C4H) 1.00 H (1.0). The TLC, HPLC, FAB-MS data are presented in Table 3.

N- and C-Terminal Modified Peptides.

D-Tic-Cys-Tyr-D-Trp-Lys-Thr-Pen-Thr-NH_2, TCTP, 8. D-1,2,3,4-tetrahydroisoquinoline-3-carboxylic acid (D-Tic) was prepared by condensation of D-Phe and formaldehyde (Pictet and Spengler, 1911), with a yield of 78.5%, m.p. = 309-311°C (uncorrected). ^{13}C NMR (250 MHz, D_2O+HCl, BB dec.): 183.47 (CO), 137.2 (Ar), 136.86 (Ar), 131.84 (Ar), 129.1 (Ar), 129.0 (Ar), 128.8 (Ar), 60.22 (α), 48.99 (N-CH_2), 34.27 (β). N^{α}-Boc-D-Tic was prepared by a standard α-amino acid protection scheme (Stewart and Young, 1984) in a yield of 63.2%, m.p. = 121-122°C, $[\alpha]^{25}_D$ = -18.1 (c=1.0, CH_3OH. ^1H NMR (250 MHz, d_6-DMSO): 19.0 (br, acid), 7.13 (m, 4H, Ar.), 4.84 (m, .5H, CH_{α}), 4.50 (m,2.5H, 0.5H + N-CH_2), 3.10 (m, 2H, CH_{β}), 1.39 and 1.46 (s+s, 9H, t-Bu). TLC of N^{α}-Boc-D-Tic R_f=0.83 (AcOH/nBuOH/Py/H_2O, 20/10/3/5. Baker Silica Gel Plates); R_f=0.64 ($CHCl_3$/MeOH/AcOH, 94/4/2, Baker Silica Gel Plates). Subsequent coupling and deprotecting of N^{α}-Boc-Thr(O-Bzl), N^{α}-Boc-Pen(S-4-MeBzl), N^{α}-Boc-Thr(O-Bzl), N^{α}-Boc-Lys(N^{ϵ}-2-ClZ), N^{α}-Boc-D-Trp, N^{α}-Boc-Tyr(O-2,6-Cl_2-Bzl), N^{α}-Boc-Cys(S-4-MeBzl), and N^{α}-Boc-D-Tic gave D-Tic-Cys(S-4-MeBzl)-Tyr(O-2,6-Cl_2-Bzl)-D-Trp-Lys(N^{ϵ}-ClZ)-Thr(O-Bzl)-Pen(S-4-MeBzl)-Thr(O-Bzl)-resin. The workup was

identical to that described for 4. The yield was 15%. Amino acids analysis; Tyr 1.0 (1.0), Thr 1.92 (2.0), Lys 1.00 (1.0). Additionally, a ^1H NMR spectrum confirmed the amino acid constitution and relative abundance (Kazmierski and Hruby, 1988): Tyr(Ar), 4H (1.0), Cys(α) 1.06 H (1.0), Pen(α) 1.08 H (1.0), D-Tic(β-CH_2) 2.13 H (1.00). The TLC, HPLC, FAB-MS data are presented in Table 3.

D-Tic-Cys-Tyr-D-Trp-Orn-Thr-Pen-Thr-NH_2, TCTOP, 9.

The title compound was synthesized in analogy to TCTP (8), except that N^{α}-Boc-Orn(Z) was used instead of N^{α}-Boc-Lys(N^{ϵ}-2-Cl-Z) in the coupling scheme to give D-Tic-Cys(S-4-MeBzl)-Tyr(O-2,6-Cl_2-Bzl)-D-Trp-Orn(Z)-Thr(O-Bzl)-Pen(S-4-MeBzl)-Thr(O-Bzl)-resin. The workup was identical to that described for 4. The yield was 13%. Amino acids analysis: Tyr 1.05 (1.0), Thr 1.93 (2.0), Orn .93 (1.0). Additionally, a ^1H NMR spectrum confirmed the amino acid constitution and relative abundance: Tyr(Ar), 4.00 H (1.0), D-Trp(Ar, C4H) .97 (1.00), Cys(α) 1.03 H (1.0), Pen(α) 1.08 H (1.0), D-Tic (β-CH_2) 2.16 H (1.00) . The TLC, HPLC, FAB-MS data are presented in Table 3.

D-Tic-Cys-Tyr-D-Trp-Arg-Thr-Pen-Thr-NH_2, TCTAP, 10.

The title compound was prepared the same way as TCTP (8) was, except that N^{α}-Boc-Arg(N^{G}-Tos) was coupled instead of N^{α}-Boc-Lys(N^{ϵ}-2-ClZ) in the coupling scheme to give D-Tic-Cys(S-4-MeBzl)-Tyr(O-2,6-Cl_2-Bzl)-D-Trp-Arg(N^{G}-Tos)-Thr(O-Bzl)-Pen(S-4-MeBzl)-Thr(O-Bzl)-resin. The workup was identical to that described for 4. The yield was 13%. Amino acids analysis: Tyr 1.02 (1.0), Thr 1.90 (2.0), Arg .96 (1.0).

Additionally, a ^1H NMR spectrum confirmed the amino acid constitution and relative abundance: Tyr(Ar) 4.00H (1.0), Cys(α) 1.03H (1.0), Pen(α) 1.10H (1.0), D-Trp(Ar, C4H) 1.12H (1.00), D-Tic(β-CH_2) 2.08H (1.00). The TLC, HPLC, FAB-MS data are presented in Table 3.

D-N-Me-Phe-Cys-Tyr-D-Trp-Orn-Thr-Pen-Thr-NH_2, 11.

N^{α}-Boc-D-N-Me-Phe was synthesized as previously described (Mc Dermott and Benoiton, 1973). The title peptide was synthesized the same way as TCTOP (9), except that N^{α}-Boc-D-N-Me-Phe was used instead of N^{α}-Boc - D-Tic in the coupling scheme. The workup was identical to that described for 4. The yield was 18%. Amino acids analysis: Tyr .99 (1.0), Orn 1.00 (1.0), Thr 1.98 (2.0). Additionally, a ^1H NMR spectrum (Kazmierski and Hruby, 1988) confirmed the amino acid constitution and relative abundance: Tyr(Ar), 4.00H (1.0), Cys(α) 1.00H (1.0), D-Trp(Ar, C4H) .98H (1.00), Pen(α) 1.00H (1.0), D-N-Me-Phe(α) 1.00H (1.00). The TLC, HPLC, FAB-MS data are presented in Table 3.

Gly-D-Tic-Cys-Tyr-D-Trp-Orn-Thr-Pen-Thr-NH_2,12.

The title compound 12 was obtained in a manner analogous to TCTOP (9), except that after coupling of N^{α}-Boc-D-Tic and deprotection, N^{α}-Boc-Gly was coupled and deprotected. The completion of this reaction was monitored by the chloranil test (Christensen, 1979). The protected Gly-D-Tic-Cys(S-4-MeBzl)-Tyr(O-2,6-Cl_2-Bzl)-D-Trp-Orn(Z)-Thr(O-Bzl)-Pen(S-4-MeBzl)-Thr(O-Bzl)-resin was worked up as 4. The yield was 11%. Amino acids analysis: Tyr 0.96 (1.0), Thr 1.98 (2.0), Orn 1.04

(1.0), Gly 1.01 (1.00). Additionally, a ^{1}H NMR spectrum confirmed the amino acid constitution and relative abundance (Kazmierski and Hruby, 1988): Tyr(Ar) 4.00 H (1.0), Cys(α) 1.00 H (1.0), Pen(α) 1.03 H (1.0), D-Trp(C4H) 0.98 H (1.00). The TLC, HPLC, FAB-MS data are presented in Table 3.

D-Trp-Cys-Tyr-D-Trp-Lys-Thr-Pen-Thr-NH_2, 13.

The title compound was synthesized in a manner analogous to 8, except that N^{α}-Boc-D-Trp was used instead of N^{a}-Boc-D-Tic in the coupling scheme, giving D-Trp-Cys(S-4-MeBzl)-Tyr(O-2,6-Cl_2-Bzl)-D-Trp-Lys(N^{ϵ}-2-ClZ)-Thr(O-Bzl)-Pen(S-4-MeBzl)-Thr(O-Bzl)-resin. The workup was identical to that described for 4. The yield was 13%. Amino acids analysis: Tyr 0.97 (1.0), Thr 1.95 (2.0), Lys 1.03 (1.0). Additionally, a ^{1}H NMR spectrum confirmed the amino acid constitution and relative abundance: Tyr(Ar), 4.00H (1.0), Cys(α) 0.94 H (1.0), Pen(α) 1.03 H (1.0). The TLC, HPLC, FAB-MS data are presented in Table 3.

D-Tic-Cys-Tyr-D-Trp-Lys-Pen-Thr-NH_2, 14.

The title compound was synthesized similarly to TCTP 8, except that N^{α}-Boc-Lys(N^{ϵ}-2-ClZ) was coupled to Pen(S-4-MeBzl)-Thr(O-Bzl)-resin, without coupling of N^{α}-Boc-Thr(O-Bzl). The obtained D-Tic-Cys(S-4-MeBzl)-Tyr(O-2,6-Cl_2-Bzl)-D-Trp-Lys(N^{ϵ}-2-ClZ)-Pen(S-4-MeBzl)-Thr(O-Bzl)-resin was worked up as described for 4. The yield was 13%. Amino acids analysis: Tyr 1.03 (1.0), Thr 0.93 (1.0), Lys 1.01 (1.0). Additionally, a ^{1}H NMR spectrum confirmed the amino acid constitution and relative abundance: Tyr(Ar), 4.00 H (1.0), Cys(α) 1.03 H (1.0),

Pen(α) 1.05 H (1.0), D-Tic(Ar) 4.20 H (1.0). The TLC, HPLC, FAB-MS data are presented in Table 3.

D-Phe-Cys-Tyr-D-Trp-Orn-Thr-Pen-NH_2, 15.

D-Phe-Cys(S-4-MeBzl)-Tyr(O-2,6-Cl_2-Bzl)-D-Trp-Orn(Z)-Thr(O-Bzl)-Pen(S-4-MeBzl)-resin was obtained by a similar coupling scheme as for TCTOP,9, except that N^{α}-Boc-D-Phe was used instead of N-Boc-D-Tic, and N^{α}-Boc-Pen(S-4-MeBzl) was directly coupled to the resin. The workup was identical to that described for 4. The yield was 14.8%. Amino acids analysis: D-Phe 0.99 (1.0), Tyr 0.99 (1.0), Thr 0.95 (1.0), Orn 1.01 (1.0). Additionally, a ^1H NMR spectrum confirmed the amino acid constitution and relative abundance: Tyr(Ar), 4.00 H (1.0), Cys(α) .98 H (1.0), Pen(α) 1.00 H (1.0), D-Trp(C4H) .93 H (1.0). The TLC, HPLC, FAB-MS data are presented in Table 3.

D-Phe-Cys-Tyr-D-Trp-Lys-Thr-Pen-NH_2, 16.

This peptide was synthesized as was 15, except that N^{α}-Boc-Lys(N^{ϵ}-2-ClZ) was used instead of N^{α}-Boc-Orn(Z) in the coupling scheme, giving D-Phe-Cys(S-4-MeBzl)-Tyr(O-2,6-Cl_2-Bzl)-D-Trp-Lys(N^{ϵ}-2-ClZ)-Thr(O-Bzl)-Pen(S-4-MeBzl)-resin. The workup was identical to that described for 4. The yield was 16.3%. Amino acids analysis: D-Phe 0.98 (1.0), Tyr 1.02 (1.0), Thr 0.95 (1.0), Lys 1.05 (1.0). Additionally, a ^1H NMR spectrum confirmed the amino acid constitution and relative abundance: Tyr(Ar), 4.00 H (1.0), Cys(α) 0.97 H (1.0), Pen(γ) 6.4 H (1.0). D-

Trp(C4H) 0.94 H (1.00). The TLC, HPLC, FAB-MS data are presented in Table 3.

D-Phe-Cys-Tyr-D-Trp-Lys-Thr-Pen-Asn-NH_2, 17.

The title compound was synthesized similarly to the synthetic scheme used for 1, except that N^{α}-Boc-Asn was coupled to the resin instead of N^{α}-Boc-Thr(O-Bzl), giving D-Phe-Cys(S-4-MeBzl)-Tyr(O-2,6-Cl_2-Bzl)-D-Trp-Lys(N^{ϵ}-2-Clz)-Thr(O-Bzl)-Pen(S-4-MeBzl)-Asn-resin. The workup was identical to that described for 4. The yield was 13%. Amino acids analysis: D-Phe 1.00 (1.0), Tyr 1.02 (1.0), Asn 1.02 (1.0), Thr 0.99 (1.0), Lys 1.02 (1.0). Additionally, a ^{1}H NMR spectrum confirmed the amino acid constitution and relative abundance: Tyr(Ar) 4.00 H (1.0), Cys(α) 1.00 H (1.0), Pen(γ) 6.00 H (1.0), D-Trp(Ar, C4H) 0.99H (1.0), Thr(γ) 3.1H (1.00). The TLC, HPLC, FAB-MS data are presented in Table 3.

D-Phe-Cys-Tyr-D-Trp-Lys-Thr-Pen-Asp-NH_2, 18.

This peptide was synthesized according to the synthetic scheme for 17, except that N^{α}-Boc-Asp(β-Bzl) was used instead of N^{α}-Boc-Asn, giving D-Phe-Cys(S-4-MeBzl)-Tyr(O-2,6-Cl_2-Bzl)-D-Trp-Lys(N^{ϵ}-2-ClZ)-Thr(O-Bzl)-Pen(S-4-MeBzl)-Asp-resin. The workup was identical to that described for 4. The yield was 13.4%. Amino acids analysis: D-Phe 1.00 (1.0), Tyr 1.01 (1.0), Asp 1.01 (1.0), Thr 0.95 (1.0), Lys 0.99 (1.0). Additionally, a ^{1}H NMR spectrum confirmed the amino acid constitution and relative abundance: Tyr(Ar) 4.00 H (1.0), Cys(α) 0.95 H (1.0), Pen(α) 1.08 H (1.0), D-Trp(Ar) 5.30 H (1.0). The TLC, HPLC, FAB-MS data are presented in Table 3.

D-Tic-Cys-Tyr-D-Trp-Lys-Thr-Pen-Val-NH_2, 19.

The title peptide was synthesized as was TCTP (8), except that N^{α}-Boc-Val was coupled to the resin instead of N^{α}-Boc-Thr(O-Bzl), yielding D-Tic-Cys(S-4-MeBzl)-Tyr(O-2,6-Cl_2-Bzl)-D-Trp-Lys(N^{ϵ}-2-ClZ)-Thr(O-Bzl)-Pen(S-4-MeBzl)-Val-resin. The workup was identical to that described for 4. The yield was 12.7%. Amino acids analysis: Tyr 0.97 (1.0), Val 0.98 (1.0), Thr 0.92 (1.0), Lys 1.06 (1.0). Additionally, a ^1H NMR spectrum confirmed the amino acid constitution and relative abundance: Tyr(Ar) 4.00 H (1.0), D-Tic(β-CH_2) 2.09 H (1.00), Cys(α) 0.97 H (1.0), Pen(α) 0.95 H (1.0). The TLC, HPLC, FAB-MS data are presented in Table 3.

D-Phe-Cys-Tyr-D-Trp-Lys-Thr-Pen-Ser-NH_2, 20.

The title peptide 20 was synthesized like 17, except that N^{α}-Boc-Ser(O-Bzl) was used instead of N^{α}-Boc-Asn in the coupling scheme, giving D-Phe-Cys(S-4-MeBzl)-Tyr(O-2,6-Cl_2-Bzl)-D-Trp-Lys(N^{ϵ}-2-ClZ)-Thr(O-Bzl)-Pen(S-4-MeBzl)-Ser(O-Bzl)-resin. The workup was identical to that described for 4. The yield was 16.3%. Amino acids analysis: D-Phe 0.98 (1.0), Tyr 1.04 (1.0), Ser 0.95 (1.0), Thr 0.94 (1.0), Lys 1.02 (1.0). Additionally, a ^1H NMR spectrum confirmed the amino acid constitution and relative abundance: Tyr(Ar) 4.00 H (1.0), Cys(α) 0.97 H (1.0), Pen(α) 0.97 H (1.0), D-Trp(Ar) 0.97H (1.0). The TLC, HPLC, FAB-MS data are presented in Table 3.

D-Tic-Cys-Tyr-D-Trp-Lys-Thr-Pen-Ser-NH_2, 21.

This peptide was synthesized similarly to **19**, except that N^{α}-Boc-Ser(O-Bzl) was coupled to the resin instead of N^{α}-Boc-Thr(O-Bzl), giving D-Tic-Cys(S-4-MeBzl)-Tyr(O-2,6-Cl_2-Bzl)-D-Trp-Orn(Z)-Thr(O-Bzl)-Pen(S-4-MeBzl)-Ser(O-Bzl)-resin. The workup was identical to that described for 4. The yield was 14.8%. Amino acids analysis: Tyr 1.00 (1.0), Ser 0.95 (1.0), Thr 0.95 (1.0), Lys 1.08 (1.0). Additionally, a ^1H NMR spectrum confirmed the amino acid constitution and relative abundance: Tyr(Ar) 4.00 H (1.0), Cys(α) 0.92 H (1.0), Pen(α) 0.94 H (1.0), D-Trp(C4H) 0.97 H (1.0). The TLC, HPLC, FAB-MS data are presented in Table 3.

Synthesis of alkylamino peptide bond isosteres.

D-Phe-Cys-$\overline{\text{Tyr-D-Tca-Orn-Thr-Pen}}$-Thr-$NH_2$, 22.

The title peptide was synthesized like 2, except that N^{α}-Boc-D-Tca was coupled to the appropriate peptide resin fragment (H)-Orn(Z)-Thr(O-2,6-Cl_2Bzl)-Pen(S-4-MeBzl)-Thr(O-2,6-Cl_2-Bzl)-resin , yielding Boc-D-Phe-Cys(S-4-MeBzl)-Tyr(O-2,6-Cl_2-Bzl)-D-Tca-Orn(Z)-Thr(O-Bzl)-Pen(S-4-MeBzl)-Thr(O-Bzl)-resin. Workup as for 4 gave the title compound 22 with the yield 23%. The structure of peptide 22 was confirmed by ^1H NMR analysis (vide infra). D-Tca (1,2,3,4-tetrahydro-β-carboline, Figure 9) was synthesized by described methods (Harvey et al., 1941). D-Trp 45g (242 mM; Sigma, 115F-0603) was suspended in 89 ml of distilled water. 9.77g (245 mM) of NaOH was added, the temperature brought up to 37°C, and the mixture stirred until D-Trp was dissolved. Then 22g of 37% formaldehyde was added, and the reaction proceeded for 3 hrs. Unlike in the original procedure (Harvey et al., 1941), nitrogen was passed through the reaction medium to prevent the

oxidation of D-Trp. The reaction was terminated and the product precipitated with a stoichiometric amount of 6N HCl (final pH was 3). The final precipitate was slightly yellow, brown if carried out under original conditions. The fine precipitate was left overnight in the refrigerator, filtered, suspended in 3/2 (v/v) EtOH/water (400 ml), and refluxed for 30 min. The suspension was filtered off, washed and dried in vacuo. Yield 88.5%.

^{13}C NMR (250 MHz, D_2O+HCl): 173.80 (CO), 139.2 (Ar), 128.2 (Ar), 127.7 (Ar), 122.47 (Ar), 120.5 (Ar), 119.52(Ar),114.13 (Ar), 106.80 (Ar), 57.07 (Cα), 43.8 (CH_2N), 23.93 (Cβ).

N^{α}-Boc-D-Tca was synthesized by standard methods in a yield of 93.4%.

^1H NMR (250 MHz, d_6-DMSO, ppm): 10.86 (indole, J=11.5), 7.41 (d, J=7.6), 7.27 (d, J=7.29), 7.04 (t, J=7.0), 6.95 (t, J=7.2), 5.14+5.04 (d, J=5.8 + d, J=5.7), 4.73+4.44 (d, J=16.3 + d, J=16.3), 4.69+4.33 (d,16.6 + d, J=16.7), 3.28 (m), 2.96 (m). $[\alpha]^{20}_D$=-83.53 (c=0.5, HOAc), R_f=.87 (n-butanol/acetic acid/water, 4/1/1, v/v/v, Analtech Silica Gel Plates).

Synthesis of Boc-Tyr(O-2,6-Cl_2-Bzl)-CHO.

1.Synthesis of Boc-Tyr(O-2,6-Cl_2-Bzl)CON(OCH_3)CH_3.

This compound was synthesized by the racemization free method of Fehrentz and Castro (1983). 4.75g (10.8mM) of Boc-Tyr(O-2,6-Cl_2-Bzl) was dissolved in 7 ml of DCM, and 1.05 g (10.4 mM) of triethylamine was added. After cooling to 0°C, 4.60g of BOP (in 7 ml of DCM) was added. After 5 min., 1.47g (14.5 mM) of O,N-dimethylhydroxylamine and 1.50g (14.9 mM) of triethylamine were added. The mixture was warmed

to RT. After 60 min., it was diluted with DCM (150 ml), then successively washed with 3N HCl (3x15 ml), saturated sodium hydrogen carbonate solution (3x10 ml) and saturated sodium chloride solution (3x20ml). The organic phase was dried with magnesium sulfate and the solvent evaporated. The crude product was purified on silica gel (230-400 mesh, Aldrich). The yield of the purified solid was 83%.

R_f=0.65 (95/5/1, v/v/v, chloroform/methanol/acetic acid, Analtech silica gel plates), R_f=0.73 (ethyl acetate, Analtech silica gel plates).

^{1}H NMR (250 MHz, d_6-DMSO): 7.50 (m,2,6-Cl_2-Bzl,3H), 7.07(d+d, J=8.5 Hz, 4H), 7.15 (d, NH, 1H), 5.176 (s, CH_2Bzl, 2H), 4.50 (m, αH,1H), 3.72 (s, OCH_3, 3H), 3.10 (s, N-CH_3, 3H), 2.76(dd+dd, 4.0 Hz,9.9 Hz, βH, 2H), 1.30+1.22 (s+s, Boc, 9H).

2.Synthesis of Boc-Tyr(O-2,6-Cl_2-Bzl)-CHO.

3.7g (7.6 mM) of Boc-Tyr(O-2,6-Cl_2-Bzl)CON(OCH_3)CH_3 was dissolved in a mixture of 100 ml of anhydrous ethyl ether and 60 ml of freshly distilled TFA, followed by cooling to 0°C. LAH (0.87g, 22.8 mM) was added portionwise while stirring over 15 min. The reaction was allowed to proceed for 20 more minutes at 0°C, and then the excess LAH was hydrolyzed with ca. 10 ml of ethyl acetate, and the lithium-amide complex (2, Figure 22) was hydrolyzed with 5% citric acid solution (added dropwise). The mixture was vigorously stirred for 30 more minutes. Then ethyl ether was added (100 ml), and the aqueous phase separated and extracted with ether (3x40 ml). The organic phases were combined, washed with 3N hydrochloric acid (3x20 ml), saturated sodium hydrogen carbonate (3x20 ml), and saturated sodium chloride solution

(3x20 ml), and then dried with magnesium sulfate. The solvents were evaporated leaving an oily product (TLC pure) in 94% yield. ^1H NMR (250 MHz, d_6-DMSO); 9.51 (s, CHO, 1H), 7.50 (m, 2,6-Cl_2-Bzl, 3H), 7.28 (d, NH, 7.6 Hz, 1H), 7.06 (d+d, 8.5 Hz, ar., 4H), 5.17 (s, CH_2Bzl, 2H), 4.03(m, αH, 1H) , 3.03 (dd, 4.5 Hz, 14 Hz,βH, 1H), 2.65(dd, 10.0 Hz, 13.9 Hz, βH, 1H), 1.34 (s, Boc, 9H). TLC:R_f=.54 (95/5/1, chloroform/methanol/acetic acid, v/v/v, Kieselgel 60 F-254 silica gel).

Synthesis of Boc-Cys(S-4-MeBzl)-CHO.

Boc-Cys(S-4-MeBzl)CON(OCH_3)CH_3 was synthesized as was Boc-Tyr(O-2,6-Cl_2-Bzl)CON(CH_3)CH_3 (vide supra), except that 5% citric acid was used instead of 3N hydrochloric acid for the extraction of the unreacted O,N-dimethylhydroxylamine. After silica gel purification (hexane/ethyl acetate, 1/1) the yield was 78%. R_f=.62 (95/5/1, v/v/v, chloroform/methanol/acetic acid, Analtech silica gel plates). ^1H NMR(250 MHz, d_6-DMSO): 7.15 (d+d, J=8.0Hz, ar, 4H), 7.14 (d, NH, 1H), 4.60 (m, α-H, 1H), 3.69 (CH_2Bzl, 2H), 2.56 (dd+dd, 5.5Hz, 8.9Hz, β-H, 2H), 2.26 (MeBzl, 3H), 1.38 (t-Bu, 9H). The synthesis of Boc-Cys(S-4-MeBzl)-CHO was carried on as described for Boc-Tyr(O-2,6-Cl-Bzl)CHO (<u>vide supra</u>), except that 5% citric acid and not 3N hydrochloric acid was used for the acidic extraction, yielding a clear oil (91.5%) R_f=.50 (95/5/1, v/v/v, chloroform/methanol/acetic acid, Analtech silica gel plates).

^{1} NMR (250MHz, d_6-DMSO): 9.43 (s,CHO, 1H), 7.43 (d, 7.9Hz, NH, 1H), 7.13 (d+d, 8.0Hz, ar, 4H), 4.05(m, α-H, 1H), 3.70 (s, CH_2Bzl), 2H), 2.79 (dd, 5.0Hz, 13.8Hz, β-H, 1H), 2.51 (dd, 9.0Hz, 13.8Hz, β-H, 1H), 2.26 (s, CH_3Bzl, 3H), 1.32 (s, t-Bu, 9H).

Boc-Tyr(O-2,6-Cl_2-Bzl)-ψ[CH_2N]-D-Tca-OMe, 28.

Boc-Tyr(O-2,6Cl_2Bzl)CHO (0.5g, 1.13 mM) and 0.96g (2.5mM) of D-Tca-OMe were dissolved in 2ml of DMF (negative ninhydrin test) and 0.02ml acetic acid. Then 0.20g (3mM) of sodium cyanoborohydride (Aldrich) was added portionwise (over 20 min.) and the mixture stirred for 2 hrs. The reaction was monitored by TLC (4/1/1 ,v/v/v, butanol/acetic acid/water, Analtech silica gel plates). DMF was evaporated in vacuo, then 10 ml of saturated $NaHCO_3$, 4 ml of saturated sodium chloride, and 20 ml of ethyl acetate were added and extracted (repeated twice, organic phase collected). The organic phase was dried over magnesium sulfate, and the solvent evaporated to yield a clear oil, yield 0.70 g, 75%. Purification was carried out on a silica gel column (Aldrich, 230-400 mesh) using 1/1 ethyl acetate/hexane. R_f=0.82 (ethyl acetate, Analtech silica gel plates). The structure was confirmed by NMR methods (vide infra).

D-Tca-OMe was obtained according to the procedure of Schwartz et al. (1957). Yield 98.3% of the final solid product. R_f=0.56 (4/1/1, butanol/water/acetic acid, v/v/v, Analtech silica gel plates). ^{1}H NMR (250MHz, d_6-DMSO): 10.85 (s,indole NH, 1H), 10.34 (broad, HCl), 7.47

(d, 7.7Hz, Ar, 1H), 7.36 (d,8.0Hz, Ar, 1HO, 7.10 (t, 7.1Hz, Ar, 1H), 7.01 (t, 7.5Hz, Ar, 1H), 4.63 (dd, 5.3Hz, 10.0Hz, α-H, 1H), 4.39 (s, N-CH_2, 2H), 3.81 ((s,OCH_3, 3H), 3.29 (5.3Hz, 16Hz, dd, β-CH_2, 1H), 3.06 (10.1Hz, 16.0Hz, dd, β-CH_2, 1H).

D-Phe-Cys-Tyr-ψ[CH_2NH]-D-Trp-Orn-Thr-Pen-Thr-NH_2, 23.

1mM of TFA·D-Trp-Orn(Z)-Thr(O-Bzl)-Pen(S-4-MeBzl)-Thr(O-Bzl)-resin fragment was synthesized as in 2. Following TFA-mediated cleavage of the t-butoxycarbonyl protecting group of D-Trp, the resin was washed 4 times with DCM without neutralization. Then, 1.66 g of Boc-Tyr(O-2,6-Cl_2-Bzl)CHO was dissolved in 30 ml of fresh DMF containing 1% acetic acid and added to the reaction vessel containing the peptide fragment on the resin. 0.19 g of sodium cyanoborohydride was added portionwise and reaction allowed to proceed for 1 hr. Due to the positive result of the ninhydrin test, reductive alkylation reaction was repeated with the same quantities of reagents and quenched after 3 hrs (negative ninhydrin test). The resulting Boc-Tyr(O-2,6-Cl_2-Bzl)-ψ[CH_2NH]-D-Trp-Orn(Z)-Thr(O-Bzl)-Pen(S-4-MeBzl)-Thr(O-Bzl)-resin was deprotected and then Boc-Cys(S-4-MeBzl) coupled and deprotected, followed by a coupling and deprotection of Boc-D-Phe. The resulting peptide resin was cleaved with HF and worked up as for 9 yielding 14.6% of the title peptide. Analytical data are given in Table 3. The composition of 23 was independently confirmed by FAB-MS and ^1H NMR investigation.

D-Phe-Cys-Tyr-ψ[CH_2N]-D-Tca-Orn-Thr-Pen-Thr-NH_2, 24.

The title peptide was synthesized in a manner similar to 23, except

that Boc-D-Tca was used instead Boc-D-Trp in the coupling scheme. Chloranil was used to monitor the extent of reductive alkylation. To perform it in a reliable way, the resin sample was carefully neutralized with DIEA, followed by DCM wash (3x). The yield of the pure peptide was 22.3%. The composition of 24 was corroborated by FAB- MS (Table 3) and ^{1}H NMR experiments.

D-Phe-Cys-Tic-D-Trp-Orn-Thr-Pen-Thr-NH_2, 25.

The synthesis of title peptide 25 was accomplished as for 2, except that Boc-Tic was used instead of Boc-Tyr(O-2,6-Cl_2-Bzl) in the coupling scheme. Coupling of the next amino acid Boc-Cys(S-4-MeBzl) was monitored by a chloranil test. The resulting Boc-D-Phe-Cys(S-4-MeBzl)-Tic-D-Trp-Orn(Z)-Thr(O-Bzl)-Pen(S-4-MeBzl)-Thr(O-Bzl)-resin was cleaved with HF and subjected to the work-up procedure described for peptide 4. Yield 18.9%. The structure of peptide 25 was confirmed by ^{1}H NMR and FAB-MS experiments (Table 3).

Boc-Tic was been obtained analogously to Boc-D-Tic with a yield of 71.3% after the first step (PictetSpengler reaction) and 94% after the Boc protection procedure. $[\alpha]^{25}_D$ = 17.8 (c=1, HOAc). ^{1}H NMR (250 MHz, d_6-DMSO): 7.25-7.11 (m, Ar, 4H), 4.86 (m, α-H, 0.5H), 4.67-4.32 (m, α-H+NCH_2, 2.5H), 3.10 (dd+dd, β-CH_2, 2H), 1.38+1.47 (s+s, t-Bu, 9H). R_f=0.64 chloroform/methanol/ acetic acid, 95/5/1, v/v/v, silica gel plates).

D-Pgl-Cys-ψ[CH_2N]-Tic-D-Trp-Orn-Thr-Pen-Thr-NH_2, 26.

The synthesis of the title peptide 26 was analogous to that of 25, except that after incorporation and deprotection of Boc-Tic, resulting in a peptide fragment Tic-D-Trp-Orn(Z)-Thr(O-Bzl)-Pen(S-4-MeBzl)-Thr(O-Bzl)-resin, reductive alkylation was carried out, analogous to that described for peptide 24. Boc-Cys(S-4-MeBzl)-CHO, (1.04 g, 3.25 mM) was dissolved in 30 ml of fresh DMF containing 1% acetic acid, followed by a stepwise addition of 0.6 g of sodium cyanoborohydride. After 80 min. the reaction was terminated and repeated with the same amounts of reagents to assure its completeness. Deprotection of the fragment Boc-Cys(S-4-MeBzl)-ψ[CH_2N]-Tic-D-Trp-Orn(Z)-Thr(O-Bzl)-Pen(S-4-MeBzl)-Thr(O-Bzl)-resin was followed by coupling and deprotection of Boc-D-Pgl. The resulting peptide-resin underwent similar work-up procedure to that of 24, yielding 17.6% of the final peptide 26. Its composition was confirmed by ^{1}H NMR and FAB-MS analysis (Table 3).

D-Phe-Cys-ψ[CH_2N]-Tic-D-Trp-Orn-Thr-Pen-Thr-NH_2, 27.

The title peptide was synthesized like 26, except that Boc-D-Phe replaced Boc-D-Pgl in the reaction scheme, giving D-Phe-Cys-ψ[CH_2N]-Tic-D-Trp-Orn(Z)-Thr(O-Bzl)-Pen(S-4-MeBzl)-Thr(O-Bzl)-resin. The work-up as for 26 gave the title peptide 27 with a yield of 20.3%. The structure was confirmed by FAB-MS analysis and ^{1}H NMR analysis (Table 3).

D-Phe-Cys-Tyr-D-Trp-Lys-Thr-D-Pen-Thr-NH_2, CTDP 29.

This peptide was synthesized similarly to 1, except that Boc-D-Pen(S-4-MeBzl) was used instead of its L isomer in the reaction scheme, yielding D-Phe-Cys(S-4-MeBzl)-Tyr(O-2,6-Cl2-Bzl)-D-Trp-Orn(Z)-Thr(O-Bzl)-Pen(S-4-MeBzl)-Thr(O-Bzl)-resin. Standard work-up as for 4 gave the title peptide 29. ^{1}H NMR analysis confirmed the structure of 29 (Sugg et al., 1988).

Experimental Conditions for the NMR Experiments.

Each sample (5 mg) was dried in vacuo, dissolved in 0.3 ml of d_6-DMSO (100% D atom, Aldrich), run through several thaw and freeze cycles and sealed. All spectra (recorded at 303 K, except for variable temperature experiments) were acquired with a Bruker AM-250 or WM- 250 spectrometer equipped with an Aspect 3000 or 2000 computer, respectively.

Signals in a 1D spectrum (digital resolution 0.1Hz/pt) were assigned by using a combination of 2D NMR techniques. Phase sensitive COSY (Marion and Wüthrich, 1983; Rance et al., 1983), employing time-proportional phase increments (TPPI), allowed the assignment of intraresidual resonances. Pulse sequence: D1-90-D0-90-D3-90-FID, D1=1.0s, D0=0.000003s.

Zero and first order phase correction from the 1D spectrum was applied, along with zero filling in the F1 dimension; shifted sine-bell multiplication was applied in both dimensions prior to FT.

Digital resolution in F1 was 5.2 Hz/pt, and in F2 was 2.6 Hz/pt, in all cases.

Homonuclear dipolar correlated 2D NMR (NOESY) was used to trace interresidual connectivities between NH^{i+1} and CH^{i}_{α}, as well as to provide important information regarding the secondary structure of the peptide. The pulse sequence was: D1-90-D0-90-D3-90-FID, D1 = 1.5s, D9 = 0.3s. Data manipulation: zero filling in F1, square sine-bell multiplication was applied in both directions prior to FT. Digital resolution in F1 and F2 = 2.6 Hz, in all cases.

Confirmation of congested spectral region assignments (β protons) was accomplished with homonuclear shift-correlated 2D NMR with delay (Bax and Freeman, 1981), emphasizing ^{4}J coupling constants between o-hydrogens of aromatic amino acids and β-protons. Thus, the characteristic AA'XX'-like signals of Tyr aromatic ring protons provided unambiguous assignment of β-CH_2 of this amino acid (Figure 23). The pulse sequence was: D1-90-D0-D2-90-D2-FID, D1 = 1.5s, D2 = 0.08s. Data manipulation: zero filling in F1, square sine-bell multiplication in both directions was applied prior to FT. Digital resolution in both dimensions was 2.6 Hz/pt, in all cases.

Temperature studies (303-328K range, 5 deg. intervals) were carried on to identify amide protons possibly involved in H-bonding, as well as to investigate the conformational rigidity of these peptides.

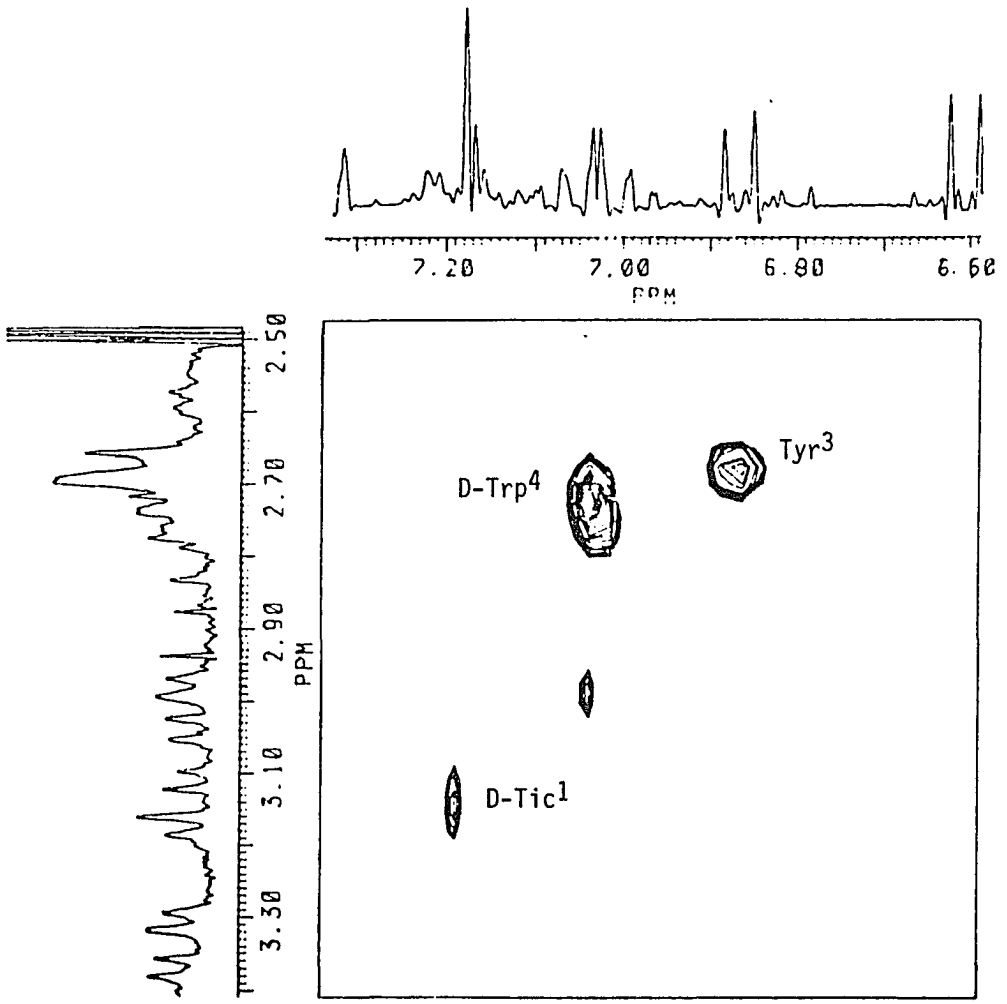

Figure 23.

Long range COSY spectrum of Gly-D-Tic-Cys-Tyr-D-Trp-Orn-Thr-Pen-Thr-NH_2 (303K, d_6- DMSO)

Chapter 3.

PHARMACOLOGICAL PROPERTIES OF THE SYNTHETIC SOMATOSTATIN ANALOGUES: RECEPTOR BINDING AND IN VITRO EXPERIMENTS.

General Remarks.

Three distinct structural and/or conformational properties of the octapeptide analogue 1 were examined with respect to their significance for interaction with mu and delta opioid receptors: 1) the importance of ring size was examined by its reduction; 2) the importance of the side chain conformation of the N-terminal D-Phe to opioid receptor potency and selectivity was examined by the design and incorporation of the the conformationally restricted amino acid D-Tic; and 3) the importance of the C-terminal Thr^8 to mu opioid potency and selectivity was examined by deleting this residue or structural changes.

Analogues with reduced size from the 20-membered ring were examined by preparing the 14-membered ring compounds 4 and 5. This ring size is comparable to the one characterizing the delta-selective disulfide-containing enkephalins (Mosberg et al., 1982; Mosberg et al., 1983), which contained a Pen^5 residue and those of Schiller et al. (1985), which did not contain a Pen^5 residue and are somewhat mu opioid receptor selective. In addition, 17-membered ring analogues 6 and 7 were made by deleting Lys^5 or Thr^6, respectively.

Peptides 1-3 (CTP, CTOP, CTAP, respectively) had been synthesized previously (Pelton et al., 1985a; Pelton et.al., 1986). These compounds were resynthesized and retested in the course of this

Table 4.

Binding Affinities and Selectivities of CTP Analogues in Competition With [^{3}H]CTOP, [^{3}H]DPDPE and [^{125}I]CGP23,996 in Receptor Binding to Rat Brain Membranes.

PEPTIDE	IC50,nM, binding vs. [^{3}H]CTOP	IC50,nM, binding vs. [^{3}H] DPDPE	IC50,nM binding vs. [^{125}I]CGP23,996	μ/δ selectivity	μ/Somatostatin selectivity
1. D-Phe-Cys-Tyr-D-Trp-Lys-Thr-Pen-Thr NH_2, CTP	3.7 ± 0.8	1,153 ± 116	1,462 ± 114	312	395
2. D-Phe-Cys-Tyr-D-Trp-Orn-Thr-Pen-Thr-NH_2, CTOP	4.3 ± 0.8	5,598 ± 317	47,704 ± 3,112	1,301	11,094
3. D-Phe-Cys-Tyr-D-Trp-Arg-Thr-Pen-Thr-NH_2, CTAP	2.1 ± 0.3	5,314 ± 278	8,452 ± 285	2,530	4,025
4. D-Tyr-Cys-Phe-Asn-Pen-Thr-NH_2	7,468 ± 297	>10,000	>100,000	>1.3	>1.3
5. D-Phe-Cys-Tyr-Asn-Pen-Thr-NH_2	17% inhibition at 10,000	>10,000	>100,000	N.D.	N.D.
6. D-Phe-Cys-Tyr-D-Trp-Thr-D-Pen-Thr-NH_2	10,000	7,822 ± 4372	N.D.	N.D.	N.D.
7. D-Phe-Cys-Tyr-D-Trp-Lys-D-Pen-Thr-NH_2	18% inhibition at 10,000	>10,000	6,103 ± 848	N.D.	N.D.
8. D-Tic-Cys-Tyr-D-Trp-Lys-Thr-Pen-Thr-NH_2,TCTP	1.2 ± 0.0	9,324 ± 546	949 ± 170	7,77	791
9. D-Tic-Cys-Tyr-D-Trp-Orn-Thr-Pen-Thr-NH_2, TCTOP	1.4 ± 0.2	15,954 ± 3,582	20,403 ± 1363	11,396	14,574
10. D-Tic-Cys-Tyr-D-Trp-Arg-Thr-Pen-Thr-NH_2,TCTAP	1.2 ± 0.2	1,274 ± 78	34,336 ± 2241	1,060	28,613
11. D-N-Me-Phe-Cys-Tyr-D-Trp-Orn-Thr-Pen-Thr-NH_2	284 ± 36	>10,000	8,054 ± 1620	>35	28
12. Gly-D-Tic-Cys-Tyr-D-Trp-Orn-Thr-Pen-Thr-NH_2	278.7 ± 0.5	5,352 ± 503	19,408 ± 6,738	19	70
13. D-Trp-Cys-Tyr-D-Trp-Lys-Thr-Pen-Thr-NH_2	6.3 ± 0.5	>10,000	1,599 ± 15	>1,587	254
14. D-Tic-Cys-Tyr-D-Trp-Lys-Pen-Thr-NH_2	9,408 ± 695	>10,000	13,610 ± 3,726	>1.0	1.5

Table 4, cont.

15. D-Phe-Cys-Tyr-D-Trp-Orn-Thr-Pen-NH_2	187 ± 40	≥10,000	47,273 ± 4,811	≥53	253
16. D-Phe-Cys-Tyr-D-Trp-Lys-Thr-Pen-NH_2	115 ± 10.2	≥10,000	1,942 ± 13	≥87	17
17. D-Phe-Cys-Tyr-D-Trp-Lys-Thr-Pen-Asn-NH_2	130 ± 17.1	≥10,000	1,801 ± 413	≥77	6.3
18. D-Phe-Cys-Tyr-D-Trp-Lys-Thr-Pen-Asp-NH_2	3,467 ± 84.5	≥10,000	8,300 ± 4597	≥2.9	2.4
19. D-Tic-Cys-Tyr-D-Typ-Lys-Thr-Pen-Val-NH_2	46.0 ± 11.	2,122 ± 13	1,992 ± 115	46	43
20. D-Phe-Cys-Tyr-D-Trp-Lys-Thr-Pen-Ser-NH_2	20. ± 4.7	≥10,000	1,888 ± 238	≥490	94
21. D-Tic-Cys-Tyr-D-Trp-Lys-Thr-Pen-Ser-NH_2	7.8 ± 2.0	3,828 ± 126	1,499 ± 131	491	192
22. D-Phe-Cys-Tyr-D-Tca-Orn-Thr-Pen-Thr-NH_2	133	>10,000			
23. D-Phe-Cys-Tyr-Ψ[CH_2NH]-D-Trp-Orn-Thr-Pen-Thr-NH_2	86	>10,000			
24. D-Phe-Cys-Tyr-Ψ[CH_2N]-D-Tca-Orn-Thr-Pen-Thr-NH_2	922	>10,000			
25. D-Phe-Cys-Tic-D-Trp-Orn-Thr-Pen-Thr-NH_2	1439	>10,000			
26. D-Pgl-Cys-Ψ[CH_2N]Tic-D-Trp-Orn-Thr-Pen-Thr-NH_2	4724	>10,000			
27. D-Phe-Cys-Ψ[CH_2N]-Tic-D-Trp-Orn-Thr-Pen-Thr-NH_2	892	>10,000			

Peptide	GPI agonism[a]	GPI antagonism[b]	pA_2
1. D-Phe-Cys-Tyr-D-Trp-Lys-Thr-Pen-Thr-NH_2	no	yes	7.10 ± 0.17
2. D-Phe-Cys-Tyr-D-Trp-Orn-Thr-Pen-Thr-NH_2	no	yes	6.37 ± .07
3. D-Phe-Cys-Tyr-D-Trp-Arg-Thr-Pen-Thr-NH_2	no	yes	7.12 ± 0.08
8. D-Tic-Cys-Tyr-D-Trp-Lys-Thr-Pen-Thr-NH_2	no	yes	8.10 ± 0.29
9. D-Tic-Cys-Tyr-D-Trp-Orn-Thr-Pen-Thr-NH_2	no	yes	7.38 ± 0.03
10. D-Tic-Cys-Tyr-D-Trp-Arg-Thr-Pen-Thr-NH_2	no	yes	8.69 ± 0.25
13. D-Trp-Cys-Tyr-D-Trp-Lys-Thr-Pen-Thr-NH_2	yes	N.D.	N.D.
19. D-Phe-Cys-Tyr-D-Trp-Lys-Thr-Pen-Val-NH_2	no	yes	6.59 ± 0.13
20. D-Phe-Cys-Tyr-D-Trp-Lys-Thr-Pen-Ser-NH_2	no	yes	6.24 ± 0.11

a Intrinsic agonist activity in GPI assay.

b Antagonism of PLO17-induced inhibition of electrically-induced contractions of GPI.

Table 5. Pharmacological characterization of selected somatostatin analogues in GPI assays.

work (Table 4, Table 5), for comparison with the new synthetic peptides. Slightly modified receptor binding protocols used in this study did not allow straightforward comparison with the old data (see Experimental).

Reduced Ring Size Analogues.

First, an effort has been made to explore the possibility of synthesizing active antagonist analogues of CTP, but with reduced ring size (from 20-membered to 14-membered and 17-membered). Peptides D-Tyr-Cys-Phe-Asn-Pen-Thr-NH_2 (4) and D-Phe-Cys-Tyr-Asn-Pen-Thr-NH_2 (5) are truncated analogues of somatostatin with 14-membered rings. They showed weak receptor binding activities (Table 4). Analogues D-Phe-Cys-D-Trp-Thr-D-Pen-Thr-NH_2 (6) and D-Phe-Cys-Tyr-D-Trp-Lys-D-Pen-Thr-NH_2 (7) which contain 17-membered rings and a D-penicillamine residue also showed little affinity to opioid or somatostatin receptors (Table 4). Peptides 4-7 all showed a dramatic decrease of affinity for both types of opioid receptors compared to 20-membered ring peptides 1-3.

Design Rationale.

NMR investigations by Sugg et al. (1988) and Pelton et al. (1988) revealed that the potent analogue CTP (1) is characterized by a type II' β-turn of the core tetrapeptide -Tyr-D-Trp-Lys-Thr- with hydrogen bonding between Tyr^3(CO) and Thr^6(NH). Furthermore, conformational analysis of CTDP D-Phe-Cys-Tyr-D-Trp-Lys-Thr-D-Pen-Thr-NH_2; (Sugg et al., 1988) also a 20-membered ring analogue with a D-Pen^7 rather than L-Pen^7 residue and possessing no significant activity for the mu opioid receptor, revealed that replacement of

L-Pen^7 (in 1) with D-Pen^7(in CTDP) is associated with a change in the helicity of the disulfide bond, being negative for CTP (1) and positive for CTDP. On the basis of these results, it was speculated that deletion of endocyclic amino acids Lys^5 or Thr^6, each of which were part of the β-turn tetrapeptide fragment, prevented these peptides from attaining the type II' β-turn in the template and also negative disulfide helicity, thus reducing their affinities for the mu opioid receptor.

Both CTP and CTDP exhibited similar conformation of the core tetrapeptide, characterized by a type II' β-turn, but have different disulfide helicities. One of the possible consequences of this observation - design of many peptides in this study was based on this assumption - is that change of the disulfide dihedral angle in CTDP caused an alteration of the relative spatial disposition of the exocyclic amino acids. Thus, the large decrease in affinity for mu receptors observed for CTDP suggested the importance of both exocyclic positions in the cyclic octapeptide for its interaction with the mu opioid receptor. This view was supported by ^{1}H NMR aided conformational analysis of the weakly potent analogue D-Pgl-Cys-Tyr-D-Trp-Lys-Thr-Pen-Thr-NH_2 (PCTP; Kazmierski and Hruby, 1988). The single substitution of D-phenylglycine for D-phenylalanine in 1 caused a dramatic decrease (about 11-fold) in its affinity for mu, and a modest affinity increase (about 2.5-fold) in binding to delta opioid receptors relative to CTP, as measured in a rat brain binding assay. It may be envisioned that D-Pgl exhibits two major conformational effects with regard to D-Phe. First, its aromatic ring has fewer rotational degrees of freedom. Second,

this ring (due to the lack of β-carbon) is located closer to the peptide backbone. To examine whether these properties have any influence on the backbone conformation, extensive conformational studies of this compound were made utilizing a variety of 1D and 2D ^1H NMR techniques (see Experimental). PCTP possesses a similar backbone conformation (βII'-turn, negative disulfide helicity; Figure 24, Figure 25, Figure 26) to CTP. Also, similar side chain conformer populations are found in both peptides suggesting that a more folded topography of PCTP (due to a lack of β-carbon atom on D-Pgl; related to this is a change of spatial relationship between putative D-Pgl and Tyr aromatic ring pharmacophores) may be of biological significance. Apparently, more folded topography of the peptide is not compatible with strong interaction with the mu opioid receptor.

In CTP, there is a large participation of the g(-) side chain rotamer for the D-Phe residue (Sugg et al., 1988), which leads to more extended topography. This suggests that freezing this particular side chain conformation (via conformational constraints) should stabilize extended topography of the peptide, potentiating its interactions with the mu opioid receptor. Tetrahydroisoquinoline carboxylic acid (Tic) would appear to be an excellent amino acid to test this hypothesis since only two discrete side chain conformations are possible for this residue (Figure 8). Furthermore it is suggested from model building that only the gauche(-) conformer, but not gauche(+), would correspond to an extended conformation. It should be emphasized that operationally D-Tic is a product of addition of a methylene unit bridging the α-N and the 2'-phenyl carbon of D-Phe (Figure 27).

Analogues With N-terminal Modifications.

Thus, D-Tic-Cys-Tyr-D-Trp-Lys-Thr-Pen-Thr-NH_2 (TCTP, 8), D-Tic-Cys-Tyr-D-Trp-Orn-Thr-Pen-Thr-NH_2 (TCTOP, 9), and D-Tic-Cys-Tyr-D-Trp-Arg-Thr-Pen-Thr-NH_2 (TCTAP, 10) were synthesized. All three peptides indeed exhibited increased affinity for the mu opioid receptor, in comparison with CTP, CTOP, and CTAP, respectively (Table 4). However, there was no major influence of this new moiety on peptide binding to the somatostatin receptor. Thus, introduction of the conformationally constrained D-tetrahydroisoquinoline carboxylate instead of D-phenylalanine results in about a 2- to 3-fold increase in mu opioid receptor binding for 8, 9, and 10. TCTP (8) showed increased affinity for mu opioid receptors (3 times relative to CTP) and lower affinity (8 times) to the delta opioid receptor with an overall mu/delta selectivity of 7,770 compared with about 312 for CTP (Table 4) in the binding assays.

In analogy to its relative binding effects, the antagonistic potency of TCTP in the guinea pig ileum assay was 10 times greater than CTP (Table 5) as measured by its pA_2 value for the antagonism of the mu agonist PLO17 (Experimental). Similarly, TCTOP (9) has 3 times higher affinity for the mu opioid receptor (in comparison with CTOP) as well as higher mu vs. delta selectivity (9 times, Table 4). Remarkably, TCTOP (10) is also 10 times more potent on peripheral opioid receptors, when compared to CTOP (Table 5). Though TCTOP is equipotent and essentially equiselective to TCTP in the central opioid

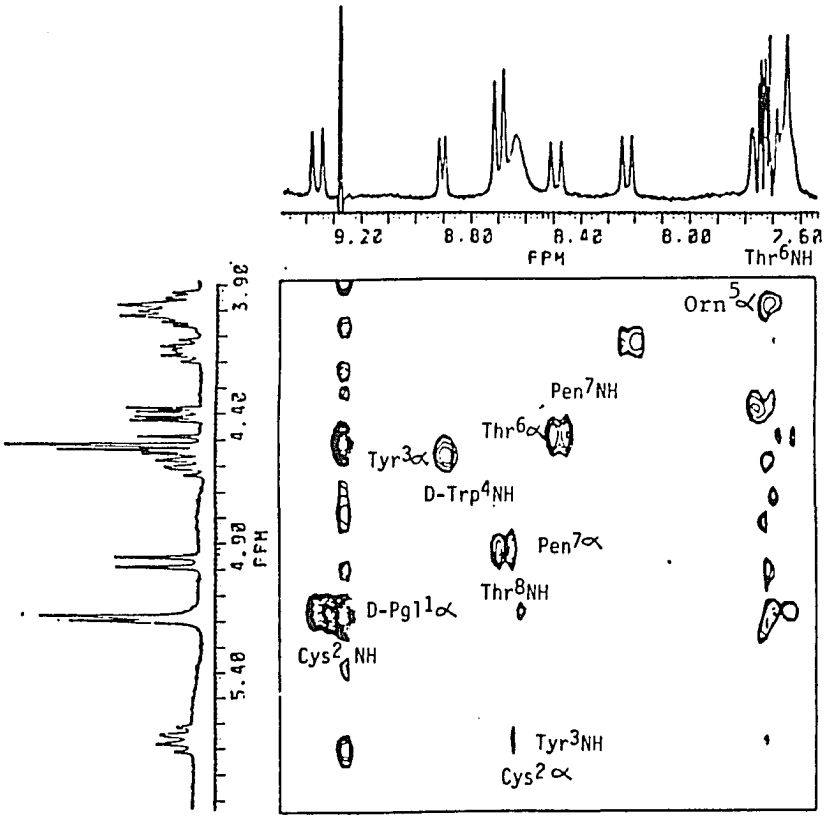

Figure 24.

NOESY spectrum of D-Pgl-Cys-Tyr-D-Trp-Lys-Thr-Pen-Thr-NH_2

(303K, d-6 DMSO)

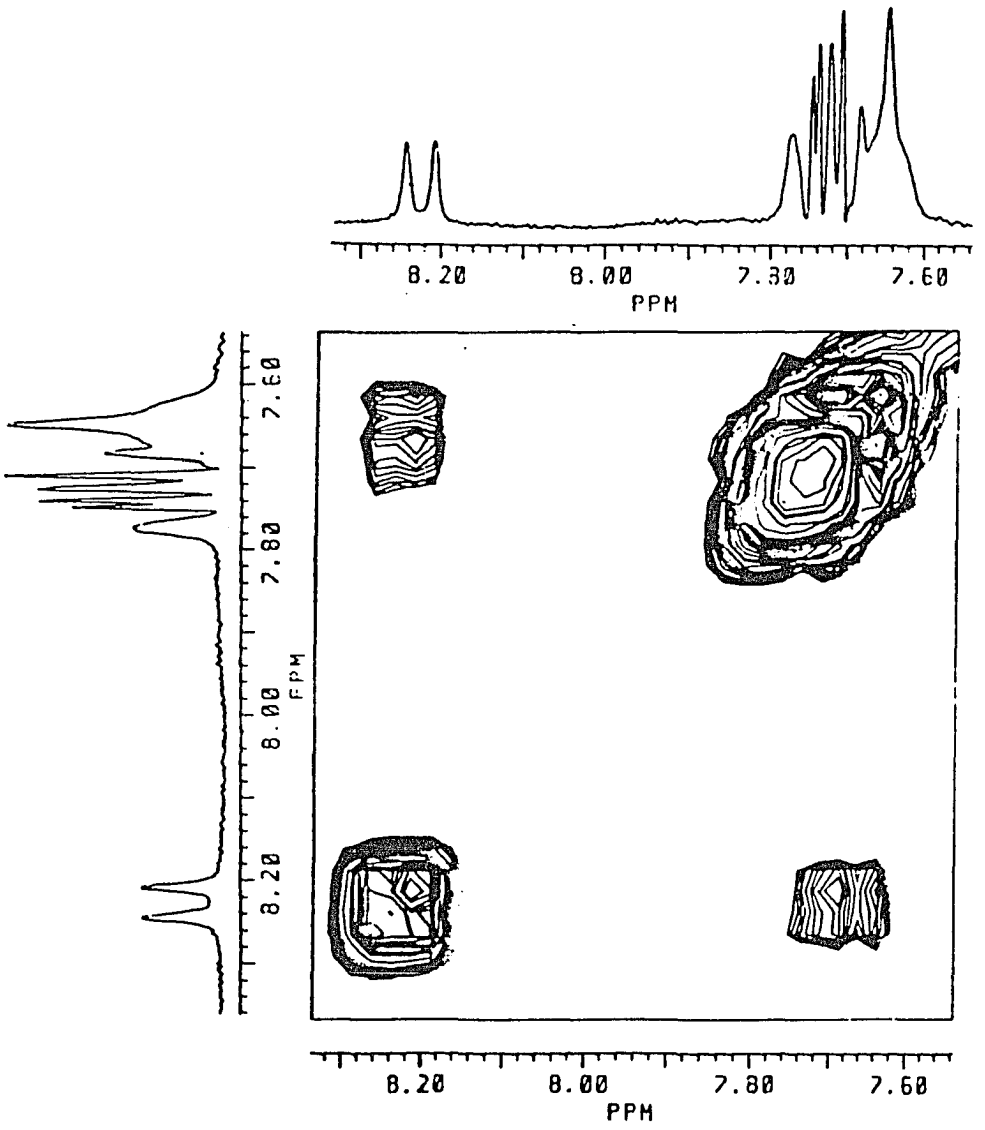

Figure 25.

NOESY spectrum of PCTP, fragment illustrating NH^5/NH^6 cross-relaxation (d_6-DMSO, 303K).

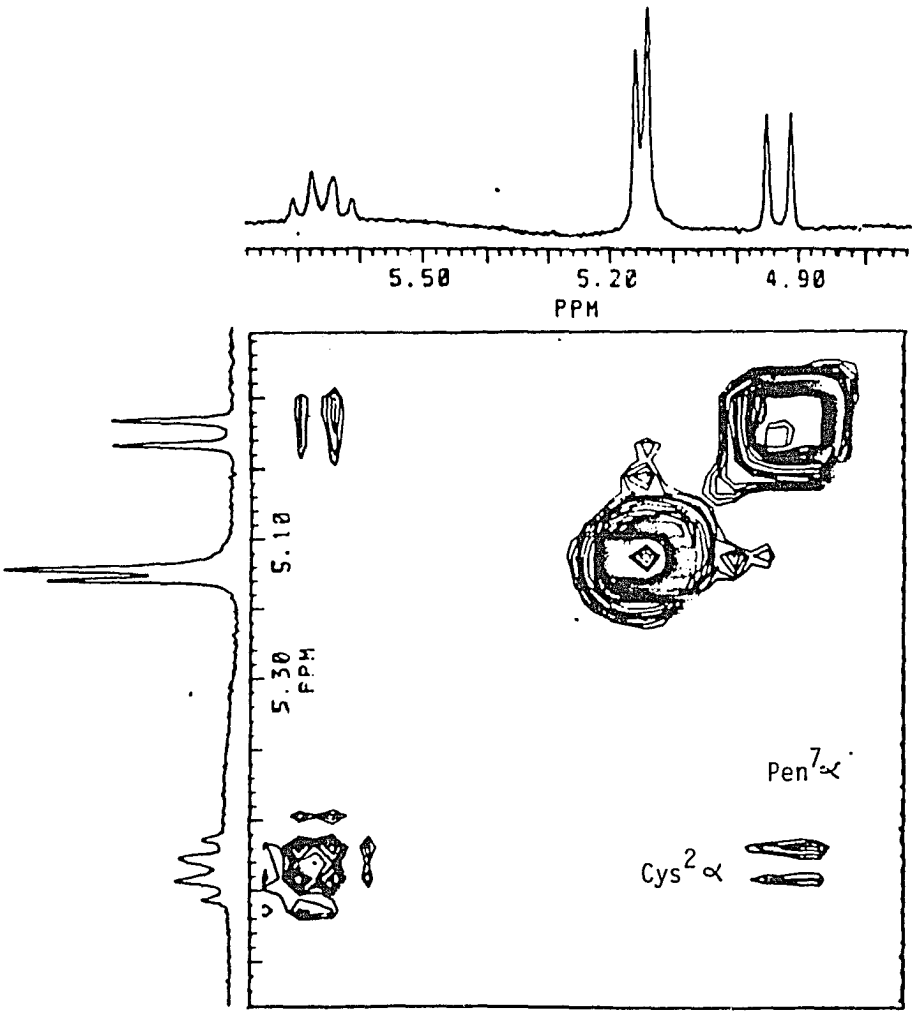

Figure 26. NOESY cross-relaxation off-diagonal signals between Cys_{α}^{2} and Pen_{α}^{7}, d_6-DMSO, 303K, PCTP.

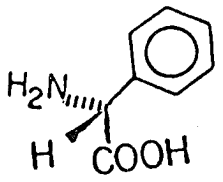

D-Pgl

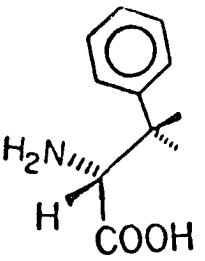

D-Phe

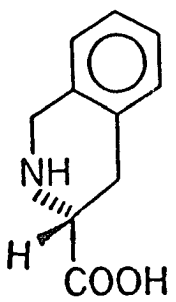

D-Tic

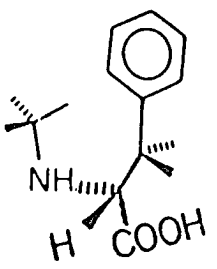

N-Me-D-Phe

Figure 27. Structures of amino acids replacing D-Phe on the N-terminal position, applied in this work.

binding assay, TCTOP was less potent in the peripheral mu opioid receptor bioassay (GPI) preparation.

Another analogue in this series - TCTAP (10)-is definitely the most potent mu opioid receptor antagonist yet synthesized (Kazmierski et al., 1988), with an <u>in vitro</u> pA_2 = 8.69 (vs. 7.12 for CTAP, 3), followed by TCTOP (9) with pA_2 = 7.38 (vs. 6.37 for CTOP, 2), and TCTP (8) with pA_2 8.10 (vs. 7.10 for CTP, 1). Replacement of Lys^5 by Orn^5 or Arg^5 has been found to be deleterious for the affinity of the cyclic hexapeptides as well as cyclic octapeptides to the somatostatin receptor (Nutt et al., 1983; Pelton et al., 1986). Indeed, rat brain receptor binding studies show that TCTOP (9) exhibits a 21-fold decrease of affinity for rat brain somatostatin receptor relatively to TCTP (8). Affinity of TCTAP (10) for somatostatin receptors is 35 times lower than that of CTP.

When the structurally, but not topographically - to be discussed further in the text (Kazmierski and Hruby, 1988) - similar amino acid D-N-Me-Phe^1 (Figure 27) is substituted for D-Tic^1 in TCTOP (9), the peptide D-N-Me-Phe-Cys-Tyr-D-Trp-Orn-Thr-Pen-Thr-NH_2 (11) is obtained, and perhaps surprisingly, it exhibits a dramatic loss of affinity for the mu opioid receptor (approximately 200-fold with respect to analogue 9), while conserving equal affinity to delta opioid and somatostatin receptors compared to 9.

The only nonapeptide in this series was Gly-D-Tic-Cys-Tyr-D-Trp-Orn-Thr-Pen-Thr-NH_2 (12), in which Gly is attached to TCTOP (9). It exhibited a sharp decrease of affinity for the mu opioid receptor

(about 200-fold with respect to 2), but a modest increase of affinity for the mu opioid receptor (about 200-fold with respect to 9). The strikingly different pharmacological profiles of peptides 11 and 12 with respect to 8 have recently been interpreted by using a combination of NMR studies and molecular modeling (Kazmierski and Hruby, 1988; Kazmierski and Hruby, manuscript in preparation). While details of conformational analysis are presented further in the text, some essential findings will be quoted here for continuity reasons. It has been convincingly shown that the backbone conformation of 8, 11, and 12 is essentially similar and can be described by a βII'-turn centered on the -Tyr-D-Trp-Orn(Lys)-Thr- tetrapeptide fragment. Also, helicity of the disulfide bridge fragment was not perturbed by structural modifications that occurred in the N-terminal position (negative dihedral angle). Detailed analysis of the side chain population distribution into the three staggered conformers, as the only detectable difference between these so pharmacologically different peptides, showed that the side chain of D-Tic (8) exists exclusively in the gauche(-), whereas that of Gly-D-Tic^1 (12) exclusively in the gauche (+) conformation.

In peptide 11, due to steric interaction of phenyl and N-methyl groups trans side chain population is significant, unlike in potent CTP, 1. Figure 28 presents stacked conformations, consistent with the NMR parameters of both peptides (8 and PCTP). While the backbone conformation is very similar, there is a dramatic topographical difference between them in their N-terminal moiety. A gauche(-) side chain of D-Tic (8) causes an increase in the distance between two

important opioid pharmacophores (D-Tic and Tyr - compare Figure 29) relative to that of PCTP, resulting in an extended topography of TCTP (8), relative to the folded topography of PCTP. Similar conclusions can be drawn from comparison of the topologies (determined from the NMR parameters) of peptides 9 and 12. The gauche(+) side chain conformation of the Gly-D-Tic dipeptide makes the topography of peptide 12 relatively compact (Figure 30), in contrast to the extended conformation of TCTP 8, Figure 31. Thus all three peptides (PCTP, 11, and 12) have similar compact topographies, and all three display very similar pharmacological properties with greatly reduced potencies at the mu opioid receptor in rat brain binding studies. In contrast, the extended topography found for CTP 8 allows this peptide to interact more strongly with the mu opioid receptors, and less readily with the delta receptors.

These results support our previously described model for opioid receptor selectivity, namely that μ and δ opioid receptors require different peptide topographies.

The importance of the N-terminal residue in these cyclic octapeptides for binding, and possibly for transduction, at opioid receptors, was further examined by design and synthesis of D-Trp-Cys-Tyr-D-Trp-Lys-Thr-Pen-Thr-NH_2 13. Rat brain binding studies (Table 4) suggest that 13 is a quite potent (IC_{50} = 6.3 nM) and selective (> 1,599) ligand for the mu receptor. However, unlike other compounds in this class, 13 has a strong agonistic action on GPI preparation at low concentrations. As this effect is only partially reversible with naloxone and ICI 174,864 in MVD preparations (data not shown), peptide

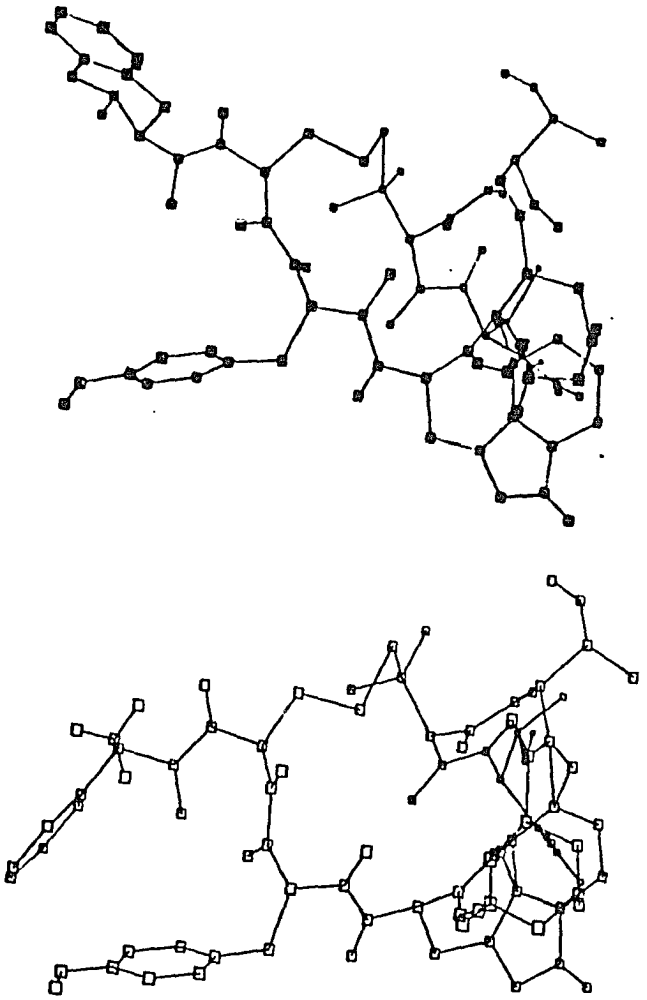

[D-Tic'] CTP

[D-Pgl'] CTP

Figure 28. Conformations of D-Tic-Cys-Tyr-D-Trp-Orn-Thr-Pen-Thr-NH_2 (top), and D-Pgl-Cys-Tyr-D-Trp-Orn-Thr-Pen-Thr-NH_2 (bottom), energy minimized with use of the NMR constraints (CHARMM).
Both structures have the same backbone conformations, but different topographies.

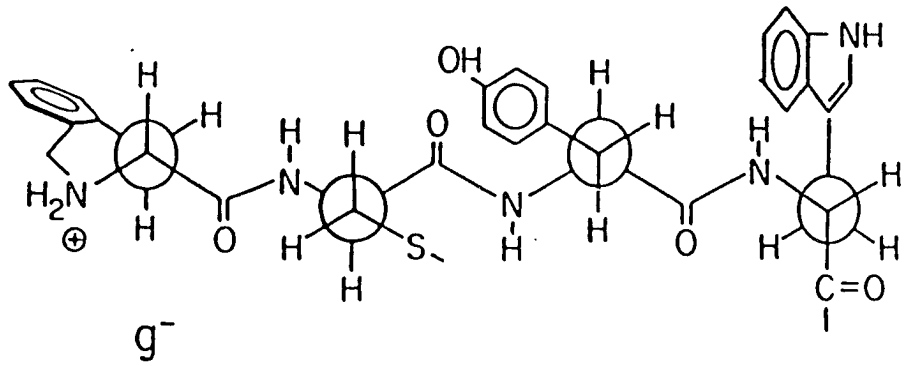

Figure 29. Newman representation of the first four residues of D-Tic-Cys-Tyr-D-Trp-Lys-Thr-Pen-Thr-NH_2.

Gly-D-Tic-Cys-Tyr-D-Trp-Orn-Thr-Pen-Thr-NH_2

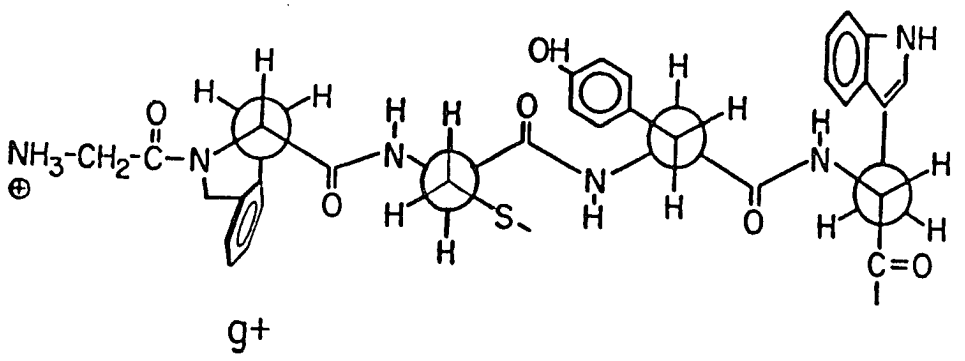

g+

Figure 30. Newman representation of relative aromatic ring relationship in Gly-D-Tic-Cys-Tyr-D-Trp-Orn-Thr-Pen-Thr-NH_2 consistent with the NMR data.

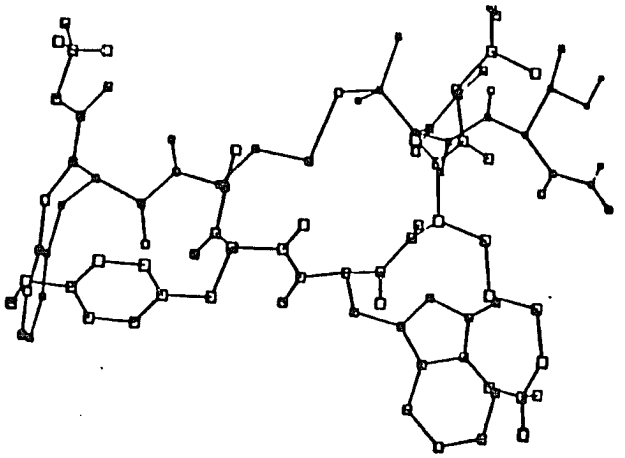

[Gly-D-Tic'] CTθP

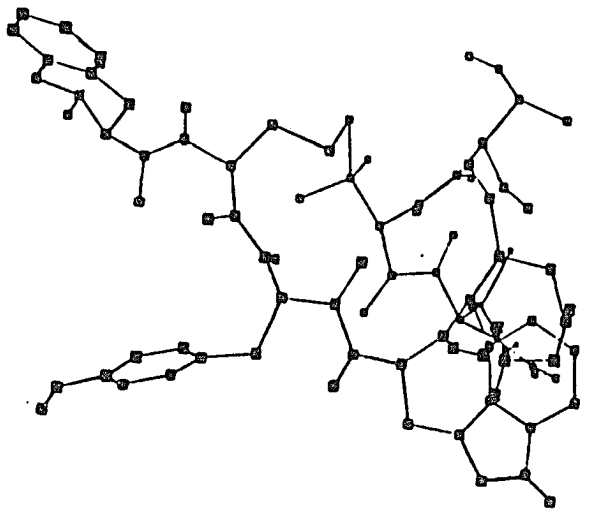

[D-Tic'] CTP

Figure 31. Conformations of Gly-D-Tic-Cys-Tyr-D-Trp-Orn-Thr-Pen-Thr-NH_2 (top) and D-Tic-Cys-Tyr-D-Trp-Orn-Thr-Pen-Thr-NH_2 (bottom), energy minimized with NMR constraints (CHARMM).
Both structures have the same backbone conformations, but different topographies.

13 may provide a unique opportunity to investigate the structural relationships of opioid agonists and antagonists. Peptide 14 is yet another truncated analogue of potent TCTP 8, in which the endocyclic Thr^6 has been deleted with respect to 8. This causes a dramatic decrease in affinity (about 7800 with respect to 8) for the mu opioid receptor.

Modifications on the C-terminal Position.

Finally we have examined the importance of The C-terminal Thr-NH_2 residue for opioid and somatostatin receptor recognition. Analogue 15, which is identical to the potent analogue CTOP (2) except for the deletion of the exocyclic Thr^8 residue, exhibited greatly reduced affinity (43 times lower than CTOP) for μ as well as δ receptors, while conserving low affinity (of the same order of magnitude as 2) for somatostatin receptors. In the same manner, 16, an analogue of 15 with Lys^5 substituting Orn^5 as in 1, showed greatly reduced affinity at the mu (approximately 31-fold, relative to 1), as well as the delta opioid receptor, but not at the somatostatin receptor.

Since previous studies had shown (Pelton et al., 1986) that a carboxamide C-terminal group greatly improves the ligand's affinity and selectivity for the mu opioid receptor relative to a carboxylate terminal group, the "double carboxamide" analogue D-Phe-Cys-Tyr-D-Trp-Lys-Thr-Pen-Asn-NH_2 (17) was synthesized in order to determine whether an increased "concentration" of carboxamide groups at the C-terminal would enhance binding to the μ receptor. 17 exhibited lower affinity (by a factor of 10 or more) in all receptor bioassays. As

expected, however, an even sharper decrease of affinity to the mu opioid receptor was found for the analogue with a mixed carboxylic acid-carboxamide terminal, D-Phe-Cys-Tyr-D-Trp-Lys-Thr-Pen-Asp-NH_2 (18, Table 4).

The SAR of analogues 15, 16, 17, and 18 (Table 4) suggested that the terminal threonine plays a very important role in binding of these analogues to mu receptors. On the basis of these findings, the relative importance of the hydrophobic β-methyl and hydrophilic β-hydroxyl moieties of Thr^8 for their interaction with the mu receptor were further examined. Thus, D-Phe-Cys-Tyr-D-Trp-Lys-Thr-Pen-Thr-NH_2 (19) and D-Phe-Cys-Tyr-D-Trp-Lys-Thr-Pen-Ser-NH_2 (20) were synthesized. In these analogues the β-OH group of Thr^8 has been replaced by a methyl group (19) or the β-methyl group has been replaced by a hydrogen (20), respectively. In the peripheral guinea pig ileum assay, both peptides were found to be moderately potent mu antagonists, although not as potent as CTP, with 19 being more potent than 20 (Table 5). In the rat binding assay order of potency is reversed, but both peptides are still less potent than CTP. Finally, D-Tic-Cys-Tyr-D-Trp-Lys-Thr-Pen-Ser-NH_2 (21) was prepared to examine the effect of the D-Tic residue in the Ser^8 series. The significant increase of affinity for mu opioid receptors (compared to 20) is consistent with our previous results.

Generally, results in the <u>in vitro</u> guinea pig ileum assay (Table 5) paralleled results obtained from binding studies (Table 4). Thus, in both systems, D-Tic^1-containing analogues (8, 9, 10) are the most potent, followed by the D-Phe^1-containing analogues (1, 2, 3),

while all chemical modification at the C-terminal Thr^8 and reduction of the ring size of CTP were detrimental to affinity for opioid receptors.

To date, only preliminary pharmacological characterization of peptides 22-27 is available (for receptor binding data see Table 4). In all cases, affinities of peptides 22-27 to δ opioid receptors are very low. None of these compounds exhibits high affinity for the μ receptor either. Nonetheless, there are several features worth noting. First, peptide 22 is much less potent at the μ opioid receptor than its parent compound 2. The fact that peptide 25 lost its affinity to μ, but conserved weak affinity for δ receptors, suggests that possibly 1,4 aromatic group relationships are important for recognition by the δ opioid receptor (most δ selective ligands feature this structural element). An attempt was therefore made in 22 to rigidize the aromatic ring of $D\text{-}Trp^4$ in a g(+) conformation (by use of 1,2,3,4-tetrahydro-β-carboline in this position), while conserving a 1,3 aromatic relationship for recognition by the μ opioid receptors (Figure 32). Conformational analysis of 22 suggests a strikingly different side chain conformation of $D\text{-}Tca^4$ in 22 from that found for tetrahydroisoquinolines. A relatively rigid g(-) conformation of that side chain may perturb (via side chain - side chain interactions) the topography of 22, resulting in its low affinity to μ opioid receptors. Substitution of the 3-4 peptide bond by a methylene amino group in 23 also results in a loss of potency for the μ opioid receptor (about 28 times relative to 2). However, NMR studies detected a conformational equilibrium for 23 (see Experimental) which will require more extensive studies

to identify the primary conformers. Similarly, motional processes of peptides 24, 26, and 27 make it difficult to delineate these structural elements that may be related to their low affinities for the μ opioid receptors. However, it seems from the chemical shift analysis that replacement of the peptide bond by the methylene amino group results in stabilization of the g(-) side chain conformation for these cyclic amino acid residues. Peptide 25 is also quite interesting. Replacement of Tyr^3 by Tic^3 in a molecule of 2 results in a substantial decrease of affinity of 25 for receptors. As suggested by conformational analysis, this can be related to the aromatic ring (on the third position) being rotated to the opposite side of the molecule (g(+) conformation, Figure 33). Only one aromatic ring pharmacophore (on the first position) is now found on the "recognition side" of the ligand. Thus, the μ opioid receptor cannot recognize the ligand's new topography. This result is complementary to the one obtained for peptide 12, in which analogous topographical modification also resulted in a decrease in affinity at the μ opioid receptor. These results suggest that, indeed, both aromatic side chains on the first and third positions are critical for the ligand's affinity to μ opioid receptors.

D-Phe-Cys-Tyr-D-Trp-Orn-Thr-Pen-Thr-NH_2

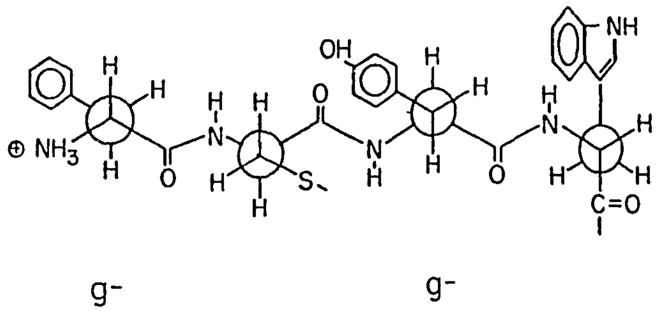

D-Phe-Cys-Tic-D-Trp-Orn-Thr-Pen-Thr-NH_2

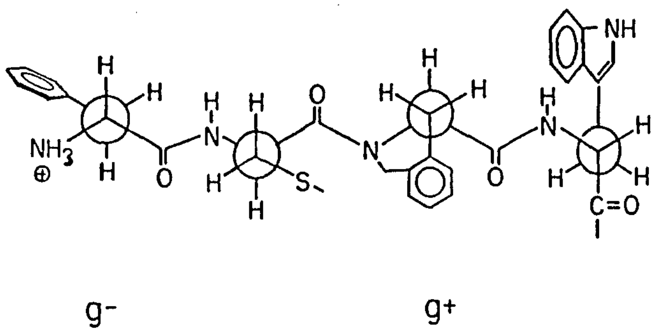

Figure 32.

Newman representations of aromatic ring determined topography in D-Phe-Cys-Tyr-D-Trp-Orn-Thr-Pen-Thr-NH_2 (top) and (determined by the ^1H NMR) D-Phe-Cys-Tic-D-Trp-Orn-Thr-Pen-Thr-NH_2 (bottom).

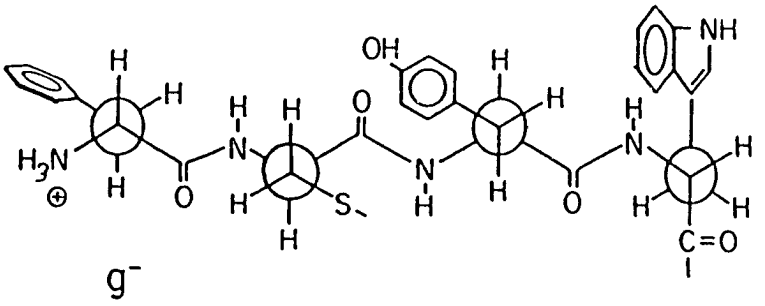

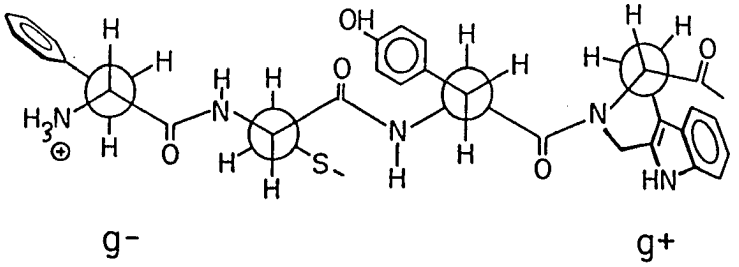

Figure 33. Newman representations of the aromatic ring topography determined for D-Phe-Cys-Tyr-D-Trp-Orn-Thr-Pen-Thr-NH_2 (top) and (putatively) in D-Phe-Cys-Tyr-D-Tca-Orn-Thr-Pen-Thr-NH_2 (bottom).

Chapter 4.

CONFORMATIONAL ANALYSIS AND DYNAMICS OF CONSTRAINED SOMATOSTATIN ANALOGUES: NUCLEAR MAGNETIC RESONANCE STUDIES

N-terminally Modified Cyclic Octapeptides.

D-Pgl-Cys-Tyr-D-Trp-Lys-Thr-Pen-Thr-NH_2, PCTP.

Unambiguous assignment of all ^1H signals in PCTP was facilitated by use of phase sensitive 2D COSY experiments (Marion and Wüthrich, 1983; Rance et al., 1983; Figure 34). Homonuclear decoupling combined with difference spectroscopy was used to selectively extract coupling constants out of crowded spectral regions. Additionally COSY experiments with delays were used to obtain the long-range couplings (Bax and Freeman, 1981) between the β protons and the ortho aromatic protons of the Tyr^3 and D-Trp^4 residues. All spectral assignments and coupling constants as well as temperature factors for the amide protons are listed in Table 6. Phi (ϕ) angles consistent with the observed coupling constants (Figure 35) were calculated by use of the Karplus-Bystrov (Bystrov, 1976) relationship and used to examine possible conformations consistent with the data. Vicinal $\alpha\beta$ coupling constants, assigned to pro-R and pro-S β-hydrogens (Kobayashi et al., 1981), enabled us to calculate side chain rotamer populations (De Leeuw and Altona,1982; Feeney, 1976; Figure 36). 2D NOE studies were helpful in differentiating between the Thr^8 and Thr^6 resonance, due to an interresidual NOE observed between Lys^5 CH_α and Thr^6 NH as well as between Pen^7 CH_α and Thr^8 NH.

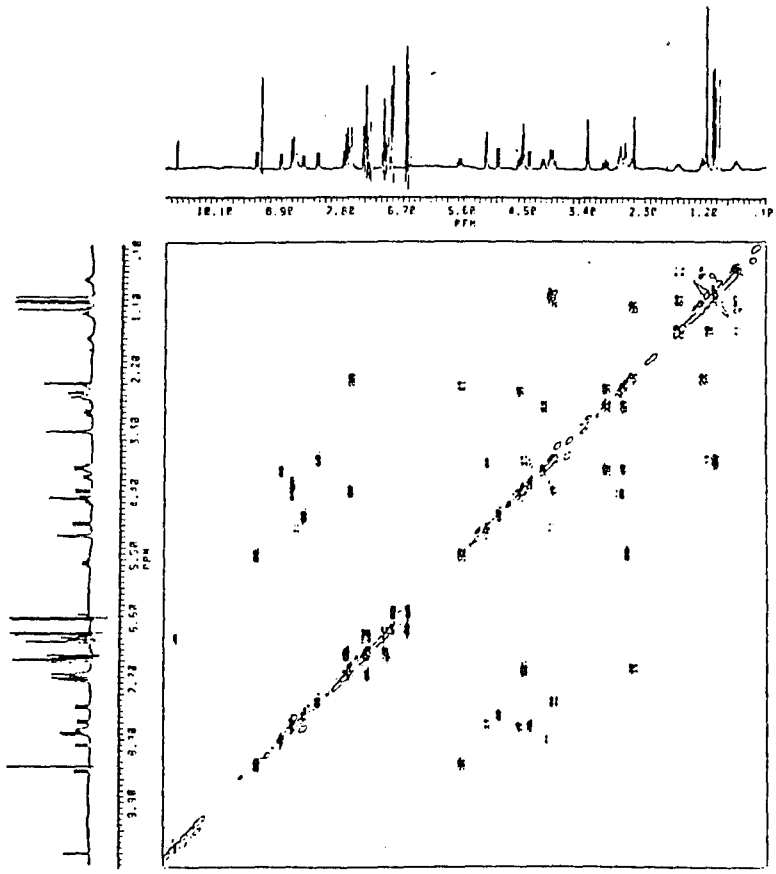

Figure 34.

Phase sensitive COSY spectrum of D-Pgl-C$\overline{\text{ys-Tyr-D-Trp-Lys-Thr-Pen}}$-Thr-$NH_2$
(303K, d_6-DMSO)

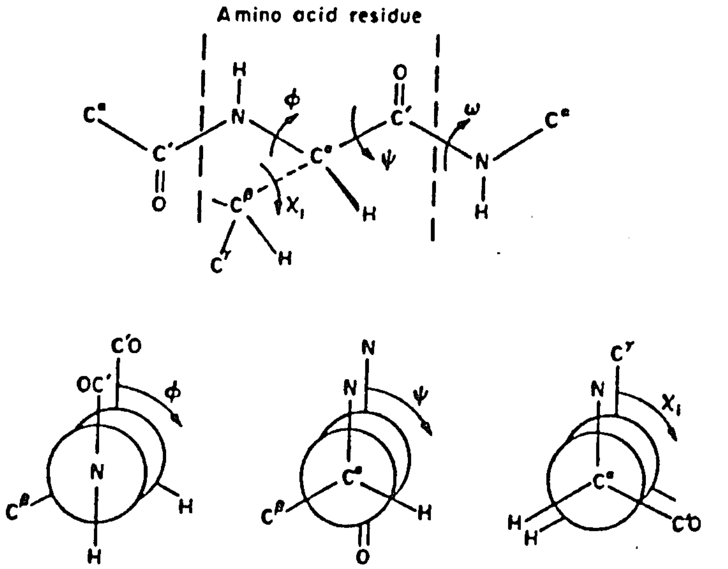

Figure 35 .

Definition of ψ, ϕ, and χ dihedral angles, determining protein/ peptide conformation.

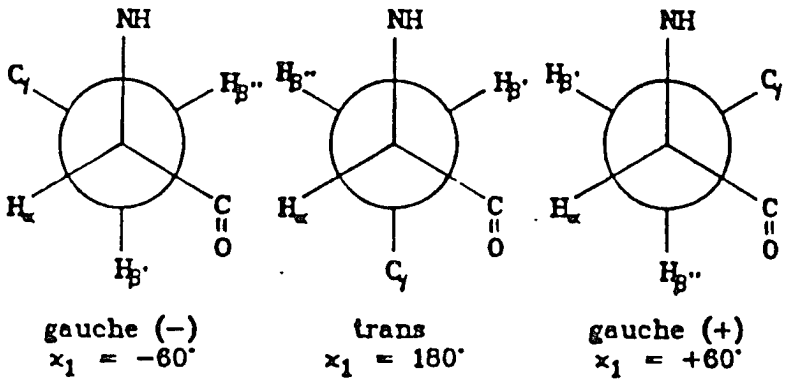

Figure 36.

Rotamer Populations About the Cα-Cβ Bond

Table 6. Spectral assignments, coupling constants and temperature factors for PCTP, 8, 11, 12.

Residue		D-Pgl[1]	D-Tic[1]	N-Me-D-Phe[1]	Gly-D-Tic[1]
Gly	NH				8.02
	CH				4.85/4.54 (J_9 = 15.4)
	NH	8.62	7.75	8.72	------
Xxx[1]	CH	5.19	4.25 ($J_{\alpha\beta}$=12.1,3.6)	4.30 ($J_{\alpha\beta}$=8.9,4.7)	5.05 ($J_{\alpha\beta}$ = 6.3, 6.3)
	CH		3.43/3.13 (J_g=16.3)	3.33/3.15 (J_g=14.3)	3.34/3.13 (J_9 = 15.4)
			$N-CH_2$ 4.37		4.57
Cys[2]	NH	9.36 (J=9.7, $\Delta\delta/\Delta T$= -5.1)	9.44 (J=9.9, $\Delta\delta/\Delta T$= -5.1)	9.35 (J=9.2, $\Delta\delta/\Delta T$=-5.9)	8.63 (J = 9.8, $\Delta\ell/\Delta T$ = -4.7)
	CH	5.66 ($J_{\alpha\beta}$=7.7,7.7)	5.64 ($J_{\alpha\beta}$=9.4,7.3)	5.53 ($J_{\alpha\beta}$=9.2,6.8)	5.37 ($J_{\alpha\beta}$ = 7.3, 3.7)
	CH	2.64	2.85 (J_g=N.D.)	2.75	2.78/2.68 (J_9 = 15.4)
Tyr[3]	NH	8.69 (J=8.1, $\Delta\delta/\Delta T$= -5.0)	8.63 (J=7.2, $\Delta\delta/\Delta T$= -3.5)	8.48 (J=8.26, $\Delta\delta/\Delta T$=-3.6)	8.56 (J = 7.8, $\Delta\ell/\Delta T$ = -4.1)
	CH	4.61 ($J_{\alpha\beta}$=8.1,6.9)	4.58 ($J_{\alpha\beta}$=8.0,6.3)	4.57 ($J_{\alpha\beta}$=8.1,6.8)	4.55 ($J_{\alpha\beta}$ = 8.7/6.1)
	CH	2.74	2.77/2.74 (J_g=14.7)	2.80/2.63 (J_g=13.6)	2.68
D-Trp[4]	NH	8.90 (J=5.3, $\Delta\delta/\Delta T$= -5.1)	8.83 (J=5.7, $\Delta\delta/\Delta T$= -3.8)	8.83 (J=5.7, $\Delta\delta/\Delta T$=-5.8	8.87 (J = 5.4, $\Delta\ell/\Delta T$ = -4.0)
	CH	4.17 ($J_{\alpha\beta}$=9.4,5.8)	4.20 ($J_{\alpha\beta}$=9.4,6.0)	4.22 ($J_{\alpha\beta}$=7.6/7.6)	4.15 ($J_{\alpha\beta}$ = 8.4/7.3)
	CH	3.00/2.69	3.04/2.71 (J_g=13.8)	3.03/2.80 (J_g=14.3)	3.00/2.73
Lys[5]	NH	8.23 (J=9.1, $\Delta\delta/\Delta T$= 7.68 -2.0)	8.24 (J=9.3, $\Delta\delta/\Delta T$= 7.75 -1.8)	8.39 (J=9.1, $\Delta\delta/\Delta T$=-4.5 7.60	NH 8.33 (J = 9.3, $\Delta\ell/\Delta T$ = -2.
Orn[5]	CH	3.98 ($J_{\alpha\beta}$=11.2,2.7)	4.02 ($J_{\alpha\beta}$=10.9,3.1)	4.10	CH_α 4.09 ($J_{\alpha\beta}$ = 10.5/3.2)
	CH	1.20/1.70	1.71/1.20	1.88/1.25	CH_β 1.85/1.14
	CH	.64	0.68	1.10	CH_γ 0.92
	CH	1.28	1.32	2.60	CH_δ 2.58
	NH	2.54	2.54	----	δNH_2 7.58
Thr[6]	NH	7.66 (J=9.00, $\Delta\delta/\Delta T$= 0.0)	7.69 (J=8.5, $\Delta\delta/\Delta T$= 0.3)	7.66 (J=9.0, $\Delta\delta/\Delta T$= -.2)	7.65 (J = 9.1, $\Delta\ell/\Delta T$ = -0.2)
	CH	4.52 ($J_{\alpha\beta}$=7.2)	4.56 ($J_{\alpha\beta}$=6.8)	4.53 ($J_{\alpha\beta}$=6.8)	4.58 ($J_{\alpha\beta}$ = 7.0)
	CH	3.95 ($J_{\beta\gamma}$=6.3)	4.00 ($J_{\beta\gamma}$=6.7)	4.02 ($J_{\beta\gamma}$=6.4)	3.92 ($J_{\beta\gamma}$ = 6.5)
	CH	1.06	1.04	1.04	1.05
Pen[7]	NH	8.49 (J=9.8, $\Delta\delta/\Delta T$= -8.5)	8.49 (J=8.7, $\Delta\delta/\Delta T$= -6.5)	8.44 (J=9.6, $\Delta\delta/\Delta T$= -3.4)	8.41 (J = 9.8, $\Delta\ell/\Delta T$ = -6.0)
	CH	4.96	4.94	4.96	4.78
	CH	1.18/.95	1.27/1.13	1.26/1.21	1.17/0.90
Thr[8]	NH	8.69 (J=8.1, $\Delta\delta/\Delta T$= -5.0)	8.39 (J=9.4, $\Delta\delta/\Delta T$= -4.3)	8.44/ J=8.4, $\Delta\delta/\Delta T$=-4.0	7.95 (J = 9.0, $\Delta\ell/\Delta T$ = -2.1)
	CH	4.40 ($J_{\alpha\beta}$=3.4)	4.30 ($J_{\alpha\beta}$=3.5)	4.36 ($J_{\alpha\beta}$=3.2)	4.23 ($J_{\alpha\beta}$ = 3.9)
	CH	4.02 ($J_{\beta\gamma}$=6.3)	4.00 ($J_{\beta\gamma}$=6.7)	4.02 ($J_{\beta\gamma}$=6.3)	4.00 ($J_{\beta\gamma}$ = 6.3)
	CH	1.02	1.05	1.04	0.99

Table 7. Relative intensities of interresidual NOE cross-relaxations for the PCTP, 8, 11, 12.

Residue	[D-Pgl^1]CTP	[D-Tic^1]CTP (8)	[N-Me-D-Phe]CTOP (11)	[Gly-D-Tic^1] (12)
NH^i/NH^{i+1}				
Lys^5/Thr^6	+++	+++		+ + +
Orn^5/Thr^6			+++	
CH^i/NH^{i+1}				
Xxx^1/Cys^2	+++	N.O.	+++	+ + +
Cys^2/Tyr^3	+++	+++	+++	+
$Tyr^3/D\text{-}Trp^4$	+++	+++	+++	+ + +
$D\text{-}Trp^4/Lys^5$	+++	+++		-----
$D\text{-}Trp^4/Orn^5$			+++	+ + +
Lys^5/Thr^6	N.O.	+		-----
Orn^5/Thr^6			+	N.O.
Thr^6/Pen^7	+++	+++	+++	+ + +
Pen^7/Thr^8	+++	+++	+++	+ + +
CH_α/CH_α				
Cys^2/Pen^7	+++	+++	+++	+ + +

[a] + = weak; +++ = strong; N.O. = not observed

Additionally, important information regarding the backbone conformation can be obtained (Table 7) from NOESY experiments. As the magnitude of magnetization transfer is inversely proportional to the sixth power of the distance between two protons, quantitative estimations of the NOE effects allow us to build up a 3D distribution of protons that can also be described by the ϕ, ψ, and χ angles (IUPAC-IUB,1970) of the amino acid residues. In this regard, NOE experiments can identify and distinguish between well known secondary structures such as the α-helices, β-turns, γ-turns, β-sheets, etc. (Shenderovich et al., 1984). Thus, type I β turns are characterized by NH^{i+1}/NH^{i+2} and NH^{i+2}/NH^{i+3} NOE signals (Wüthrich et al., 1984), type II β turns by CH^{i+1}/NH^{i+2} and NH^{i+2}/NH^{i+3} (Rao et al., 1983), γ turns by CH^{i+1}/CH^{i+2} (Grathwohl et al.,1975), etc. Analysis of the 2D NOE spectrum of PCTP reveals very important interactions between the Lys^5 NH and Thr^6 NH protons as well as between the D-Trp^4 CH_α and Lys^5 NH protons (spectra not shown) suggesting the presence of a type βII' turn (Sugg et al.,1988). This is supported by a near zero temperature dependence of the Thr^6 amide chemical shift (Table 6), suggesting an intramolecular H-bond to the i+3 (Thr^6) NH.

The ϕ angles required for the type βII' turn are found among those available from analysis of the coupling data from Table 6 using the Bystrov (1976) relationship, which further validates our conformational considerations.

Wüthrich et al. (1984) analyzed distance vs. ψ angles for cis and trans isomers of the Pro-Pro dipeptide, and showed that for peptides with trans peptide bonds, the distance between the CH_α and CH_2

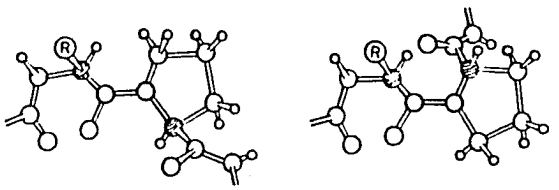

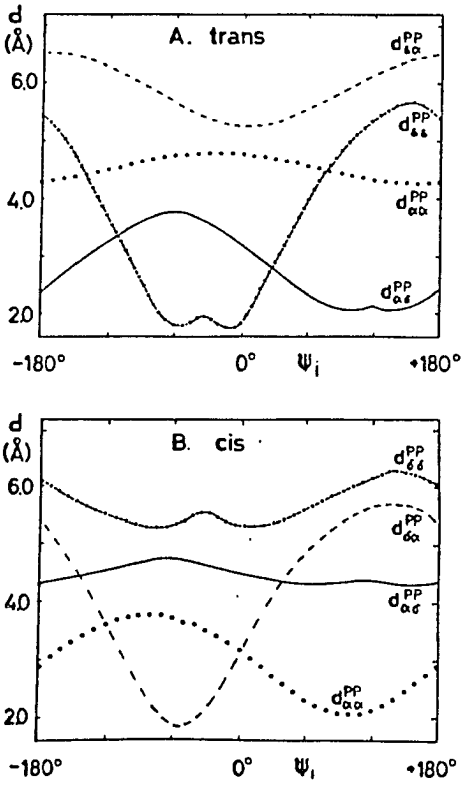

Figure 37. Distance vs dihedral angle ψ for cis and trans peptide bond of the Pro-Pro dipeptide. by Wüthrich et al., (1984).

reaches the minimum (and the NOE reaches the maximum) for ϕ_i <+60 to 180> degrees (Figure 37). In the case of a cis peptide bond, no ψ rotation can place the protons $CH_\alpha{}^i$ and $CH_{2\delta}{}^{i+1}$ (NH^{i+1}) spatially within 4.2 angstroms, where the NOE is observable. Cis peptide bonds occur rather rarely in linear or large cyclic peptides, except for N-substituted amino acids. Table 7 reveals that in CTP strong NOEs exist between CH^i and NH^{i+1} of the peptide pairs 1/2, 2/3, 3/4, 4/5, 6/7, 7/8. It is thus reasonable to assume that all these peptide bonds are trans (180 degrees).

No ψ angle can be directly determined from ^1H NMR coupling constant experiments. However, NOESY experiments suggest that for the L-amino acids ψ = 60° to 180° and for D-amino acids (D-Pgl^1,D-Trp^4) ψ = - 60 to -180° (Figure 24). The latter value is in the range expected for ψ^{i+1} of a type II'β turn, which has an idealized value of -120°. It should be noted that the existence of a strong NH_5/NH_6 NOE precludes a strong $CH^{\alpha}{}_5/NH_6$ NOE. Thus, assuming a trans bond, ψ_5 = -120 to 0°; this range is expected for the ψ_{i+2} of a type II'β turn which has an idealized value near 0 degrees.

Also, an interresidual NOE for the Cys^2CH_α to Pen^7CH_α was detected (Figure 26) which suggests a disulfide bond helicity similar to that of CTP (1). Comparisons of the spectral parameters for CTP and PCTP, as well as their side chain populations (Table 6) leads to the conclusion that both compounds have very similar backbone conformations as well as topologies of the aromatic side chain residues. Therefore, the only major difference between their topographies is the closer proximity of the aromatic rings (believed to be pharmacophores)

of the 1st and the 3rd residues in PCTP (Figure 28, empty square structure) than in CTP. This closer spatial relationship results in a somewhat more folded conformation of PCTP as compared with CTP (1), which seems to be responsible for the observed loss of potency and selectivity at the μ opioid receptors. Thus, by a proper topological adjustment of critical interresidual distances, one can alter receptor affinity and selectivity, respectivelly to other receptor classes.

A compact topography in this region by PCTP leads to a large decrease of affinity for μ receptors and a relative increase in selectivity to δ opioid receptors. In CTP (1), a large population of the gauche(-) side chain rotamer of D-Phe^1 results in a more extended conformation, apparently well recognized by the μ but not the δ opioid receptors. Qualitatively, therefore, one would expect that a rigidization of the side chain of D-Phe^1 in the gauche(-) conformation would further enhance the peptide's affinity and selectivity for μ opioid receptor. The Tic residue was chosen to examine this hypothesis. Analysis of the conformational properties of [D-Tic^1]CTP, 8. [D-Tic^1]CTP (8) was synthesized and indeed was found to be more selective and potent towards the μ opioid receptor than CTP (1), Table 4. The immediate questions arise as to which of the two allowed side chain conformations is present in this analogue, and whether the overall topology of the neuropeptide is perturbed due to the rigidity and structural properties of D-Tic. As with PCTP, all of the ^{1}H NMR spectral signals were assigned (Table 6), the ϕ angles calculated (Table 8), and the side chain rotamer populations determined. NOESY cross peaks (Table 7) indicated a type II' β turn for the Tyr-D-Trp-

Lys-Thr fragment of this peptide as well, and this was strongly supported by the presence of an H-bonded amide of Thr^6 (Table 6). Analysis of other spectral parameters, including side chain rotamer populations, decisively excluded any major perturbation of the cyclic structure of the peptide due to the D-Tic amino acid. Moreover, the disulfide bond helicity is not altered by the substitution at the N-terminal position, as deduced from a strong transannular Cys^2CH_α to Pen^7CH_α NOE cross peak (Table 7; Figure 38). Most of the cross-relaxation CH^i/NH^{i+1} interresidual NOEs found for PCTP were also observed in 8 (Table 7), with the exception of 1/2 NOE. As cis peptide bonds generally are not formed by α-amino acids, it is reasonable to assume a trans 1/2 peptide bond with a possible ψ_1=<0;120> degrees. Other ψ angles are in the same range as for PCTP, and all ω angles are 180 degrees (all trans peptide bonds).

To determine the two conformations possible for Tic, gauche(-) and gauche(+) (Figure 8), the ^1H NMR splitting pattern for the vicinal protons of D-Tic was examined. Comparison of these coupling constants (Table 6) demonstrated that in [$D\text{-}Tic^1$]CTP the Tic residue has a gauche(-) conformation about the C_α-C_β (χ^1) bond. Thus, the aromatic ring of $D\text{-}Tic^1$ becomes rigidized in a conformation (the carbonyl group is equatorial) that results in an extended structure of peptide 8 (Figure 28, solid squares). In light of the other NMR data, and consistent with that of the weakly potent PCTP, this topographical feature seems to be exclusively responsible for the observed biological properties of 8 relative to CTP 1. The spatial relationship of the

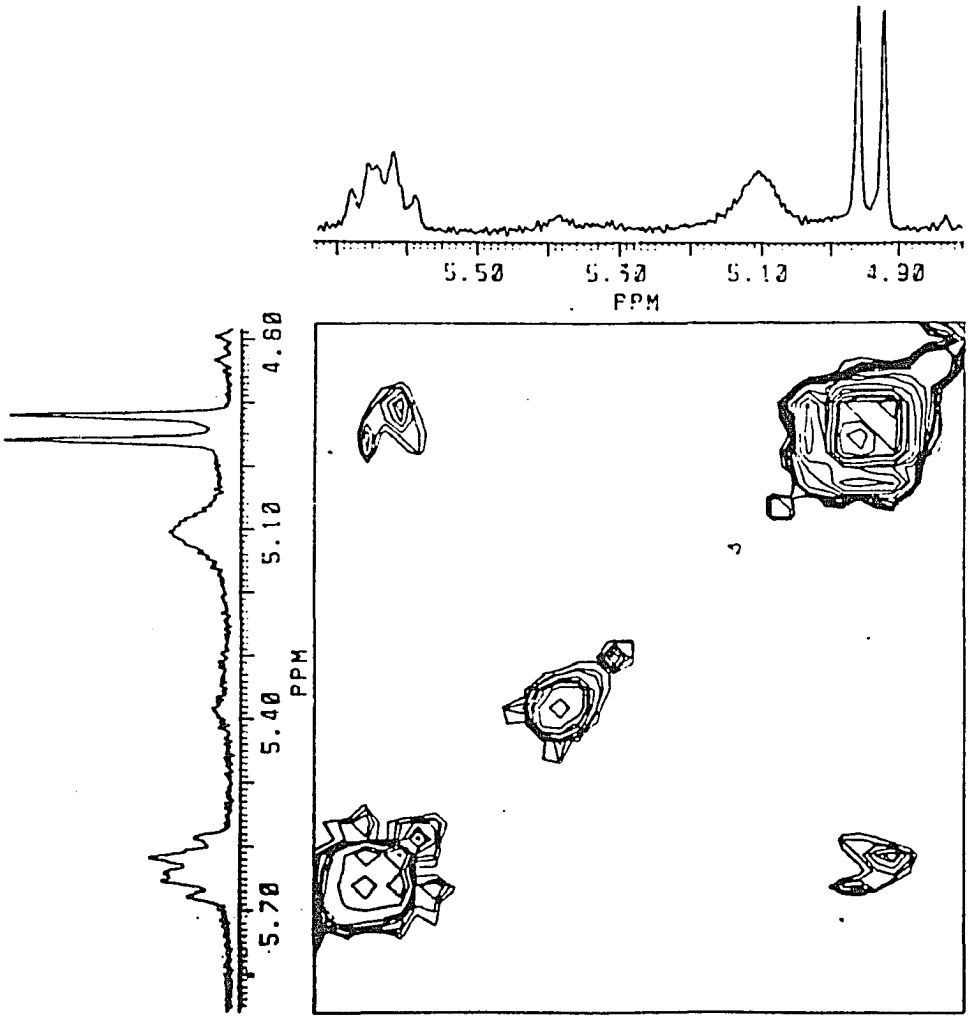

Figure 38. 2D NOESY spectrum for TCTP in d_6-DMSO, with emphasis on αH region of Cys and Pen.

aromatic pharmacophores can be examined using Newman representations (Figure 29), and is characterized by increased distance between them compared to PCTP.

Analyzing Table 6, one notices very similar chemical shifts for peptides 1 and 8. There is a small upfield shift of the $Thr^{8}CH_{\alpha}$ (0.08 ppm) and the Thr^{8} NH (0.16 ppm), and the chemical shift difference for the β,β-geminal methyl groups of Pen^{7} is larger for 8 than for 1 (0.14 vs. 0.08 ppm, respectively). This parameter is remarkably large for PCTP (0.23 ppm), consistent with the constrained nature of the peptide, and spatial proximity of D-Pgl aromatic ring to the disulfide moiety, thus exerting strong ring current anisotropy.

D-N-Me-Phe-Cys-Tyr-D-Trp-Orn-Thr-Pen-Thr-NH_2, 11.

A dramatic change in the pharmacological properties of peptide 11 was observed. This compound exhibited a very weak (300 times less than 8) binding at the μ opioid receptor (Table 4). Comparison of coupling constants, chemical shifts (Table 6), ϕ angles (Table 8), population of side chain rotamers, and the magnitude of NOE cross-relaxations suggest that 11 still conserves a type II' β conformation with a negative disulfide helicity. As in PCTP but not 8, the CH^{i}_{α}/NH^{i+1} interresidual signals are strong for all, but the 5/6 case, indicating $\psi_1 \approx$ -60 to -180°. Again, an important differences was noticed only for the 1st position. As calculated from vicinal coupling constants, there is a substantial participation of the trans side chain rotamer, with a lesser amount of the gauche(-) and gauche(+) populations of $D\text{-N-Me-Phe}^{1}$. This effect can be explained in terms of

nonbonded interactions between the N-methyl and phenyl groups which lead to destabilization of the usually energetically more favorable gauche(-) conformation. In terms of topography, the phenyl ring of residue 1 in peptide 11 is rotated towards the tyrosyl ring to a larger extent than in peptide 1.

Furthermore, the consistency of other parameters throughout the molecule relative to peptides 1, 8 and PCTP gives support to the suggestion that conformational changes occur only at the N-terminal position, pointing out that the observed pharmacological effects can be directly attributed to the relative spatial relationships of the position 1 amino acid with other pharmacophore elements of the ligand.

Gly-D-Tic-Cys-Tyr-D-Trp-Orn-Thr-Pen-Thr-NH_2, 12.

The topographical features of this peptide will be contrasted with these of peptide 8, so as to determine those differences that may have led to such a remarkably different affinity to opioid receptors, as a result of glycine coupling to peptide 8. Assignments of all proton signals, coupling constants and temperature factors for labile protons are presented in Table 6. Phi angles were calculated by the method of Bystrov (1976) and are given in Table 8.

The principale information about the backbone conformation can be obtained from NOE analysis (Table 7). As previously observed for compounds of this class, there are two important NOEs between $CH^4{}_\alpha$/NH^5 (Figure 39) and NH^5/NH^6 (Figure 40) for peptide 12. The presence of these and the absence of other cross-relaxation effects suggest that a type II' β-turn represents backbone conformation for 12 (Kes-

Table 8. Possible dihedral angles ($NH\text{-}CH_\alpha$) for PCTP, 8, 11, 12, determined from ^1H NMR coupling constants.

Residue	D-Pgl	D-Tic (8)	N-Me-D-Phe(11)	Gly-DTic (12)
Xxx[1]	N.D.	N.D.	N.D.	N.D.
Cys[2]	-140/-135 -113/-94	-157/-130 -112/-92	-154/-140 -101/-86,48/72	-149/-134 -112/ -94
Tyr[3]	-162/-152 -110/-94 38/82	-156/-146 -83/-76 32/42 78/92	-159/-140 -101/-86 48/72	-162/-152 -89/ -82 37/ 88
D-Trp[4]	67/163,79/66 -19/-23, -92/-102	172/166, 75/68 -20/-28 -92/-102	172/163,76/68 -21/-28,-94/-105	168/ 174 68/ 74 -19/ -25 -94/-105
Lys[5]	-154/-141 -101/-88	-152/-140 -103/-86 52/71	-154/-141 -101/-88 47/74	-152/-140 -103/ -86 52/ 71
Orn[5]	47/74			
Thr[6]	-156/-143, -100/-87, 47/75	-159/-149 -93/-82 40/80	-156/-143 -100/-87 47/75	-154/-141 -101/ -88
Pen[7]	-150/-135 -112/-93	-156/-146 -94/-84 42/59	-145/-135 -105/-92	-150/-135 -112/ -93 47/ 74
Thr[8]	-161/-150 -86/-83 38/82	-152/-140 -103/-89	-161/-150 -92/-83 40/82	-156/-143 -100/-87 47/ 75

sler et al., 1983; Rao et al., 1983). This assumption identifies ϕ_{i+1}, ψ_{i+1} and ϕ_{i+2}, ψ_{i+2} being in good conformity with those predicted for the ϕ angles by the ^3J couplings (Table 8). Interresidual NOEs between CH^i_α and NH^{i+1} for 12 (Table 7) require a few comments. A type II' β turn backbone conformation precludes any close contact between the CH^{i+2}_α and NH^{i+3}. In agreement with that, only a weak NOE peak was detected in the 2D NOE spectrum of 8, and none in the case of peptide 12. Strong cross-relaxation between, respectively, alpha and amide protons of D-Tic^1/Cys^2, Tyr^3/D-Trp^4, D-Trp^4/Orn^5, Thr^6/Pen^7 and Pen^7/Thr^8 pairs suggests that there are no cis peptide bonds present in 12, and also defines the possible range of ψ angles (vide supra). The absence of a D-Tic/Cys NOE for 8 should not be attributed to a cis peptide bond formation, but rather to ψ_1 = 0 to 120°. The D-Tic$_\alpha$/Cys NH cross-relaxation signal for 12 suggests α ψ_1 completely different from that found in 8, possibly in the range of 180 to 300°. These interesting differences between the two compounds may be due to different compatibilities of the relatively rigid side chains of Tic with the adjacent parts of the molecule. In view of negligibly small size of the Gly residue attached to D-Tic in 12, one may expect some significant conformational differences for the tetrahydroisoquinoline residue in both peptides. This important point will be explored further in the text in more detail. Another observation (Table 6) is that the chemical shifts of the β-turn forming residues are fairly comparable for both 8 and 12, whereas significant deviations can be noticed for both exocyclic residues. Yet, the prominent cross-relaxation signal observed between the alpha protons of Cys^2 and Pen^7 of

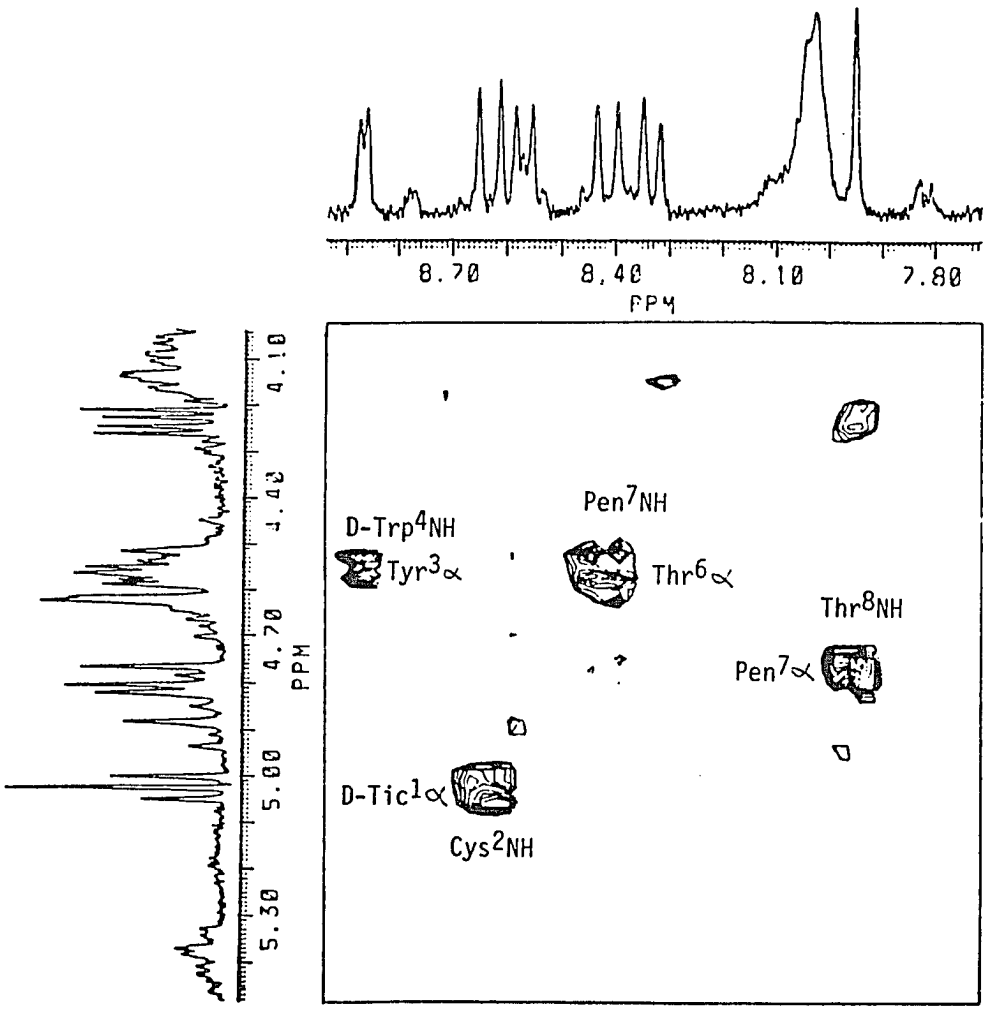

Figure 39.

NOESY spectrum of Gly-D-Tic-Cys-Tyr-D-Trp-Orn-Thr-Pen-Thr-NH_2

(303K, d_6- DMSO)

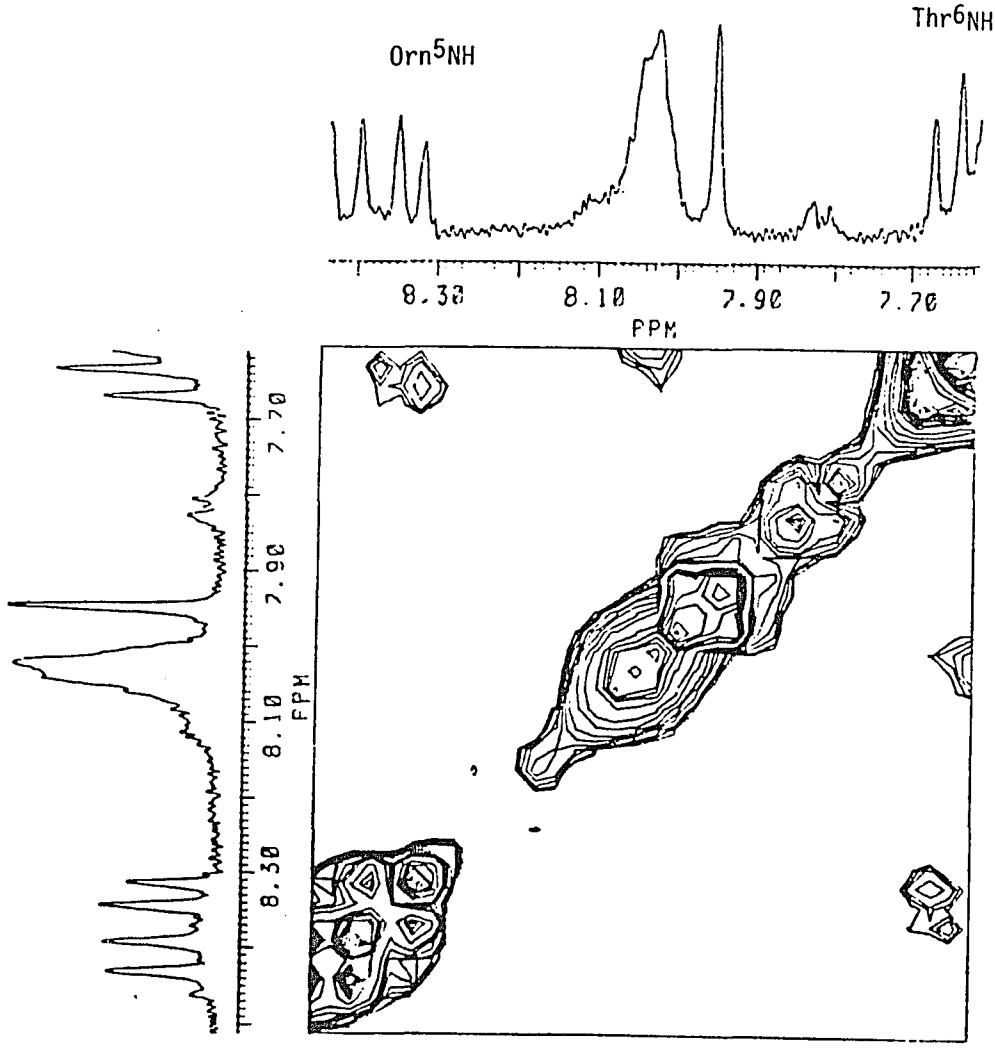

Figure 40 .

NOESY spectrum of Gly-D-Tic-Cys-Tyr-D-Trp-Orn-Thr-Pen-Thr-NH_2

(303K, d_6-DMSO)

12 indicates that the disulfide helicity in peptide 12 is similar to that of peptide 8. Analysis of side chain populations (Table 9) suggests significant differences in their distribution only for Cys^2 (in 12).

It can be concluded, therefore, that the conformations of the cyclic hexapeptide domain in both 8 and 12 are very similar. However, important conformational perturbations occur in the N-terminal exocyclic position, which may be of relevance for the opioid receptor selectivities for both peptides. Therefore, the focus of the analysis will now be directed towards the topography of the N-terminal residues in both 8 and 12. As observed in Table 6, both vicinal coupling constants of the D-Tic residue in 12 are equal and small and suggest a gauche(+) conformation of its side chain.

It needs to be emphasized at this point, before further discussion, that the gauche (+) conformation is the least stable for most amino acids. Such a configuration of substituents results in two strongly repulsive gauche interactions, whereas the generally more stable gauche(-) conformation shows only one gauche relationship of substituents around the C-C bond (Figure 8). This unexpected conformational behavior of D-Tic in 12 can be explained by a concept of pseudoallylic strains (Sugg et al., 1985; Johnson 1968). Tetrahydroisoquinoline carboxylic acid in the N-terminal position of a peptide sequence prefers the gauche(-) conformation (Figure 41). However, when any amino acid is coupled to the amine of Tic (e.g. Gly in 12) so that the Tic residue occupies an internal position in the peptide sequence a change of amine nitrogen hybridization to a partial sp^2 hybridiza-

Table 9. Rotamer side chain populations for peptides 8 and 12, as calculated from vicinal coupling constants.

Residue	D-Tic			Gly-DTic		
	g^-	t	g^+	g^-	t	g^+
Xxx[1]	100	0	0	0	0	100
Cys[2]	47.7	52.3	0	47.9	10.1	42
Tyr[3]	58.6	40.2	1.2	61.7	38.3	0
D-Trp[4]	62.5	37.5	0	32.8	67.2	0
Lys[5]	89.9	5.2	4.9	-------		
Orn[5]	------			85.3	6.1	8.6
Thr[6]	$			$		
Pen[7]	mostly g^+ or trans			mostly g^+ or trans		
Thr[8]	!			!		

$^{\$3}J_{\alpha\beta}$ indicates free rotation of this side chain

$^{!}$Low $^{3}J_{\alpha\beta}$ indicates that gauche αβ relationship takes place suggesting restricted rotation around C_α-C_β bond of this amino acid.

tion occurs. This has dramatic effects on the pipecolic acid ring conformation. Ring flattening results in strong 1,2 diequatorial repulsive interactions between the N- and C- substituents (Gly and Cys, respectively) of the Tic amino acid (Figure 41). This highly energetic configuration, I, is unstable and undergoes a flip to the ring chair conformation II (Figure 41), in which the N- and C- substituents are in 1,2 diaxial relationship. This rearrangement causes the pipecolic acid ring to attain a gauche(+) conformation. The increased stability of the gauche(+) form is due to replacement of the strong 1,2 diequatorial repulsions by weak 1,2 diaxial interactions. This mechanism seems to be fairly general, as it has been found in several other cases (vide infra, other experiments in progress). J coupling analysis is completely consistent with the distinct conformational properties of the Tic residue in 12 and with observed chemical shift differences.

First, a huge (-0.79 ppm) upfield shift of Cys^2 NH is observed. Similarly, though not as significant, an upfield shift can be noticed for the Thr^8 amide (-0.44). In light of earlier considerations it seems reasonable to assume that a D-Tic ring anisotropy effect, nonequivalent for different Tic conformations, causes these remarkable effects. Furthermore, a very meaningful difference in the alpha CH chemical shifts of tetrahydroisoquinoline resudues in both 8 and 12 occurs (4.15 vs. 5.05 ppm, respectively). In peptide 8 the gauche(-) conformation of Tic places the Tic αCH proton in an axial position, leading to a weak upfield shift caused by the aromatic ring anisotropy. When the Tic conformation is gauche(+) as in 12, the CH_α is in the

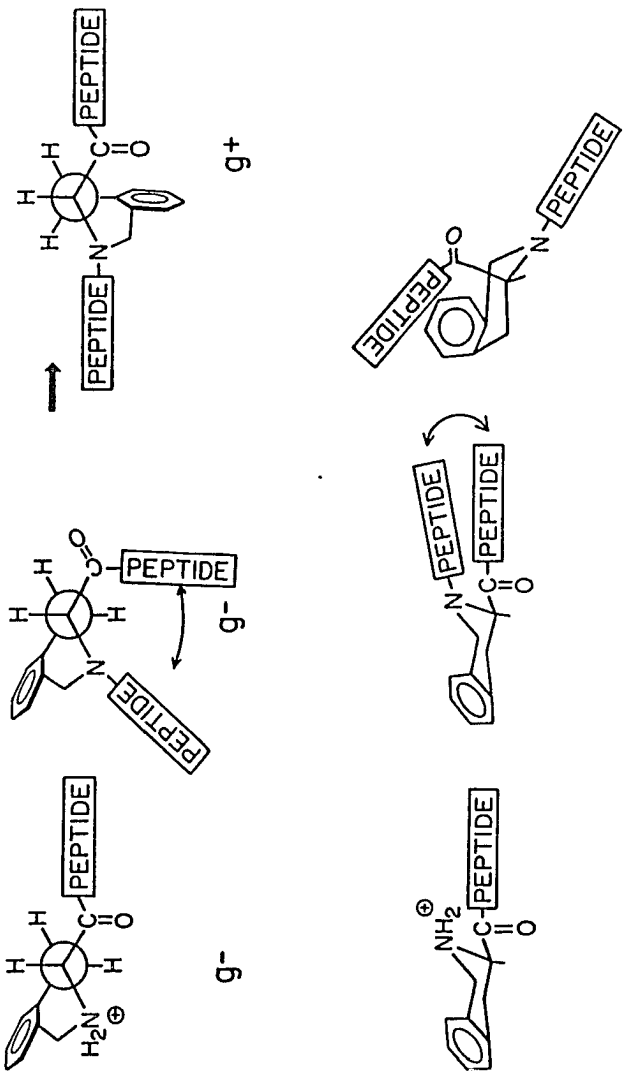

Figure 41. Conformational transformations of tetrahydroisoquinoline carboxylic acid (Tic).

deshielding cone of the aromatic ring, causing a downfield shift. All these independent observations support the model shown in Figure 41, and are explained well only by the ability of tetrahydroisoqunoline to adopt different conformational states.

Glycine residues may be used as a dynamic probe of peptide flexibility in their vicinity (Kessler et al., 1985). The chemical shift difference between the diastereotopic protons of 0.31 ppm (Table 6) suggests a relatively slow rotation of the Gly residue, probably due to steric compression with C-terminal Threonine. Additionally, the geminal coupling constants (Titlestad et al., 1973; Siemion, 1971) can be attributed to orientation of the π orbital of the glycine C=O bond. Thus, possible ψ angles for this residue are ±40° and ±140° (Bystrov, 1976).

Pseudopeptides and Bicyclic Peptides.

Design rationale of pseudopeptides.

The mechanism, schematically shown in Figure 41, that enables a tetrahydroisoquinoline to select the preferred conformation of its side chain, carries important consequences. It may be envisioned that strong 1,2 diequatorial interaction of substituents (carboxylic and the secondary amino group) can be relieved if the N-substituent is forced to attain a conformation out of the CH_2-N-C_α plane. To achieve this, properties that cause its planar arrangement (resonance of the carbonyl group with the free electron pair of the amino group) need to be removed. That can be done by replacement of the carbonyl group with a methylene unit. The resulting alkylamine may synthetically be

obtained by reductive alkylation of a picolic acid derivative bearing a peptide with an amino aldehyde in the presence of sodium cyanoborohydride. Since this procedure has not yet been described in the literature of solid-phase peptide synthesis technology for the case of secondary amino acids, the synthetic details are given in the Experimental.

If, indeed, lack of sp^2 hybridization in the nitrogen atom allows for nonplanarity of the proper ring fragment and N-substituent, then it may be anticipated that even a 1,2 diequatorial relationship of substituents may be energetically tolerated by the molecule. If that is the case, then even internally positioned (but alkylated) picolic acid derivatives may show a preference for the g(-) side chain conformation. To test validity of this theory compounds 21-27 (Table 4) have been synthesized, and characterized biologically and physicochemically.

Boc-Tyr(O-2,6-Cl_2Bzl)-ψ[CH_2]-D-TcaOMe (21).

Initially to establish the side chain preference of alkylated 1,2,3,4-tetrahydro-β-carboline, conformational studies were performed on a simple model title compound 21, the synthesis of which additionally allowed us to establish the best conditions for the desired series of reductive alkylation reactions on the resin.

Spectral assignments were obtained on the basis of a phase sensitive COSY experiment, and are tabulated in Table 10. The serious spectral overlap of CH_α/CH_2 signals of D-Tca required detailed spectral decoupling experiments. The nonequivalence of both vicinal

coupling constants and relatively low value of $J_{\alpha\beta''}$ suggest a dynamic equilibrium between g(+) and g(-) side chain conformers. This result encouragingly showed, however, that alkylated 1,2,3,4-tetrahydro-β-carboline indeed exhibits decreased bias towards the g(+) side chain conformation observed for acylated tetrahydroisoquinoline.

D-Phe-Cys-Tyr-D-Tca-Orn-Thr-Pen-Thr-NH_2, 22.

Total spectral assignments, as well as coupling constants for 22 are shown in Table 11, and were acquired as described in the Experimental section. Side chain conformer population and accessible $\phi(NH\text{-}CH_\alpha)$ angles are given in Table 12. Several features of these data are worth notice. First, quite unexpectedly, acylated D-Tca has a side chain conformation strongly biased towards a g(-) conformation. For reasons already discussed, in peptide 22 it is postulated that a dynamic equilibrium between at least two conformational states g(-) and g(+) takes also place ($J_{\alpha\beta}$=2.5;6.8 Hz).

At present the different behavior of D-Tic (in peptides 12 and 25) and of D-Tca in 22 is not clear, since both amino acids are based on a pipecolic acid structure. Further investigations, particularly molecular mechanics and dynamics calculations, will have to be carried out to characterize the contrasting conformational properties of both amino acids.

A comparison of ϕ angles with those of CTP (Sugg et al., 1988), TCTP (8; Kazmierski and Hruby, 1988a), and GTCTOP (12; Kazmierski and Hruby, manuscript in preparation) suggests that they are still compatible with a type II' β conformation (Table 12).

Table 10. Chemical shift and coupling constant assignments for model compound Boc-Tyr-(O-2,6-Cl_2-Bzl)-ψ[CH_2N]-D-TcaOMe, 28, d_6-DMSO, 303K.

Residue	Chem.shift [ppm]		Coupl. const. [Hz]
Tyr			
Bu^t	1.29	(s)	
NH	6.67		8.7
α	3.80	(m)	
β'	2.84	(dd)	α/β'=4.4
			β'/β''=13.9
β''	2.55	(dd)	α/β''=8.9
CH_2	2.75	(d)	$\alpha/\psi CH_2$=7.0
D-Tca			
α		(dd)	α/β'=3.3
			α/β''=5.9
β	2.99	(m)	
N-CH_2	4.07	(d)	NCH/NCH=14.8
	3.93	(d)	
OMe	3.53	(s)	

Table 11. Chemical shifts, coupling constant assignments and amide temperature coefficients for peptides D-Phe-Cys-Tyr-D-Tca-Orn-Thr-Pen-Thr-NH_2, 22, and D-Phe-Cys-Tic-D-Trp-Orn-Thr-Pen-Thr-NH_2, 25, d_6-DMSO, 303K.

Residue	Chem. shift [ppm] Temp. Factor [10^{-3}ppm/deg] 22	25	Coupl. const. [Hz] 22	25
D-Phe[1]				
NH_3^+	8.07 (m),	8.06 (m)		
	-1.04	-0.44		
α	4.20 (m)	4.02	α/β'=5.2	4.8
β'	3.29	3.23	α/β''=9.9	9.5
β''	3.00	2.96	β'/β''=14.0	13.8
Cys[2]				
NH	9.21	9.25	α/NH=10.2	8.7
	-5.1	-4.08		
α	5.32	5.47	α/β'=5.9	4.6
β'	3.05	3.20	α/β'=10.2	10.0
β''	2.80	2.92	β'/β''=15.5	13.6
Tyr[3] 22 Tic[3] 25				
NH	8.59	-----	α/NH=7.9	
	-4.0			
α	5.03	5.22	α/β'=7.0	4.1
β'	2.99	2.95	α/β''=8.5	5.8
β''	2.80	2.84	β'/β''=13.2	15.8
N-CH_2	----	4.89 (m)	----------	
D-Tca 22 D-Trp 25				
NH	---	8.09	------	6.2
		-4.7		
α	5.25	4.27	α/β'=2.5	6.6
β'	3.07	3.04	α/β''=6.8	8.8
β''	2.93	2.96	β'/β''=16.5	14.2
N-CH_2	4.70/4.50 (dd)	----	14.8	---
Orn[5]				
NH	8.4	8.29	α/NH=7.5	8.0
	-2.2	-3.1		
α	4.00	4.07	α/β'=4.8	4.7
β'	1.92	1.70	α/β''=6.4	9.1
β''	1.54	1.25		
γ	1.49	1.18		
δ	2.65	2.58		

δ-NH_3^+	.51	7.63 .23		
Thr[6]				
NH	7.40 -0.10	7.28 -0.84	α/NH=7.4	7.8
α	4.43	4.39	α/β=7.4	4.5
β	4.03	3.88	β/γ=6.3	6.3
γ	1.03	0.91		
OH	≈4.8	≈4.9		
Pen[7]				
NH	8.27 -6.3	7.92 -2.0	α/NH=9.4	9.0
α	4.88	4.80		
γ	1.24/1.28 .041	1.27/1.40 0.131		
Thr[8]				
NH	8.31 -4.7	8.32 -4.4	α/NH=9.7	8.3
α	4.30	4.26	α/β=3.6	3.9
β	3.98	4.01	β/γ=6.3	6.4
γ	1.06	1.05		
OH	≈5.01	4.90		

Similarly to CTP, the side chain conformation of peptide 22 is biased towards g(-) for D-Phe, but there is a high population of a trans rotamer of Cys^2 (t and g(-) for CTP). Also, the side chains of the amino acid preceding and following D-Tca (Tyr^3 and Orn^5, respectively) exhibit some extent of conformational disorder in comparison with CTP. While the side chain of Orn^5 in 22 seems to be almost equally divided among all three staggered states (mostly g(-) for Lys^5 in CTP), Tyr^3 has a preference for a trans (g(-) in CTP) side chain conformation. These perturbations at the 3 and 5 positions are almost certainly caused by the unusual conformational properties of D-Tca^4 (in 22), whereas the origin of the discrepancies for the 2^{nd} position amino acid (vide supra) is difficult to account for at present. Comparing 22 with the CTP 1 there is an upfield shift of the $Cys^2{}_\alpha$ (-0.32 ppm) and amide protons (-0.13), a downfield shift of the $Tyr^3{}_\alpha$ (0.44 ppm), as well as a dramatic downfield shift of $Orn^5{}_\alpha$ (0.80 ppm with respect to Lys^5 of CTP) protons. Similar to effects observed for other peptides with constrained amino acids, the ring current anisotropy of D-Tca residue seems to be responsible for these effects. Ring current effects of tryptophane and its derivatives are known to be much stronger than for any other naturally occurring aromatic amino acid (Giessner-Prettre and Pullman, 1971).

Nuclear Overhauser effects are in good agreement with the above analysis. There is a very strong cross-relaxation signal for alpha protons of Cys^2 and Pen^7, attributed to a negative disulfide helicity (Figure 42). Additionally, the characteristic $CH^i{}_\alpha/NH^{i+1}$

Table 12. Side chain conformer population and accessible ϕ angles derived from ^{1}H NMR analysis of D-Phe-Cys-Tyr-D-Tca-Orn-Thr-Pen-Thr-NH_2, 22, d_6-DMSO, 303K.

Residue	ϕ angles	rotamer population (%)
D-Phe[1]	---	
g(+)		0
t		28.6
g(-)		71.3
Cys[2]	-120	
g(+)		0
t		83.5
g(-)		16.5
Tyr[3]	-156, -87, 60	
g(+)		0
t		64.7
g(-)		35.3
D-Tca[4]	----------	*
Orn[5]	-160, -82, 38 82	
g(+)		39.5
t		39.6
g(-)		20.9
Thr[6]	-162, -80, 36, 84	---
Pen[7]	-144, -96, 60	---
Thr[8]	-150, -100	---

* see the text for a discussion.

cross-relaxation signals are observed for the following pairs of amino acids: 1/2, 4/5, 6/7, 7/8 (Figure 43). According to the explanation given before (vide supra) these pairs of amino acids are linked via trans peptide bonds. No $Cys^2{}_\alpha/Tyr^3NH$ (2/3) or Orn^5CH_α /Thr^6NH (5/6) cross-relaxations have been observed, but a significant effect was detected for Orn^5NH/Thr^6NH. In light of our earlier discussion (vide supra) and despite the presence of a conformationally constrained D-Tca residue in the core of the turn, a type II' β turn is the best descriptor of the backbone conformation of peptide 22. This is supported by a very low temperature coefficient of Thr^6NH suggesting that the amide is either hydrogen bound (to the Tyr^3 carbonyl group) or solvent shielded.

In summary, substitution of D-Trp^4 by D-Tca^4 in CTOP 2, resulting in peptide 22, does not seem to alter the peptide backbone conformation. The constrained nature of this cyclic amino acid, and its apparent ability to flip between both gauche(-) and gauche(+) conformational states, perturbs the side chain conformation of the neighboring residues: Cys^2, Tyr^3, and Orn^5. Another interesting observation from the NOESY experiments is a strong cross-correlation between the Tyr^3CH_α and both protons N-CH_2 of D-Tca. Further quantitative studies of this effect (peak volume estimation) will allow a more detailed description of the topographical consequences of D-Tca^4 substitution.

D-Phe-Cys-Tyr-ψ[CH_2NH]-D-Trp-Orn-Thr-Pen-Thr-NH_2, 23.

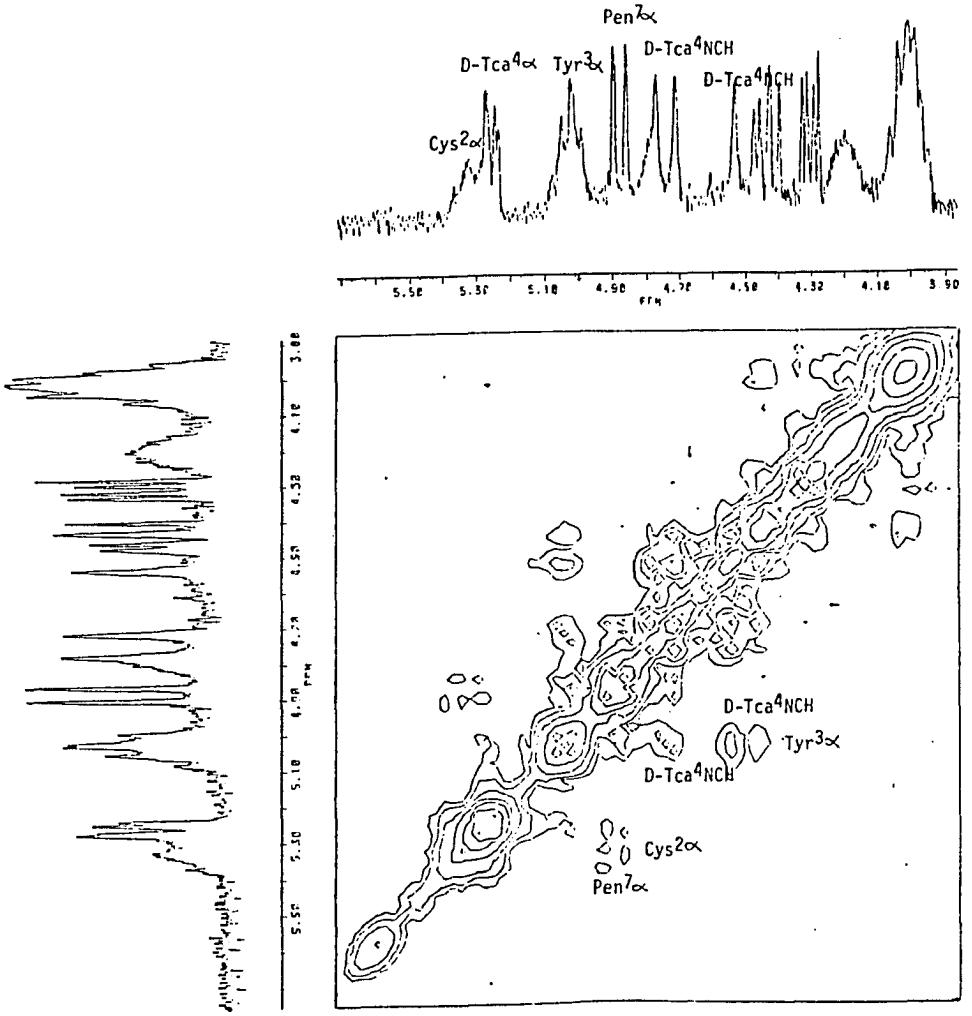

Figure 42.

NOESY spectrum of D-Phe-Cys-Tyr-D-Tca-Orn-Thr-Pen-Thr-NH_2

(303K, d_6- DMSO)

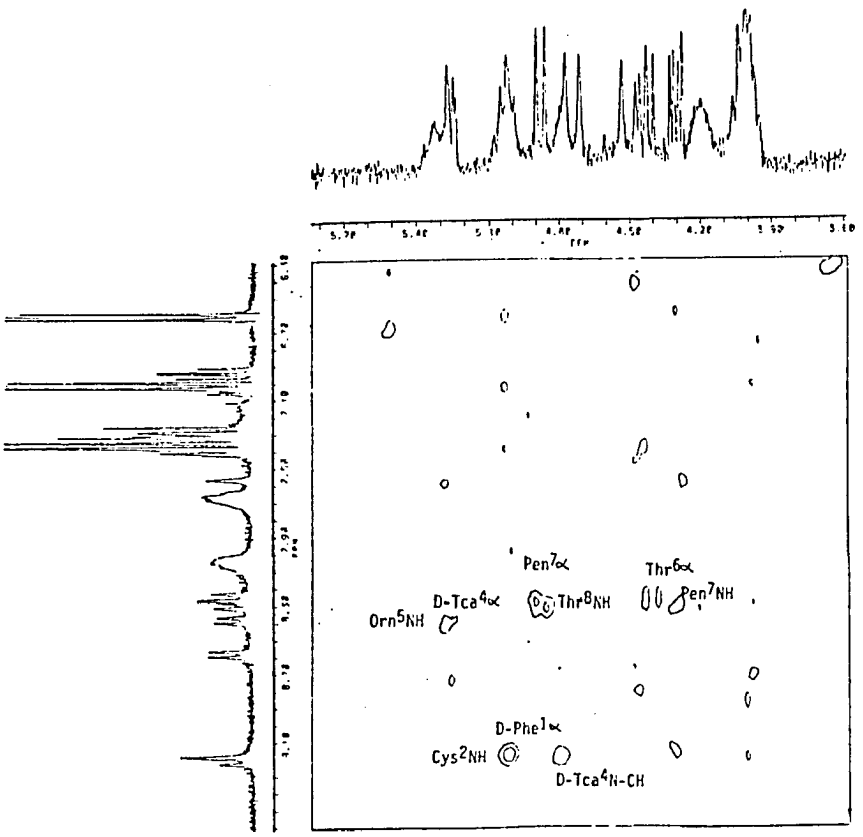

Figure 43.

NOESY spectrum of D-Phe-Cys-Tyr-D-Tca-Orn-Thr-Pen-Thr-NH_2

(303K, d_6- DMSO)

Peptide 23 is a model compound, with a simple peptide bond isostere modification in CTOP (2), that was to test whether there is any significant influence of CH_2/C=O substitution on peptide conformation, before considering more complex cases involving cyclic amino acids. Since chemical shift anisotropy was proven to be an important analytical tool (vide supra), it was of considerable interest to establish the magnitude of influence of this structural modification upon thec chemical shifts of the neighboring nuclei. Signal assignment and coupling constant analysis have been achieved using ^{1}H NMR techniques, as described in the Experimental and previous chapters (Table 13). There are several interesting points that can be immediately noticed. First of all, it was possible to obtain only limited information about vicinal coupling constants of D-Trp^4, and the signal of D-Trp^4 NH was not found. Additionally, the Tyr^3 amide appeared as a hump instead of the expected doublet. These startling irregularities in the ^{1}H NMR spectrum of 23 were all found for the 3rd and 4th residues only. Instead of the commonly seen pair of doublets of a AA'XX' system of Tyr (2,6 and 3,5 going upfield, respectively), a split signal (two doublets of uneven intensity) for the 2,6 protons were found at 303K (Figure 44). With an increase in temperature both signals fused and at 333K they coalesced into one doublet. Crude estimation of the activation enthalpy for the two site jump of the tyrosyl ring gives about 77.3 kJ/mol. This finding represents a rare experimental demonstration of restricted rotation of an aromatic side chain in a peptide, which is slow enough to observe on the NMR time scale (less than $10^3 s^{-1}$; Romanowska and Kopple, 1987). In a densely

packed structure such as peptide 23, the rotation of the ring between the two equilibrium orientations must displace neighboring side chains to some extent, in a concerted manner. Consequently, a rotational jump ($\pm 180°$ about C_β-C_1) depends on a degree of cooperativity with motions of surrounding groups. In principle, the rate and mechanism of this type of molecular motion can provide information about the conformational flexibility of neighboring residues. Activation energy measurements for tyrosine have been performed in several instances using ^2H quadrupole echo NMR line shape analysis and spin-lattice relaxation times in crystalline tyrosine-containing peptides (Rice, 1987). These studies detected 180° rotational jumps with the rate varying between 10^3-10^6 s^{-1}. Combined X-Ray/NMR studies of the molecular structure and dynamics of crystalline p-F-D,L-Phe showed that the phenyl ring exhibits two types of motion: a) a rapid, small-amplitude rolling motion about the C_β-Cl bond axis, b) a slower 180° flip about the C_β-Cl axis. The relatively small value of the activation energy (E_a) measured for the PFF ring (less than 20 kcal/mol) strongly suggests that the ring flip is a cooperative process involving rolling motions of phenyl rings that are neighbors of the ring that flips (Hiyama, 1986). The activation energy of aromatic ring two-site oscillation in ferricytochrome c has a similar value, whereas in BPTI (Figure 45) it is equal to about 15 kcal/mol, although some rings are immobile up to 80°C (Wagner, 1976; Hetzel et al., 1976; Figure 45).

Hindered rotation of tyrosine aromatic ring in oxytocin bound to neurophysin was also reported (Blumenstein et al., 1980).

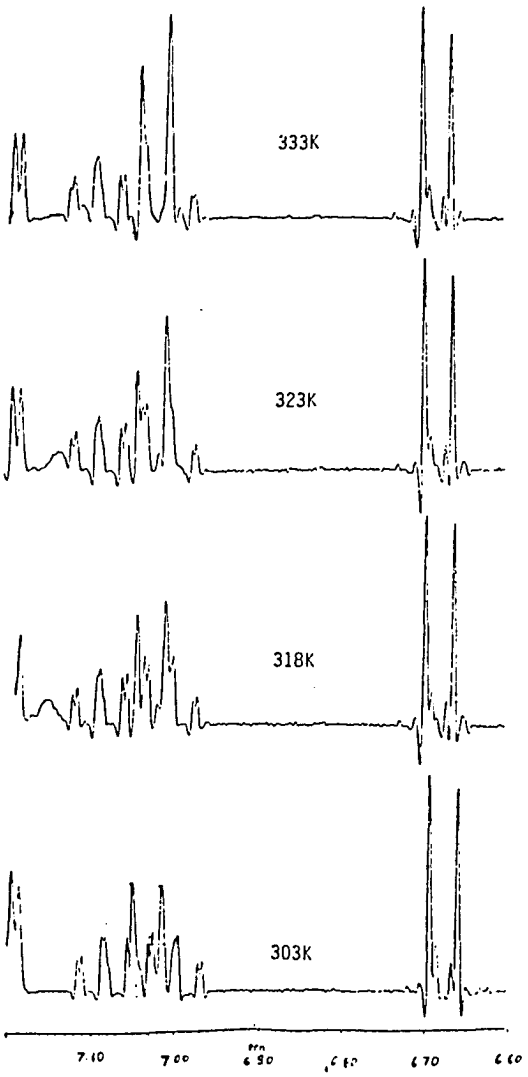

Figure 44 . Temperature dependence of aromatic resonances in D-Phe-Cys-Tyr-ψ[CH_2NH]-D-Trp-Orn-Thr-Pen-Thr-NH_2, d_6-DMSO.

In sufficiently hindered aromatic amines, besides stereomutation inverting the nitrogen atom, a second motion corresponding to a torsional process (rotation of the aromatic ring) has also been detected by NMR methods (Casarini et al., 1988; Casarini et al., 1987).

The observation of restricted aromatic ring rotation in peptide 23 is very puzzling, as one would expect that the $CH_2/C{=}O$ peptide bond replacement should increase peptide flexibility in that region, thus allowing the aromatic ring to find an energy well. Further investigations of this rare effect are in progress.

Table 13 shows a number of chemical shift differences for 23 in comparison with CTP, 1. The expected upfield shifts (as a result of isosteric peptide bond replacement) of the Cys^2 NH (-0.32 ppm) and the Tyr^3 NH (-0.46 ppm) are easily identified. Other significant upfield shifts include the Thr^6 NH (-0.41 ppm), Pen^7 NH (-0.34 ppm) and Thr^8 NH (-0.49 ppm), whereas a downfield shift is observed for the Orn^5 amide proton (0.32 ppm). Similarly, for alpha protons, there are dramatic upfield shifts of Cys^2 (-0.81 ppm), Pen^7 (-0.32 ppm), and Tyr^3 (-0.42 ppm), all a consequence of the peptide bond replacement. Some of the unexpected shifts (e.g. for Pen^7) may be related to the oscillation of the tyrosine aromatic ring between two sites. Analysis of NH-CH_α dihedral angles (obtained from Table 13) still supports the possibility of a type II' β-turn of the backbone, though the temperature coefficient of Thr^6 NH is not as small as usually observed in H-bonded amides (vide supra). On the other hand, the NOE cross-relaxation signals for the D-$Trp^4{}_\alpha/Orn^5$NH and Orn^5NH/Thr^6NH

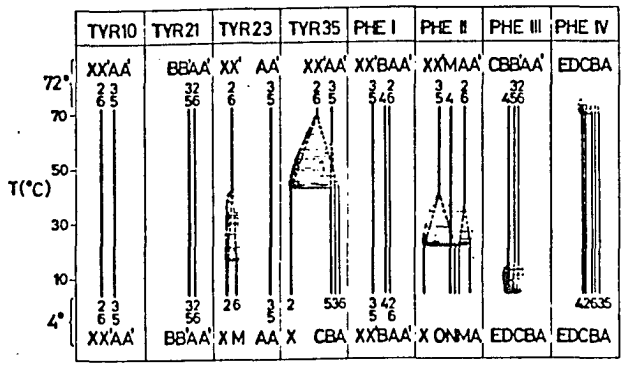

FAST EXCHANGE

$\nu_e \gg |\nu_2 - \nu_6|, |\nu_3 - \nu_5|$

A A' B B'

INTERMEDIATE EXCHANGE

$\nu_e \sim |\nu_2 - \nu_6|, |\nu_3 - \nu_5|$

A A' B C

SLOW EXCHANGE

$\nu_e \ll |\nu_2 - \nu_6|, |\nu_3 - \nu_5|$

A B C D

Figure 45. Spectral types of the aromatic residues in peptides and proteins, due to their restricted rotation around the C_2 axis (BPTI example).

pairs of protons are diagnostic for type II' β-turns. There also is, somewhat obscured by the proximity of the diagonal, cross-relaxation between the alpha protons of Cys^2 and Pen^7, and unexpectedly cross-relaxation between Cys^2 $_\beta$ and Pen^7 $_\alpha$ protons (Figure 46). Other NOE cross-peaks, expected if the peptide bond is trans, are also found: CH^i_β /NH^{i+1}, for i and i+1 = 1/2, 2/3, 6/7, 7/8. As a type II' β turn precludes the spatial proximity of Orn^5CH_α and Thr^6 NH, crossrelaxation from these residues is, indeed, not detected.

Side chain population analysis is, unfortunately, incomplete. Internal flexibility of some parts of the backbone makes it impossible to extract appropriate vicinal coupling constants. Briefly, there is a pronounced trans side chain population of Cys^2 (90%, compared with the almost equal distribution among trans and gauche(-) states for CTP, 1). Also, the side chain of Tyr $CH_2{}^3$ is mostly trans populated (gauche(-) for Tyr in CTP). This effect may cause observed chemical shift variations between equivalent residues of CTP and peptide 23. The low value of the Thr^6 vicinal coupling constant $J_{\alpha\beta}$ (4.5 Hz) vs. 6.8 Hz for CTP is another discrepancy between these two peptides.

In summary, peptide 23 still may be best characterized by a type II' β-turn conformation of its backbone, though there is substantial flexibility of its backbone, best manifested by a two site slow jump of the Tyr ring.

D-Phe-Cys-Tyr-ψ[CH_2N]-D-Tca-Orn-Thr-Pen-Thr-NH_2, 24.

Chemical shifts, coupling constants, and temperature coefficients are listed in Table 13. Due to low resolution of some signals

Table 13. Chemical shifts, coupling constants and amide temperature coefficients for D-Phe-Cys-Tyr-ψ[CH_2NH]-D-Trp-Orn-Thr-Pen-Thr-NH_2 (23), D-Phe-Cys-Tyr-ψ[CH_2N]-D-Tca-Orn-Thr-Pen-Thr-NH_2 (24), D-Phe-Cys-ψ[CH_2N]-Tic-D-Trp-Orn-Thr-Pen-Thr-NH_2 (26), d_6-DMSO.

Residue	Chem. shift [ppm]			Coupl. constant		
	Temp. factor 10^{-3}[ppm/deg]					
	23	24	26	23	24	26
	333K	365K	333K			
D-Pgl[1] 26						
D-Phe[1] 23						
24						
NH_3^+	8.04	8.21	8.63			
α	4.13	4.19	5.26	α/β'=4.5	5.1	
β'	3.23	3.23	--	α/β''=9.4	9.1	
β''	2.97	2.95	--	β'/β''=14.3	14.1	
Cys[2]						
NH	9.02	8.80	7.67*	α/NH=8.9	8.3	$
	-4.6	-4.5	$			
α	4.86	4.80	4.60	α/β'=3.5	$	$
β'	3.23	3.15	≈3.12	α/β''=9.4	$	$
β''	2.97	2.95	≈3.08	β'/β''=14.3	$	$
CH_2 26	----	----	2.77			
Tyr[3]						
Tic[3] 26						
NH	8.15	7.87	----	α/NH=m	7.6	---
	-5.5	-5.7	----			
α	4.17	4.16	3.88*	α/β'=5.7	$	$
β'	2.87	2.72	2.82	α/β''=9.7	$	$
β''	2.61	2.66	2.75	β'/β''=14.3	$	$
CH_2 23 24	#	2.81	----			
D-Tca 24						
D-Trp 23 26						
NH	$	----	8.44	α/NH=$	---	7.8
α	4.01	4.18	4.65	α/β'=$	$	6.2
β'	3.24	$	3.16	α/β''=8.7	9.1	8.2
β''	3.14	2.96	3.04	β'/β''=13.5	$	16.6
Orn[5]						
NH	8.56	8.20	8.44	α/NH=7.8	8.0	7.8
	-1.7	-1.4	$			
α	3.92	4.25	4.12	α/β'=$	$	$
β'	1.32@	1.85	1.75	α'/β''=$	$	$
β''	1.02@	1.61	1.38			
γ	0.98@	1.61	1.32			

δ	2.44@	2.81	2.67			
δ-NH_3^+	7.70	7.77@	7.70			
Thr[6]						
NH	7.28	7.57	7.32	α/NH=7.6	7.2	3.9
	-1.8	-3.8				
α	4.32	4.35	4.31	α/β=4.5	5.3	6.1
β	3.93	4.00	3.94	β/γ=6.3	5.9	6.3
γ	0.98	1.06!	0.98			
OH	≈5.3@					
Pen[7]						
NH	8.15	8.04	7.78	α/NH=9.1	9.0	6.9
	-2.4	-4.5				
α	4.69	4.64	4.51			
γ	1.31	1.32	1.19			
	1.37	1.38	1.22			
	.052	.052	.033			
Thr[8]						
NH	7.90	7.80	7.96	α/NH=8.5	8.5	8.6
	-1.6	-3.4				
α	4.26	4.24	4.20	α/β=3.9	3.7	3.8
β	4.00	4.00	4.01	β/γ=6.3	6.3	6.3
γ	1.05	1.08!	1.06			
OH	4.98@					

* putative assignment
$ not determined
# to be yet determined
m multiplet
@ 303K
! assignments could be reversed

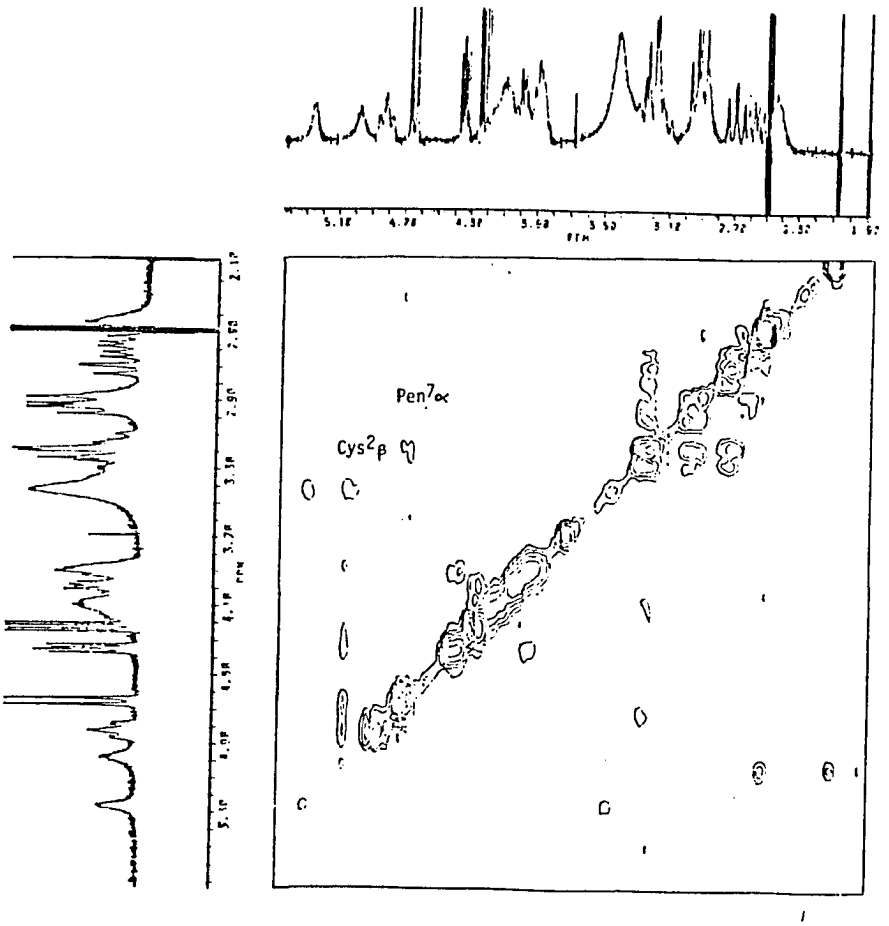

Figure 46.

NOESY spectrum of D-Phe-Cys-Tyr-Ψ[CH_2NH]-D-Trp-Orn-Thr-Pen-Thr-NH_2

(303K, d_6- DMSO)

in the 1D spectrum (its possible origin will be discussed later) at 303K, it was improved by increaseing the temperature to 365K. On the other hand 2D experiments (low spectral resolution is acceptable) were carried out at 303K. Differential decoupling experiments failed to extract the vicinal coupling constants for amino acids directly connected with the flexible peptide bond isostere (Cys^2, $TyrCH_2{}^3$, D-Tca^4, Orn^5). Visible broadening of amide and alpha proton signals for these residues may be attributed to conformational averaging. Otherwise, signals of residues isolated from the "flexibility domain" (Thr^6, Pen^7, Thr^8) are manifested as sharp signals. Interestingly, peptide 24 consists of two domains, a flexible one (amino acids 2-4) and a rigid one (amino acids 6-8). Coupling constants can be obtained for rigid domain amino acids, but not from the flexible domain. Comparison of the 1D spectra of 24 at 303 and 365K (Figure 47) besides improving spectral resolution (due to faster molecular tumbling of the peptide in otherwise viscous DMSO (James, 1975)) revealed some interesting dynamic processes. The diastereotopic protons of the methylene group adjacent to the amino group are in intermediate exchange at 303K, and as such are observed as broad humps at 4.14 and 3.78 ppm (Figure 47, bottom). At 365K, conformational averaging is fast enough to result in two relatively sharp doublets, at 4.18 and 3.78 respectively. This observation may be related to an oscillation between the gauche(-) and gauche(+) conformations for the D-Tca^4 side chain. The ϕ dihedral angles between NH^i-$CH^i{}_\alpha$ are compatible with either a type II'β turn or a reverse γ turn conformation.

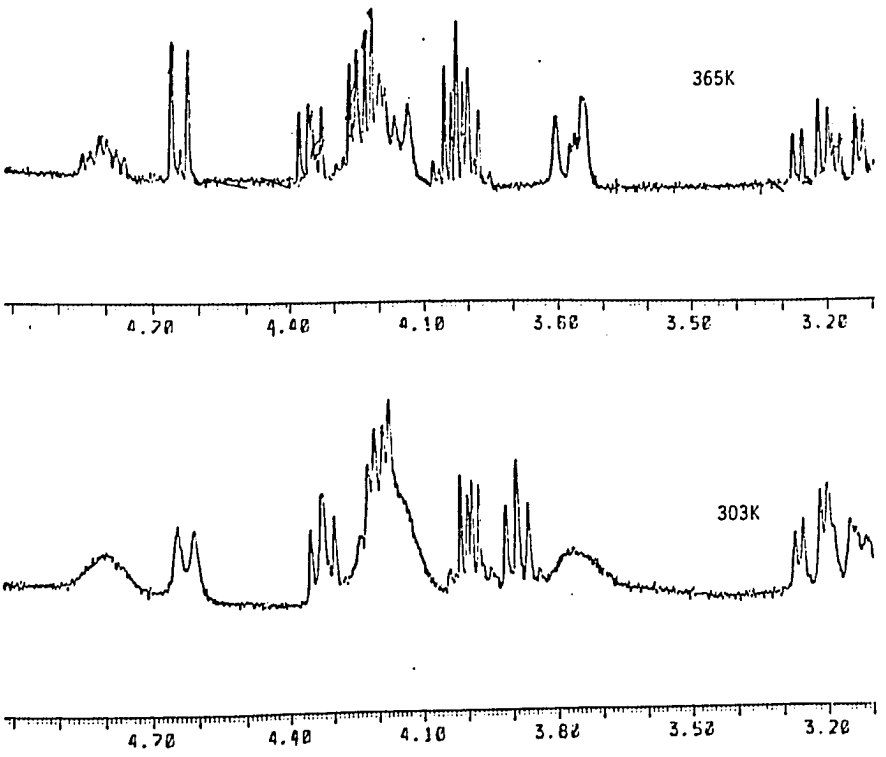

Figure 47. Possible manifestation of the mobility of the pipecolic ring fragment in D-Phe-Cys-Tyr-ψ[CH_2N]-D-Tca-Orn-Thr-Pen-Thr-NH_2, by temperature spectral dependence.

Analysis of the NOESY experiment reveals that two important cross- peaks between D-Phe$^1{}_\alpha$/Cys^{2}NH and Cys$^2{}_\alpha$/Tyr $CH_2{}^3$NH are not found. Not incidentally these amino acids were identified previously as constituting a flexibility domain in peptide 23, and presumably the same occurs for peptide 24. It is well known that internal flexibility in molecules greatly influences the magnitude of NOE cross-peaks. This aspect will be discussed later. The presence of a 4/5 and the absence of a 5/6 $CH_\alpha{}^i$/NH^{i+1} NOE has been interpreted here (vide supra) as strong proof for a type II' β-turn conformation involving residues 3-6. That really is the case for peptide 24, but another important cross-relaxation between amide protons of Orn^5 and Thr^6 is missing. The suggested mobility of the D-Tca^4 side chain, may require concerted motions of the neighboring Orn^5 side chain. Indeed, the dynamics of this residue may have caused a failure to extract reliable and unambiguous vicinal coupling constants for this amino acid. In addition, the chemical shift difference for Orn$^5{}_\beta$ protons in 24 is significantly lower (0.24 ppm) than in 22 (0.38 ppm), which is usually attributed to conformational averaging in peptides (Kessler, 1982). Thus, the magnitude of the cross-relaxation may be affected here. The presence of 6/7 and 7/8 NOESY signals again reflects a higher degree of order in the C-terminal part of peptide 24.

Analysis of amide temperature factors does not indicate H-bond formation by the Thr^6 NH. The low temperature factor for the Orn^5 amide NH may be indicative of a γ or inverse γ turn involving residues 3-5 (Smith and Pease, 1980). Side chain rotamer analysis is incomplete at this point (Table 13), however, the side chain popula-

tions for D-Phe^1, Thr^6, and Thr^8 are similar to those found in CTP (Sugg et al., 1988) and related compounds.

Analysis of the amide chemical shifts for compounds 22, 23, 24 (Table 11 and Table 13, respectively) reveals no essential differences. The major discrepancy, an upfield shift of the Tyr^{3}CH$_2$ amide proton (-0.72 ppm relative to 23) is expected as a result of the peptide bond replacement. The same, to a lesser extent, is true for the Cys^2 amide proton (-0.22 ppm upfield shift relative to 23). Otherwise, the chemical shifts for other residues are amazingly uniform (with only a small exception for the Thr^8 amide).

As previously discussed, the alpha protons of tetrahydroisoquinoline have different chemical shift values as a function of the pipecolic acid ring conformation. Comparison of relevant chemical shifts for peptides 23 and 24, in the absence of the appropriate vicinal coupling constants, suggest similar D-Tca^4 side chain conformations in both molecules. This comparison reveals some startling differences in the conformational behavior of tetrahydroisoquinolines and tetrahydrocarbolines, of unknown origin. Replacement of the carbonyl group (in 22) by a methylene moiety (24) does not introduce a conformational bias in the side chain of D-Tca^4. This result is not unexpected, however, since in 22 (unlike in 25, vide infra) there already is significant preference of the D-Tca side chain to attain a gauche(-) conformation.

In the absence of more sensitive parameters (coupling constants), the similar chemical shifts of Orn^5 γ protons is yet further evidence for similar topographies of both peptides in that region. This chemical

shift has been used as a diagnostic tool probing the spatial relationship of the D-Trp^4 and Lys^5 residues in a related class of octapeptides (Hallenga et al., 1980; Wynants et al., 1985). A decrease in the spectral range (a difference between the highest and the lowest chemical shift values for the same class of protons) has usually been interpreted as evidence for conformational averaging (Kessler, 1982). For amide protons this range is 1.27 ppm for 24 and 1.81 ppm for 22. Among alpha protons the chemical shift range is 0.64 ppm for 24 in contrast to 1.32 ppm for 22. Also, the chemical shift difference of the diastereotopic Pen^7 methyl groups in 22, 23, 24 is fairly consistent, confirming similar rigidity of the C-terminal peptide region in these molecules.

The implications of these stereochemical and dynamic properties on affinities and selectivities for opioid receptors will be discussed in the later text.

D-Phe-Cys-Tic-D-Trp-Orn-Thr-Pen-Thr-NH_2, 25.

The chemical shifts, coupling constants, and temperature coefficients were obtained by methods described in the Experimental and are listed in Table 11. Unlike previously discussed 23 and 24, the title compound 25 has a further conformational constraint applied to the i position of the putative type II' β-turn. A Tic derivative was incorporated into the peptide chain, replacing Tyr in 2. The appropriate cyclic derivative of tyrosine is very difficult to synthesize (a multistep synthesis has been published by Miyake et al., 1984),

whereas classical Pictet-Spengler reaction of tyrosine with formaldehyde results in polymeric material of Bakelite type. Nonetheless, it has been found (Pelton et al., 1985a) that the replacement of Tyr^3 with Phe^3 results in only a modest (3 times) decrease of peptide affinity to the mu opioid receptor. Karplus-Bystrov (Bystrov, 1976) analysis of accessible ψ angles does not indicate any major discrepancy with these of CTP. Also, analysis of side chain populations suggests that the overall topographies of these two molecules (excluding the Tic^3 residue, which will be discussed later) are similar. Another, relatively minor difference was detected in the side chain population in Cys^2 of 25 which is mostly trans. For CTP the population is equally divided between trans and gauche(-) conformations. The origin of this effect is probably related to a dramatic, though expected, side chain conformational change at the 3rd position in 25 (relative to 2). Analysis of the coupling constants (Table 11) indicates that both vicinal coupling constants are almost equal, as a result of the somewhat skewed gauche(+) conformation of the Tic^3 side chain group (Figure 33).

Similarly to peptide 23, one observes an increased trans side chain population of Cys^2 (probably the result of repulsions from the Tic^3 aromatic ring). This does not allow one to detect any cross-relaxation between the alpha protons of Cys^2 and Pen^7 (only minor effect is detected in the case of peptide 23)-Figure 48. This result should be contrasted, however, with a very strong cross-relaxation found in peptide 22, in spite of an overwhelmingly trans population of the Cys^2 side chain. On the other hand NOESY experiments reveal two important

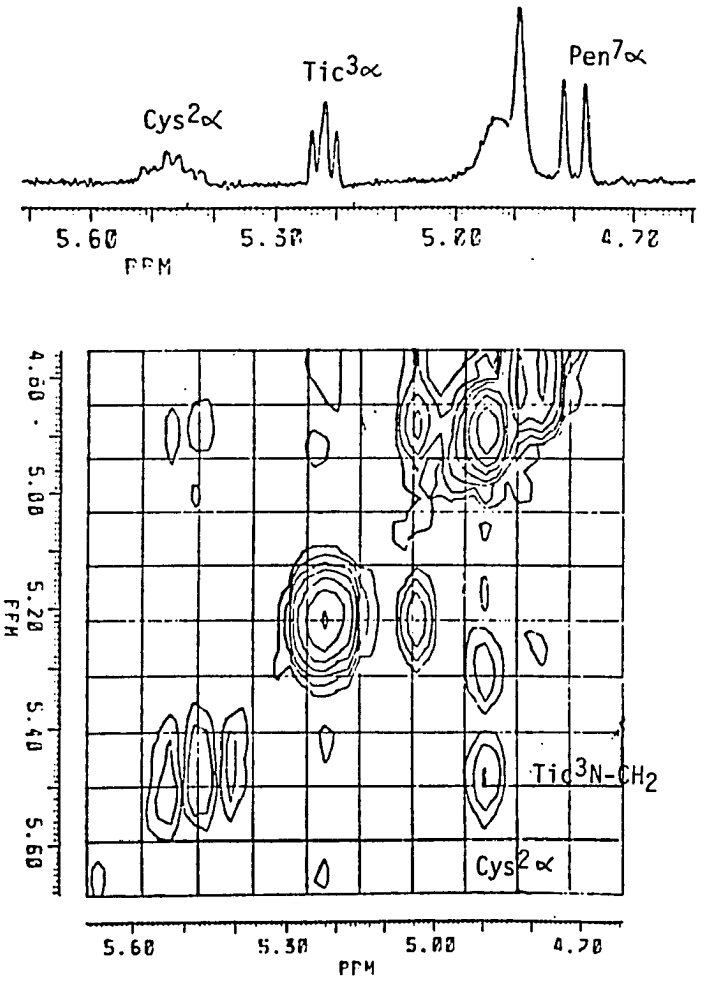

Figure 48.

NOESY spectrum of D-Phe-Cys-Tic-D-Trp-Orn-Thr-Pen-Thr-NH_2

(303K, d_6- DMSO)

cross peaks: Cys^2 CH_α/Tic^3 NCH_2 and Tic^3 CH_α/Tic^3 NCH_2. The first effect may only be observed if the corresponding peptide bond is in a trans configuration (vide supra). The 1D spectrum of 25 suggests that there is only one conformer observed. Thus, in contrast to the proline ring where cis and trans peptide bond isomers are often in equilibrium (Montelione et al., 1986; Piela et al., 1987; Thomas, 1976), the tetrahydroisoquinoline ring seems to exclusively prefer a trans conformation of the peptide bond.

NOESY experiments reveal that the following pairs of protons $CH^i_\alpha/$ NH^{i+1} are in spatial proximity: 1/2, 3/4, 4/5, 6/7, 7/8. These peptide bonds are trans. Lack of 5/6 cross-relaxation in the presence of a strong NH^5/NH^6 signal again is interpreted as evidence for a type II' β-turn backbone conformation.

The chemical shift difference between the diastereotopic methyl groups of Pen^7 was much larger in 25 (0.132 ppm), than in 1 (0.06 ppm). Perhaps an overall increase of peptide rigidity (transmitted via side chains) yields better stereodifferentiation of both methyl groups for 25. Table 11 reveals that there is a substantial upfield shift of the D-Trp^4NH (-0.74 ppm in comparison to 1), which possibly is a result of ring anisotropy from the gauche(+) populated side chain of Tic, in contrast to the mostly gauche(-) populated side chain of Tyr in CTP. Erratic upfield shifts of Thr^6, Pen^7, Thr^8 amide resonances; and the absence of this phenomenon for Orn^5NH, indicate transannular ring current anisotropy effects on these residues. Information of this type will be very helpful in molecular modelling studies.

D-Pgl-Cys-ψ[CH_2N]-Tic-D-Trp-Orn-Thr-Pen-Thr-NH_2, 26.

Strong indications of conformational averaging were identified for the title peptide 26 in the form of broad lines for some signals at 303K. Increased resolution was achieved by carrying NMR experiments at 333K (James, 1975).

Chemical shifts and coupling constants (where obtained) are listed in Table 13. However, even at elevated temperatures the signals of the 2nd, 3rd, and 7th residues still stayed sufficiently broadened that no accurate coupling constant information could be extracted. To obtain approximate information about the conformation and dynamics of this molecule, chemical shift analysis (in a similar manner as done before) was utilized. It was noted first that D-Pgl in the 1st position has similar ring anisotropy effects to D-Phe (Kazmierski and Hruby, 1988). Considering the alpha protons first, there was a significant upfield shift of the Cys^2 CH_2 protons in 26 (-0.87 ppm with respect to 25). This is much higher than one would expect solely as a result of isosteric peptide bond replacement with an alkyl amino group (about -0.4 ppm). Due to increased distance the influence of this replacement should be even less pronounced for the Cys^2CH_2 amide in peptide 26. On the contrary, there was a tremendous upfield shift of this resonance in 26 relative to 25 (- 1.58 ppm). These results strongly imply dramatic ring current anisotropy effects, suggesting very different orientations of the Tic aromatic side chains in both 26 and 25 (where the gauche(+) conformation was found). Both the alpha and amide protons of D-tryptophan in 26, on the contrary, experience a downfield shift relative to 25 (0.38 and 0.35 ppm, respectively). A

closer look at both the alpha and amide protons of both peptides 25 and 26 (Table 11 and Table 13) reveals, with the exception of the alpha protons of Pen^7, that the corresponding resonances are almost identical. A small upfield shift (-0.29 ppm) experienced by the $Pen^7{}_\alpha$ resonance will be discussed later. Additionally, the alpha proton of Tic in 26 experiences an upfield shift of -1.34 ppm, which is much larger than expected from alkyl amine peptide bond modification. Again, conformational effects must be involved. Figure 8 clearly shows that both the gauche(-) and gauche(+) Tic conformers differ in the relationship of the aromatic ring (ring current anisotropy) to an alpha proton.

Analysis of a 1D spectrum of 26 revealed that while D-Trp, Orn, and Thr^6 gave reasonably sharp signals, the next amino acid Pen^7 again gave broad (slow exchange) alpha and amine proton resonances. The already mentioned small upfield shift of Pen^7 CH_α may be related to this phenomenon. Most convincing, however, is a comparison of the chemical shift difference between the diastereotopic methyl groups of Pen^7. This value is only 0.033 ppm for 26, compared to 0.131 ppm for rigid 25 (Table 11 and Table 13). The existence of two domains of different flexibility in 26 separated by the relatively rigid D-Trp-Orn-Thr fragment suggests that flexibility originating from the peptide bond isostere substitution may be transmitted through the disulfide bonds and is manifested in the form of a more flexible Pen^7 residue. ϕ angles calculated from the vicinal coupling constants for D-Trp and Thr^6 exhibit a significant deviation compared with the corresponding values in CTP (1). NOESY experiments did not add any additional

information. Only some intraresidual NOE signals were detected. At present it is difficult to come up with any reasonable model for peptide 26. The apparent flexibility of this compound in conjunction with the lack of any distance information is especially challenging and will require more extensive work.

Motional averaging in peptides and proteins has recently been the subject of elaborated studies involving molecular dynamics simulations and their correlations with cross-relaxation rates accessible from the time development of the nuclear Overhauser effect (Olejniczak et al., 1984; Olejniczak et al., 1981). These studies, limited to the effects of subnanosecond fluctuations because of limited length of the available dynamics run, showed that cross-relaxation rates are reduced by motional averaging on a picosecond time scale. The ratio of experimentally determined cross-relaxation rate (σ) to that estimated for a rigid, isotropically tumbling protein reflects the degree of internal motions that occur in the molecule. For intraresidual protons, where the internuclear separation is fixed, the resulting ratio is equal to the order parameter S^2 (Levy, 1986), which can also be determined from the dynamics simulations. Studies on lysozyme (Olejniczak et al., 1984) showed that unlike for Trp-28, experimental values of S^2 for Ile-98 and Met-108 are smaller than the values of S^2 predicted from simulations. This suggests that motions on a long time scale (nanosecond range dihedral angle fluctuations involving transitions between minima), compared with those from simulations, are present and have non-negligible effects on the cross-relaxation rates. Even interresidue subnanosecond motions can, on the average, decrease NOE

intensity about 20%. Motions other than these fast fluctuations are by no means eliminated. The magnitudes of fast fluctuations would be reduced if additional slower motions were present, to satisfy experimental results. In the absence of the fast motions any slower motion must involve greater angular fluctuations (Olejniczak et al., 1981). Therefore, it is perceived that even slower molecular motions, such as those involving peptides 23, 24, and 26 that may be manifested on the NMR time scale, will even further reduce observable NOEs. Further investigation of the dynamic and conformational properties of these peptides, in conjunction with the unique pharmacological properties of some of them, may give many important insights into structural requirements for affinity to different classes of opioid receptors.

Comparison of Results Obtained in this Work With the Literature Data.

This work provides structural evidence for opioid receptor selection mechanism. Treatment of type II' β-turn-forming amino acids on a relatively rigid conformational template allowed us to examine very local, selective manipulations in the peptide's topography. The very distinct conformational properties of H-(D-)N-Me-Phe, H-(D-)Tic, as well the acylated D- and L-Tic and Tca residues constitute an approach that allows design of desired topographical features in a predictable manner. A gauche(-) side chain conformation of D-Tic in 8 corresponds to an extended form of the peptide (Figure 29) , recognized well by the mu but not the delta opioid receptors. A gauche(+)

side chain conformation of Gly-D-Tic^1 in 12 is responsible for enforcing an overall more folded topography of this peptide, a feature not well recognized by the mu opioid receptor, but slightly better recognized by delta receptors.

It is interesting to compare results obtained in this work with some recent findings from other laboratories. Salvadori et al. (1986) incorporated Z-dehydrophenylalanine (Δ^ZPhe) into the third position of the naturally occurring mu opioid agonist- dermorphin, H-Tyr-D-Ala-Phe-Gly-Tyr-Pro-Ser-NH_2. This structural modification resulted in a 74-fold decrease of <u>in vitro</u> activity in the GPI system (activity on mu receptor) and a 27-fold decrease in its analgesic properties. No systematic studies on conformational properties of this peptide have been carried out. However the aromatic ring of the Δ^ZPhe is directed (due to Z-isomerism) towards the Tyr^1 moiety, leading to a decrease of the critical distance (in light of our results) between these important aromatic pharmacophores ("folded" conformation).

The pharmacological consequences of the Phe^4 replacement by both isomers of dehydrophenylalanine in the enkephalin series has been tested by Nitz et al. (1986). As indicated by competitive binding experiments in a radioligand receptor assay, the Δ^ZPhe^4-containing peptide conserved a high affinity, whereas the analogue bearing Δ^EPhe exhibited about 1000 weaker affinity to delta opioid receptors, in comparison with the enkephalins. Again, as no conformational studies accompanied these findings, it can only be speculated that the Δ^ZPhe^4 isomer probably constitutes a compact conformation of the peptide, exhibiting therefore preferential binding to delta opioid receptors.

Finally, recent conformational investigations of the cyclic delta opioid selective peptide Tyr-D-Pen-Gly-Tyr-D-Pen-OH suggested the spatial proximity of both aromatic rings, on the basis of indirect NOE effects (Hruby et al., 1988). Similar conclusions, on the basis of relaxation data, have been drawn for linear enkephalins (Niccolai et al., 1980). This finding confirms that the delta opioid receptor recognizes compact molecular topographies. This result is complementary to our finding based on mu selective octapeptides that an extended topography is recognized by mu but not the delta receptors.

Summary and Future Perspectives.

This research has attempted to contribute to several essential problems of contemporary molecular biology.

The relationship between primary and secondary structure. Unlike most recent approaches to control and design of peptide secondary structure (Gierasch et al., 1981; Mutter, 1985; Kemp and Carter, 1987, etc.) that concentrate on the backbone conformation, the approach presented here treats backbone as a relatively rigid structure, upon which side chains can be arranged in predetermined topographies. NMR based conformational analysis of peptides 22 and 25 suggests that turn structures are not perturbed by the cyclic aromatic amino acids, which enforce certain topographical properties, essentially by forming stable bicyclic structures. The fact that N-terminal (D-)Tic (8) and internal (D-)Tic (12 and 25) possess strikingly different side chain χ^1 angles (g(-) vs g(+), respectively) is the basis of this new

approach to peptide/protein topography design. Besides the cyclic derivative of phenylalanine, similar work was initiated with cyclic derivatives of tryptophane (carbolines), and in principle could be extended to other amino acids (such work is in progress in this laboratory). Pseudopeptides were synthesized to stabilize the g(-) side chain conformation for internally coupled pipecolic acid derivatives. At present, the detected mobility of the backbone in the area of the alkylamine does not make it possible to unequivocally support this approach to establish the topography; however the chemical shifts of the α-H's of amino acids involved in pseudopeptide bonds seem to support this possibility. Further studies, particularly on peptide 23, are in progress.

Topographical models for the bioactive state of a peptide. As demonstrated by conformational analysis of a large number of peptides, the type II' β-turn backbone structure is a stable conformational feature of this class of peptides. This, as well our ability to determine side chain conformations of cyclic amino acids, renders unique insights into elements of bioactive conformation of μ opioid ligands. It was demonstrated that the sequential flip of the aromatic side chain of the first amino acid (in 12) and the third (in 25) resulted a in sharp decrease of the peptide's affinity for the μ opioid receptor, whereas both side chains located on the same side of the molecule and separated by a proper distance (8) were extremely important pharmacophores for recognition by the μ opioid receptor. Correlation of the described topography design on a rigid conformational template, in

conjunction with receptor binding data, may be a very useful tool in searches for bioactive conformations in general.

Design of potent and selective μ opioid antagonists and agonists.

Any hypothesis, such as the topographical design on a rigid templates model proposed here, requires experimental verification. To date, design of the most potent and selective class of μ opioid antagonists utilized the above stated principles. An interesting step towards design of μ agonists should be substitution of D-Tca on the N-terminus of octapeptides. Its precursor peptide 13 showed significant agonistic character, enhanced in [D-Tca^1]CTP, with the expected increase of its selectivity for the μ opioid receptor, analogously to the influence of D-tetrahydroisoquinoline vs. D-phenylalanine on this position.

It is admitted that this study brought up as many questions as it tried to answer. Careful model studies on selected cyclic amino acids incorporated in different peptide sequences will have to be carried out to verify the scope and limitations of the proposed approach to the topography design on a backbone template. However, the results to date in terms of topographical insight and biological potency and specificity have been most promising, suggesting that further work is justified.

REFERENCES

Atherton, E., Fox, H., Hapkiss, D., and Sheppard, R.C.(1978).J.Chem.Soc.Chem.Commun.,539-540.

Banwell, C.N., and Primas, H.(1963).Mol.Phys.,6,225-256.

Bauer, W., Briner, V., Doepfner, W., Haller, R., Huguenin, R., Marbach, P., Petcher, T.J., and Pless, J.(1982).Life Science,31,1133-1140.

Bax,A., and Freeman, R.(1981).J.Mag.Res.,44,542-561.

Beamont, S.M., Handford, B.O., and Young, G.T.(1965).Acta Chim.Acad.Sci.Hung.,44,37-43.

Bergman, M. and Zervas, L.(1932).Ber.Dtsch.Chem.Ges.,65,1192- 1201.

Blumenstein, M., Hruby, V.J., and Viswantha,V.(1980). Biochem.Biophys.Res.Commun.,94,729-736.

Bonora, G.M., Toniolo, C., Di Blascio, B., Pavone, V., Pedone, C., Benedetti, E., Lingham, I., and Hardy, P.(1984).J.Am.Chem.Soc., 106,8152-8156.

Bryan, W.M.(1986).J.Org.Chem.,51,3371-3372.

Bystrov, V.F.(1976).Prog.NMR Spectroscopy,10,41-81.

Camerman, A., Mastropaolo, D., Karle, I., Karle, J., and Camerman, N.(1983).Nature,306,447-450.

Casarini, D., Lunazzi, L., Placucci, G., and Maciantelli,D.(1987). J.Org.Chem.,52,4721-4726.

Casarini, D., Lunazzi, L., and Maciantelli, .(1988).J.Org.Chem.,53, 182-185.

Chang, K.-J., Cooper, B.R., Hazum, E., and Cuatrecasas, P.(1979).Mol.Pharmacol.,16,91-104.

Christensen,T.(1979).In"Peptides, Structure and Function"(E.Gross, J.Meienhofer,eds.),pp.385-388,Pierce.

Clore, G.M., and Gronenborn, A.M.(1982).J.Mag.Res.,48,402-417.

De Leeuw, F.A.A.M., and Altona, C.(1982).Int.J.Peptide Protein Res.20,120-125.

Di Maio, J., Bayly, C.I., Villeneuve, G., and Michel, A.(1986).J.Med.Chem.,29,1658-1663.

Doi, M., Tanaka, M.,Ishida, T., and Inoue, M.(1987).FEBS Letters,213,265-268.

Epelbaum, I., Brazeau, P., Tsang, D., Brawer, J., Martin, J.B.(1977).Brain Res.,126,309.

Erickson,B.W., and Merrifield, R.B.(1973a).J.Am.Chem.Soc., 95,3750-3756.

Erickson, B.W., and Merrifield, R.B.(1973b).J.Am.Chem.Soc., 95,3757-3763.

Feeney,J.(1976).J.Mag.Res.,21,473-478.

Fehrentz, J.A., and Castro, B.(1983).Synthesis,676-678.

Feigel, M.(1986).J.Am.Chem.Soc.,108,181-182.

Fournie-Zaluski, M.C., Prange, T., Pascard, C., and Roques, B.P.(1977).Biochem.Biophys.Res.Commun.,79,1199-1206.

Gierasch, L.M., Deber, C.M., Madison, V., Niu, C.-H., and Blout, E.R.(1981).Biochemistry,20,4730-4738.

Giesner-Pretre, C., and Pullman, B.(1971).J.Theor.Biol.,31,287-289.

Glaser, J.A., and Borer, P.N.(1986).Bioch.Biophys.Res.Commun., 1267-1273.

Gorin, F.A., and Marshall, .R.(1977).Proc.Natl.Acad.Sci.USA, 74,5179-5183.

Grathwohl, C., Tun-Kyo, A., Bundi, A., Schwytzer, R., and Wüthrich, K.(1975).Helv.Chim.Acta,58,415-423.

Gupta, F.A., Sarma, R.H., and Dhingra, M.M.(1986).FEBS Letters,198,245-250.

Hallenga, K., Van Binst, G., Scarso, A., Michel, A., Knappenberg, M., Dremier, C., Brison, J., and Dirkx, J.(1980).FEBS Lett.,119,47-52.

Hansen, P.E., and Morgan, B.A.(1984).In"The Peptides; Analysis, Synthesis, Biology",Vol.6.(S. Udenfriend and J. Meienhofer, eds.),269-321,Academic Press.

Harvey, D.G.(1941).J.Chem.Soc.,153-159.

Hetzel, R., Wüthrich, K., Deisenhofer, J., and Huber,R.(1976). Biophys.Struct.Mech.,2,159-180.

Hiyama, Y., Silverton, J.V., Torchia, D.A., Gerig, J.T., and Hammond, S.J.(1986).J.Am.Chem.Soc.,108,2715-2723.

Hruby, V.J.(1981).In"Topics in Mol.Pharmacology"(A.S.V. Burgen and G.C.K. Roberts, eds),100-126, Elsevier/North-Holland, Amsterdam.

Hruby, V.J.(1982).Life Sciences,31,189-199.

Hruby, V.J., Kao, L.-F., Pettitt, B.M., and Karplus, M.(1988). J.Am.Chem.Soc.,3351-3359.

Isogai, Y., Nemethy, G., and Scheraga, H.A.(1977). Proc.Natl.Acad.Sci.USA.,74,414-418.

IUPAC-IUB Commission on Biochemical Nomenclature.(1970). Biochemistry,9,3471-3479.

Jakubke. H.D.(1965).Z.Naturforsch.,20b,273-274.

James,T.L.(1975).In"Nuclear Magnetic Resonance in Biochemistry;Principles and Applications",Academic Press.

Johnson, F.(1968).Chem.Rev.,68,375-413.

Kaiser, E., Colescott, R.L., Bossingor, C.D., and Cook, P.I.(1970).Anal.Biochem.,34,595-598.

Kastin, A.J., Coy, D.H., Jacquet, Y., Schally, A.V., and Plotnikoff, N.P.(1978).Metebolism,Suppl.1,27,1247.

Kazmierski, W. and Hruby, V.J.(1988).Tetrahedron.(1988).44,697-710.

Kazmierski, W., Wire, W.S., Lui, G.K., Knapp, R.J., Shook, J.E., Burks, T.F., Yamamura, H.I., and Hruby, V.J.,J.Med Chem.,submitted.

Kazmierski, W., and Hruby, V.J.(1988b)., manuscript in preparation.

Kemp, D.S., and Carter, J.S.(1987).Tetrahedron Letters,28,4645-4648.

Kessler, H., Müller, A., and Oschkinat, H.(1985).Mag.Res.Chem.,23,844-852.

Kessler, H.(1982).Angew.Chem.Int.Ed.Engl.,21,512-523.

Kessler, H., Berndt, M., Kogler, H., Zarbock, J., Sorensen, O.W., and Bodenhausen, G.(1983).J.Am.Chem.Soc.,105,6944-6952.

Kessler, H., Holzemann, G., and Zechel, C.(1985).Int.J.Peptide Protein Res.,25,267-279.

Kobayashi, J., Higashijima,T., Sekido,S., and Miyazawa, T.(1981).Int.J.Peptide Protein Res.,17,486-494.

Levy, R.M.(1986).Isr.J.Chem.,27,173-179.

Loew, G.H., and Burt, S.K.(1978).Proc.Natl.Acad.Sci.USA,75,7-12.

Loew, G.H., Toll, L., Uyeno, E., Cheng, A., Judd, A., Lawson, J., Keys, C., Amsterdam, P., and Polgar, W.(1986).In"Opioid peptides:Medicinal Chemistry"(R.S. Rapaka, G. Barnett, R.L. Hawks, eds),NIDA Research Monograps,69,231-265.

Loew, G., Keys, C., Luke, B., Polgar, W., and Toli, L.(1986).Molecular Pharmacology,29,546-553.

Lord, J.A.H., Waterfield, A.A., Hughes, J., and Kosterlitz, H.W.(1977).Nature,267,495-499.

Mapelli, C., Kimura, H., and Stammer, C.H.(1985).In"Peptides:Structure and Function"(C.M. Deber, V.J. Hruby and K.D. Kopple, eds.), 503-506. Pierce.

Marion, D., and Wüthrich, K.(1983).Biochem.Biophys.Res.Commun., 113,967-974.

Martin, W.R., Eades, C.G., Thompson, J.A., Huppler, R.E., and Gilbert, P.E.(1976).J.Pharmacol.Exp.Thr.,197,517-523.

Maurer, R., Gaehwiler, B.H., Buescher, H.H., Hill,R.C., and Roemer, D.(1982).Proc.Natl.Acad.Sci.USA.,79,4815-4817.

Mc Dermott, J.R., and Benoiton, N.L.(1973).Can.J.Chem.,51,1915-1919.

Meraldi, J.-P., Hruby, V.J., and Brewster, A.I.R.(1977). Proc.Natl.Acad.Sci.USA,74,1373-1377.

Merrifield, R.B.(1964).J.Am.Chem.Soc.,86,304-305.

Merrifield, R.B.(1978).J.Org.Chem.,43,2845-2852.

Mitchell, A.R., Kent, S.B.H., Englelhard, M., and Merrifield, R.B.(1978).J.Org.Chem.,43,2845-2852.

Miyake,A., Itoh,K., Aono,T., Kishimoti,S., Natsushita, Y., Inada, Y., Nishikawa, K., and Oka, Y.(1984).Journal of the Takeda Research Laboratories,43,53-76.

Montelione, G.T., Hughes,P., Clardy,J., and Scheraga, H.A.(1986). J.Am.Chem.Soc.,108,6765-6773.

Mosberg, H.I., Hurst, R., Hruby, V.J., Galligan, J.J., Burks, T.F., Gee, K., and Yamamura, H.I.(1982).Biochem.Biophys.Res.Commun., 106,506-518.

Mosberg, H.I., Hurst, R., Hruby, V.J., Gee, K., Yamamura, H.I., Galligan, J.J., and Burks T.F.(1983).Proc.Natl.Acad.Sci.USA, 80,5871-5874.

Motta, A., Tancredi, T., and Temussi, P.A.(1987).FEBS Letters,215,215-218.

Mutter, M.(1985).Angew.Chem.,Int.Ed.,24,639-653.

Mutter, M.(1988).In"Peptides,Chemistry and Biology"(G.R. Marshall, ed.), pp.349-353, ESCOM, Leiden.

Niccolai, N., Garsky, V., and Gibbons, W.A.(1980).J.Am.Chem.Soc., 102,1517-1520.

Nitz, T.J., Shimohigashi, Y., Costa, T., Chen, H.-C., and Stammer, C.H.(1986).Int.J.Peptide Protein Res.,27,522-529.

Nutt, F.R., Weber, D.F., Curley, P.E., Saperstein, R., and Hirschmann, R.(1983).Int.J.Peptide Protein Res.,21,66-73.

Olejniczak, E.T., Dobson, C.M., Karplus, M., and Levy, R.M.(1984). J.Am.Chem.Soc.,106,1923-1930.

Orlowski, R.C., Walter, R., and Winkler, D.(1976).J.Org.Chem., 41,3701-3705.

Pelton, J.T., Gulya,K., Hruby, V.J., Duckles, S.P., and Yamamura, H.I.(1985a).Proc.Natl.Acad.Sci.USA,.82,236-239.

Pelton, J.T., Gulya, K., Hruby, V.J., Duckles, S., and Yamamura, H.I.(1985b).Peptides,6,Suppl.1,159-163.

Pelton, J.T., Kazmierski, W., Gulya, K., Yamamura, H.I., and Hruby, V.J.(1986).J.Med.Chem.,29,2370-2375.

Pictet, A., and Spengler, T.(1911).Chem.Ber.,44,2030-2036.

Piela,L., Nemethy, G., and Scheraga, H.A.(1987).J.Am.Chem.Soc., 109,4477-4485.

Prasad, V.V., and Balaram, P.(1984).CRC Crit.Rev.Biochem.,307-348.

Rance, M., Sorensen, O.W., Bodenhausen, G., Wagner, G., Ernst, R.R., and Wüthrich, K.(1983).Biochem.Biophys.Res.Commun.,117,471-478.

Rao, B.N.N., Kumar, A., Balaram, H., Ravi, A., and Balaram. P.(1983).J.Am.Chem.Soc.,105,7432-7428.

Renaud, L.P., Martin, J.B., and Brazeau, P.(1975).Nature.,325,233-235.

Rezek, M., Havlicek, V., Leybin, L.,LaBella, F.S., and Friesen, H.(1981).Can.J.Pharmacol.,56.227-231.

Rice, D.M., Meinwald, Y.C., Scheraga, H.A., and Griffin, R.G.(1987). J.Am.Chem.Soc.,109,1636-1640.

Romanowska, K., Kopple, K.D.(1987).Int.J.Peptide Protein Res., 30,289-298.

Rudinger, J.(1973).In"The Chemistry of Polypeptides"(P.G. Katsoyannis, ed.),pp.87-123.Plenum, New York.

Salvadori, S., Marostoni, M., Balboni, G., Marzola, G., and Tomatis, R.(1986).Int.J.Peptide Protein Res.,28,262-273.

Sato, K., and Nagai, U.(1986).J.Chem.Soc.Perkin Trans.,1,1231.

Schiller, P.W., Yam, C.F., and Lis, M.(1977).Biochemistry,16,1831-1838.

Schiller, P.W., DiMaio, J., and Nguyen, T.M.- D.(1985).In"Proceedings of the 16th FEBS Congress"(Y.A.Ovchinnikov, ed.),457-462, Utrecht Univ. Science Press.

Schwartz, H., Bumpus, F.M., and Page, I.H.(1957).J.Am.Chem.Soc., 5697-5703.

Sheehan, J.C., and Hess, G.P.(1955).J.Am.Chem.Soc.,77,1067-1068.

Shenderovich, M.D., Nikiforovich, G.V., and Chipens, G.I.(1984). J.Mag.Res.,59,1-12.

Siemion, I.Z.(1971).Liebigs Annln.Chem.,748,88-95.

Smith, J.A., and Pease, L.G.(1980).Crit.Rev.Biochem.,8,315-399.

Solomon, I.(1955).Phys.Rev.,99,559-565.

Spackman, D.H., Stein, W.H., and Moore, S.(1958).Anal.Chem.,30, 1190-1206.

Stewart, J.M., and Young, J.D.1984.In"Solid Phase Peptide Synthesis",Pierce,sec.ed.

Sugg, E.E., Griffin, J.F., and Portoghese, P.S.(1985).J.Org.Chem., 50,5032-5037.

Sugg, E.E., Tourve, D., Kazmierski,W., Hruby, V.J., and Van Binst, G.(1988).Int.J.Peptide Protein Res.,31,192-200.

Terenius, L.(1976).Eur.J.Chem.,38,211-213.

Thomas, W.A.(1976).In"Annual Reports on NMR Spectroscopy",Vol.6B(E.F.Mooney,ed.),p.12,Academic Press.

Titlestad, K., Groth, P., and Ali, M.I.(1973).J.Chem.Soc.Chem.Commun., 346-347.

Upson, D.A., and Hruby, V.J.(1976).J.Org.Chem.,41,1353-1358.

Vale, W., Rivier, C., and Brown, M.(1977).Ann.Rev.Physiol.,39,473-527.

Van de Ven, F.J.M., and Hilbers, C.W.(1983).J.Mag.Res.,54,512-520.

Veber, D.F., Freidinger, R.M., Schwenk-Perlow, D., Paleveda, Jr., W.J., Holly, F.W., Strachan, R.G., Nutt, R.F., Arison, B.H.(1981).Nature,292,55-58.

Veber, D.F., Holly,F.W.(1979).Nature,280,512-514.

Veber, D.F., Saperstain, R., Nutt, R.F., and Freidinger, R.M.(1984).Life Sciences,34,1371-1378.

Vitoux,B., Aubry, A., Lung, M.T., and Marraud, M.(1986).Int.J.Peptide Protein Res.,27,617-632.

Voelter, W.(1980).In"Polypeptide Hormones"(R.F. Beers,Jr. and E.G. Basset,eds.).pp.135-147,Raven Press, New York.

Wagner, G., De Marco, A., and Wüthrich, K.(1976).Biophys.Struct., 2,139-158.

Weygand, F., Steglicg, W., and Chytil, N.(1968).Z.Naturforsch., 23b,1391-1392.

Wilkes, B.C., and Schiller, P.W.(1987).Biopolymers,1431-1444.

Wüthrich, K., Billeter, M., and Braun, W.(1984).J.Mol.Biol.,180,715-740.

Wynants,C., Van Binst, G., and Loosli, H.R.(1985).Int.J.Peptide Protein Res.,25,615-621.